

**CHARACTERISATION AND SUBSTITUTION  
KINETICS OF DIFFERENT COBALT(III) TRIPOD  
COMPLEXES**

*A thesis submitted to meet the requirements for the degree of*

**MAGISTER SCIENTIAE**

in the

**Department of Chemistry**

**Faculty of Natural and Agricultural Sciences**

*at the*

**University of the Free State**

by

**Phillip Sechaba Molosioa**

*Promotors*

**Dr. H.G. Visser**

**Prof. W. Purcell**

**March 2006**

# Acknowledgements

---

I would like to express my sincere gratitude to the Almighty for giving me this precious opportunity in life and guiding me throughout the course of the study.

My sincere gratitude also goes to:

Dr. H.G. Visser (my promotor) and Prof. W. Purcell (my co-promotor), for their great ideas and the keen interest they showed towards this project. Their valuable time devoted in helping out in difficult circumstances in the course of this study is highly appreciated.

The NRF and Prof. A. Roodt for financial assistance throughout the duration of this project.

My parents, Stephen and Maria Molosioa, my sister Brenda Molosioa for their valuable encouragements, understanding, generous and tolerance during the time of this study. Words will never be sufficient to express my gratitude in this regard. This work is dedicated to all of you.

Neo Molosioa (my daughter) for being such a wonderful child and you are the greatest gift from God.

A special word of thanks to Thato Mshali and Wade Davis for their willingness to always offer help and for their beneficial comments and contribution to this thesis any way.

Finally, to all the personnel of the Department of Chemistry, for all the friendship and help in all my years of study.

**Sechaba Molosioa**

# Table of contents

---

<b>List of abbreviations</b>	<b>iv</b>
<b>List of figures</b>	<b>v</b>
<b>List of schemes</b>	<b>ix</b>
<b>List of tables</b>	<b>x</b>
<b>Chapter 1 Introduction and aim</b>	<b>1</b>
1.1 Introduction	1
1.2 Aim of this Study	17
<b>Chapter 2 Literature overview</b>	<b>18</b>
2.1 Reaction Kinetics	18
2.2 Octahedral Substitution Reactions	24
<b>Chapter 3 Synthesis and identification of Cobalt(III)-lda and-pda complexes</b>	<b>43</b>
3.1 Introduction	43
3.2 Chemicals and Instrumentation	44
3.3 Synthesis and isolation	45
3.3.1 <i>l</i> -Leucine- <i>N,N</i> -diacetic acid (lda)	45
3.3.2 <i>l</i> -Phenylalanine- <i>N,N</i> -diacetic acid (pda)	46
3.3.3 Complexes of <i>l</i> -leucine- <i>N,N</i> -diacetic acid (lda)	46
3.3.4 <i>In situ</i> synthesis of [Co(lda)(H <sub>2</sub> O) <sub>2</sub> ]	47
3.3.5 Isolation of [Co(lda)(H <sub>2</sub> O)(NCS)] <sup>-</sup>	48
3.3.6 Complexes of <i>l</i> -phenylalanine- <i>N,N</i> -diacetic acid (pda)	48
3.3.7 <i>In situ</i> synthesis of [Co(pda)(H <sub>2</sub> O) <sub>2</sub> ]	49

## Table of contents

3.3.8	Isolation of $[\text{Co}(\text{pda})(\text{H}_2\text{O})(\text{NCS})]^-$	49
3.4	Results and discussion	50
3.4.1	<i>l</i> -Leucine- <i>N,N</i> -diacetic acid (lda)	50
3.4.2	<i>l</i> -Phenylalanine- <i>N,N</i> -diacetic acid (pda)	52
3.4.3	Complexes of <i>l</i> -leucine- <i>N,N</i> -diacetic acid (lda)	54
3.4.4	Complexes of <i>l</i> -phenylalanine- <i>N,N</i> -diacetic acid (pda)	64
3.5	Conclusion	70
<b>Chapter 4 Kinetic study of the reactions of Cobalt(III)-lda and-pda complexes</b>		<b>72</b>
4.1	Introduction	72
4.2	Experimental Procedures	73
4.3	Kinetic Results	74
4.2.1	Influence of $\text{H}^+$ ions on the Co(III)-lda and-pda system	74
4.2.2	Substitution reactions of $[\text{Co}(\text{lda})(\text{H}_2\text{O})_2]$ and $[\text{Co}(\text{pda})(\text{H}_2\text{O})_2]$ with $\text{NCS}^-$ ions	81
4.4	Discussion of kinetics results	94
<b>Chapter 5 Critical evaluation</b>		<b>98</b>
<b>References</b>		<b>100</b>

<b>Table of contents</b>
--------------------------

**Appendix A****Supplementary data** **104**

## Section I

Kinetic data for Chapter 4 104

## Section II

Theoretical aspects of kinetics 112

**Abstract** **120****Opsomming** **123**

## List of abbreviations

---

py	pyridine
CoPP	cobalt-protoporphyrin
bcmpa	bis- <i>N,N</i> -carboxymethyl-phenylalanine
bcmlc	bis- <i>N,N</i> -carboxymethyl-leucine
aa	amino acid
nta	nitrilotriacetic acid
lda	<i>l</i> -leucine- <i>N,N</i> -diacetic acid
pda	<i>l</i> -phenylalanine- <i>N,N</i> -diacetic acid
Im	imidazole
pK <sub>a</sub>	acid dissociative constant
L	ligand
dmap	dimethylaminopyridine
<i>N,N</i> -Et <sub>2</sub> en	<i>N,N</i> -diethylethylenediamine
IR	infrared
<sup>1</sup> H NMR	proton nuclear magnetic resonance
NMR	nuclear magnetic resonance
apda	<i>N</i> -(2-carboxyethyl)iminodiacetic acid
k <sub>obs</sub>	observed rate constant
ΔH <sup>#</sup>	activation enthalpy
ΔS <sup>#</sup>	activation entropy
UV/VIS	ultraviolet/visible spectroscopy
ppm	parts per million
<i>N</i> -Eten	<i>N</i> -ethylethylenediamine
nm	nanometer
M	molar
λ	wavelength
δ	chemical shift
TPPS	<i>meso</i> -tetra( <i>p</i> -sulphonatophenyl)porphyrine

# List of figures:

---

## Chapter 1

<b>Figure 1.1:</b>	Nitrilotriacetic acid (nta).	4
<b>Figure 1.2:</b>	<i>l</i> -Leucine- <i>N,N</i> -diacetic acid (lda).	4
<b>Figure 1.3:</b>	<i>l</i> -Phenylalanine- <i>N,N</i> -diacetic acid (pda).	4
<b>Figure 1.4:</b>	Structure of [(Co(bcmlc)( <i>l</i> -phen)].	6
<b>Figure 1.5:</b>	Structure of [(Co(bcmpa)( <i>l</i> -phen)].	6
<b>Figure 1.6:</b>	Structure of [Cr((S)-lda)(Im) <sub>2</sub> ].	7
<b>Figure 1.7:</b>	Structure of [Cr((S)-pda)(Im) <sub>2</sub> ].	7
<b>Figure 1.8:</b>	Structure of [Co(nta)(μ-OH)] <sub>2</sub> <sup>2-</sup> .	9
<b>Figure 1.9:</b>	UV/VIS spectra of different Co(III)-nta species in solution.	10
<b>Figure 1.10:</b>	Structure of [Co(nta)(enR <sub>1</sub> R <sub>2</sub> )] (enR <sub>1</sub> R <sub>2</sub> = substituted ethylenediamines).	12
<b>Figure 1.11:</b>	Structure of [Co(nta)(CO <sub>3</sub> )] <sup>2-</sup> .	12
<b>Figure 1.12:</b>	<i>N</i> -(2-carboxyethyl)iminodiacetic acid (apda).	14
<b>Figure 1.13:</b>	Structure of the [Co(apda)(H <sub>2</sub> O) <sub>2</sub> ] complex.	14
<b>Figure 1.14:</b>	Octahedral distortion around cobalt(III) centres of anionic units, [Co(Hapda) <sub>2</sub> ], A and B.	15
<b>Figure 1.15:</b>	UV/VIS spectra of different Co(III)-apda species in solution.	16

## Chapter 2

<b>Figure 2.1:</b>	General substitution reactions of octahedral complexes.	24
<b>Figure 2.2:</b>	Base hydrolysis mechanism.	26

### Chapter 3

<b>Figure 3.1:</b>	IR spectrum of lda ligand.	50
<b>Figure 3.2:</b>	The structure of <i>l</i> -leucine- <i>N,N</i> -diacetic acid (lda).	51
<b>Figure 3.3:</b>	<sup>1</sup> H NMR spectrum of lda.	52
<b>Figure 3.4:</b>	IR spectrum of pda ligand.	53
<b>Figure 3.5:</b>	The structure of <i>l</i> -phenylalanine- <i>N,N</i> -diacetic acid (pda).	53
<b>Figure 3.6:</b>	<sup>1</sup> H NMR spectrum for pda.	54
<b>Figure 3.7:</b>	IR spectrum of [Co(lda)(μ-OH)] <sub>2</sub> <sup>2-</sup> .	55
<b>Figure 3.8:</b>	<sup>1</sup> H NMR spectrum for [Co(lda)(μ-OH)] <sub>2</sub> <sup>2-</sup> .	56
<b>Figure 3.9:</b>	Glycinato rings in Co(III)-nta complexes.	57
<b>Figure 3.10:</b>	Glycinato and 4-methyl pentionato rings in Co(III)-lda complexes.	57
<b>Figure 3.11:</b>	UV/VIS spectra of different Co(III)-lda species in solution.	59
<b>Figure 3.12:</b>	UV/VIS spectra of different Co(III)-lda species in solution.	60
<b>Figure 3.13:</b>	IR spectrum of [Co(lda)(H <sub>2</sub> O)(NCS)] <sup>-</sup> .	62
<b>Figure 3.14:</b>	UV/VIS spectral changes for the reaction between [Co(lda)(H <sub>2</sub> O) <sub>2</sub> ] with NCS <sup>-</sup> ions.	63
<b>Figure 3.15:</b>	IR spectrum of [Co(pda)(μ-OH)] <sub>2</sub> <sup>2-</sup> .	64
<b>Figure 3.16:</b>	<sup>1</sup> H NMR spectrum for [Co(pda)(μ-OH)] <sub>2</sub> <sup>2-</sup> .	65
<b>Figure 3.17:</b>	Glycinato and 3-phenylpropionato rings in Co(III)-pda complexes.	66
<b>Figure 3.18:</b>	UV/VIS spectra of different Co(III)-pda species in solution.	67
<b>Figure 3.19:</b>	UV/VIS spectra of different Co(III)-pda species in solution.	68
<b>Figure 3.20:</b>	IR spectrum of [Co(pda)(H <sub>2</sub> O)(NCS)] <sup>-</sup> .	69
<b>Figure 3.21:</b>	UV/VIS spectral changes for the reaction between [Co(pda)(H <sub>2</sub> O) <sub>2</sub> ] with NCS <sup>-</sup> ions.	70

### Chapter 4

<b>Figure 4.1:</b>	Plot of Abs (λ = 400 nm ) vs. pH for [Co(lda)(H <sub>2</sub> O) <sub>2</sub> ] (2 × 10 <sup>-3</sup> M), 25.1 °C, μ = 1.0 M (NaClO <sub>4</sub> ).	75
--------------------	--	----

<b>List of figures</b>
------------------------

- Figure 4.2:** Plot of Abs ( $\lambda = 400$  nm) vs. pH for [Co(pda)(H<sub>2</sub>O)<sub>2</sub>] ( $2 \times 10^{-3}$  M), 25.2 °C,  $\mu = 1.0$  M (NaClO<sub>4</sub>). 76
- Figure 4.3:** Plot of  $k_{\text{obs}}$  vs. [H<sup>+</sup>] at different temperatures,  $\mu = 1.0$  M (NaClO<sub>4</sub>),  $\lambda = 355$  nm, [Co(lda)(H<sub>2</sub>O)<sub>2</sub>] =  $1 \times 10^{-2}$  M. 78
- Figure 4.4:** Plot of  $k_{\text{obs}}$  vs. [H<sup>+</sup>] at different temperatures,  $\mu = 1.0$  M (NaClO<sub>4</sub>),  $\lambda = 355$  nm, [Co(pda)(H<sub>2</sub>O)<sub>2</sub>] =  $1 \times 10^{-2}$  M. 79
- Figure 4.5:** UV/VIS spectral changes for the reaction between [Co(lda)(H<sub>2</sub>O)<sub>2</sub>] ( $7.9 \times 10^{-3}$  M) with NCS<sup>-</sup> ions. T = 25.3 °C, [NCS<sup>-</sup>] =  $1.7 \times 10^{-2}$  M 82
- Figure 4.6:** UV/VIS spectral changes for the reaction between [Co(pda)(H<sub>2</sub>O)<sub>2</sub>] ( $7.2 \times 10^{-3}$  M) with NCS<sup>-</sup> ions. T = 25.3 °C, [NCS<sup>-</sup>] =  $1.5 \times 10^{-2}$  M. 82
- Figure 4.7:** Plot of Abs ( $\lambda = 400$  nm) vs. [NCS<sup>-</sup>] for [Co(lda)(H<sub>2</sub>O)<sub>2</sub>] ( $1 \times 10^{-3}$  M), 25.1 °C, pH = 2.0 and  $\mu = 1.0$  M (NaClO<sub>4</sub>). 84
- Figure 4.8:** Plot of Abs ( $\lambda = 400$  nm) vs. [NCS<sup>-</sup>] for [Co(pda)(H<sub>2</sub>O)<sub>2</sub>] ( $1 \times 10^{-3}$  M), 25.3 °C, pH = 2.0 and  $\mu = 1.0$  M (NaClO<sub>4</sub>). 84
- Figure 4.9:** Plot of  $k_{\text{obs}}$  vs. [NCS<sup>-</sup>] for the first reaction ( $k_1$  step) at different temperatures,  $\mu = 1.0$  M (NaClO<sub>4</sub>),  $\lambda = 400$  nm, [Co(lda)(H<sub>2</sub>O)<sub>2</sub>] =  $1 \times 10^{-3}$  M. 87
- Figure 4.10:** Plot of  $k_{\text{obs}}$  vs. [NCS<sup>-</sup>] for the first reaction ( $k_1$  step) at different temperatures,  $\mu = 1.0$  M (NaClO<sub>4</sub>),  $\lambda = 400$  nm, [Co(pda)(H<sub>2</sub>O)<sub>2</sub>] =  $1 \times 10^{-3}$  M. 88
- Figure 4.11:** Plot of  $k_{\text{obs}}$  vs. [NCS<sup>-</sup>] for the second reaction ( $k_3$  step) at different temperatures,  $\mu = 1.0$  M (NaClO<sub>4</sub>),  $\lambda = 400$  nm, [Co(lda)(H<sub>2</sub>O)<sub>2</sub>] =  $1 \times 10^{-3}$  M. 88
- Figure 4.12:** Plot of  $k_{\text{obs}}$  vs. [NCS<sup>-</sup>] for the second reaction ( $k_3$  step) at different temperatures,  $\mu = 1.0$  M (NaClO<sub>4</sub>),  $\lambda = 400$  nm, [Co(pda)(H<sub>2</sub>O)<sub>2</sub>] =  $1 \times 10^{-3}$  M. 89
- Figure 4.13:** Plot of  $k_{\text{obs}}$  vs. pH at 25.0 °C for the first reaction between [Co(lda)(H<sub>2</sub>O)<sub>2</sub>] and NCS<sup>-</sup> ions.  $\mu = 1.0$  M (NaClO<sub>4</sub>),  $\lambda = 400$  nm, [NCS<sup>-</sup>] =  $1.25 \times 10^{-2}$  M. 90

<b>List of figures</b>
------------------------

**Figure 4.14:** Plot of  $k_{\text{obs}}$  vs. pH at 25.0 °C for the first reaction between [Co(pda)(H<sub>2</sub>O<sub>2</sub>)] and NCS<sup>-</sup> ions.  $\mu = 1.0$  M (NaClO<sub>4</sub>),  $\lambda = 400$  nm, [NCS<sup>-</sup>] =  $1.25 \times 10^{-2}$  M. 90

**Figure 4.15:** Plot of  $k_{\text{obs}}$  vs. [NCS<sup>-</sup>] for the first reaction at pH = 7.00, 25.0 °C,  $\mu = 1.0$  M (NaClO<sub>4</sub>),  $\lambda = 400$  nm, [Co(lda)(H<sub>2</sub>O<sub>2</sub>)] =  $2 \times 10^{-4}$  M. 91

**Figure 4.16:** Plot of  $k_{\text{obs}}$  vs. [NCS<sup>-</sup>] for the first reaction at pH = 7.00, 25.0 °C,  $\mu = 1.0$  M (NaClO<sub>4</sub>),  $\lambda = 400$  nm, [Co(pda)(H<sub>2</sub>O<sub>2</sub>)] =  $2 \times 10^{-4}$  M. 91

## List of schemes:

---

### Chapter 1

- Scheme 1.1:** Reactions of  $[\text{Co}(\text{nta})(\text{H}_2\text{O})_2]/[\text{Co}(\text{nta})(\text{H}_2\text{O})(\text{OH})]^-$  with  $\text{NCS}^-$  ions. 11
- Scheme 1.2:** Mechanism for the reaction between  $[\text{Co}(\text{nta})(\mu\text{-OH})]_2^{2-}$  and L (L = dmap, py). 11

### Chapter 3

- Scheme 3.1:** Synthesis and reactions of  $[\text{Co}(\text{L})(\mu\text{-OH})]_2^{2-}$  (L = lda, pda). 43
- Scheme 3.2:** Acidic cleavage of  $[\text{Co}(\text{nta})(\mu\text{-OH})]_2^{2-}$ . 61

### Chapter 4

- Scheme 4.1:** Formation and reactions of  $[\text{Co}(\text{L})(\text{H}_2\text{O})_2]$  (L = lda, pda). 73
- Scheme 4.2:** pH dependence of  $[\text{Co}(\text{L})(\text{H}_2\text{O})_2]$  (L = lda, pda). 74
- Scheme 4.3:** Reaction of  $[\text{Co}(\text{L})(\text{H}_2\text{O})_2]$  (L = lda, pda) with  $\text{H}^+$  ions. 76
- Scheme 4.4:** Proposed mechanism for the reaction of  $[\text{Co}(\text{L})(\text{H}_2\text{O})_2]$  (L = lda, pda) with  $\text{H}^+$  ions. 79
- Scheme 4.5:** Reactions of  $[\text{Co}(\text{L})(\text{H}_2\text{O})_2]/[\text{Co}(\text{L})(\text{H}_2\text{O})(\text{OH})]^-$  (L = lda, pda) with  $\text{NCS}^-$  ions. 83

# List of tables:

---

## Chapter 1

- Table 1.1:** Different bond lengths and angles in metal-lda and-pda complexes. 8
- Table 1.2:** Different bond lengths and angles in cobalt(III)-nta complexes. 13

## Chapter 2

- Table 2.1:** Rate constants for the acid hydrolysis reaction of  $[\text{Co}(\text{NH}_3)_5\text{X}]^{2+}$  with different ions at 25.0 °C. 33
- Table 2.2:** Rate constants for the acid hydrolysis reactions of  $[\text{Co}(\text{NH}_3)_5(\text{H}_2\text{O})]^{3+}$  with different ions at 45.0 °C. 34
- Table 2.3:** Rate constants for the acid hydrolysis reactions of  $[\text{Co}(\text{N-N})_2\text{Cl}_2]^+$  with different diamine chains at 25.0 °C. 36
- Table 2.4:** Rate constants for the acid hydrolysis reactions of  $[\text{Co}(\text{N}_4)\text{LCI}]^{n+}$  at 25.0 °C. 38

## Chapter 3

- Table 3.1:** Summary of  $^1\text{H}$  NMR data for four distinguishable doublets of Co(III)-lda and-pda complexes. 71

## Chapter 4

- Table 4.1:** Observed rate constants for the reaction between  $[\text{Co}(\text{L})(\text{H}_2\text{O})_2]$  (L = lda, pda) and different acids and anions. 77
- Table 4.2:** Rate constants and activation parameters for the reaction between  $[\text{Co}(\text{L})(\text{H}_2\text{O}_2)]$  (L = lda, pda) and  $\text{H}^+$  ions. 81

<b>List of tables</b>
-----------------------

**Table 4.3:** Rate constants and activation parameters for the reaction between [Co(L)(H<sub>2</sub>O<sub>2</sub>)] (L = lda, pda) and NCS<sup>-</sup> ions. 93

# 1

## Introduction and aim

---

The first part of this chapter deals mainly with the history and the significance of cobalt and cobalt(III) complexes while the different aims of this study are discussed in the second part of the chapter.

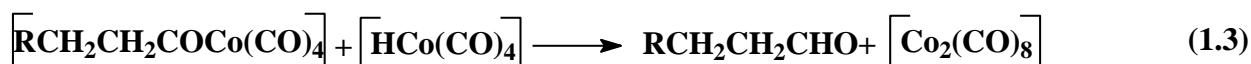
---

### 1.1 INTRODUCTION

#### *Cobalt Chemistry – where it started*

The use of cobalt dates as far back as 2000 BC when the Egyptians used it as a colouring agent for glass making. The common use of cobalt compounds in colouring glass led to their import into China under the name of Mohammedian blue. Cobalt amine complexes containing pyridine ligands such as  $[\text{CoCl}(\text{dien})(\text{py})_2](\text{NO}_3)(\text{ClO}_4)$  and  $[\text{CoCl}(2,3\text{-tri})(\text{py})_2]\text{ZnCl}_4$ , were discovered in the early twentieth century by Werner (House *et al.*, 1999:181) and are regarded to form the basis for the formulation of the coordination theory in inorganic chemistry.

The uses of cobalt compounds in industry are very widespread and are used for example as catalysts (Tannenbaum & Bor, 2004:33) in hydroformylation of olefins (see **Eq. 1.1 - 1.3**),



as well as pigments and electroplaters. It is also used in ceramics, as dryers for paints and varnishes, animal and human nutrients, high temperature alloys, high-speed tools, magnetic alloys,

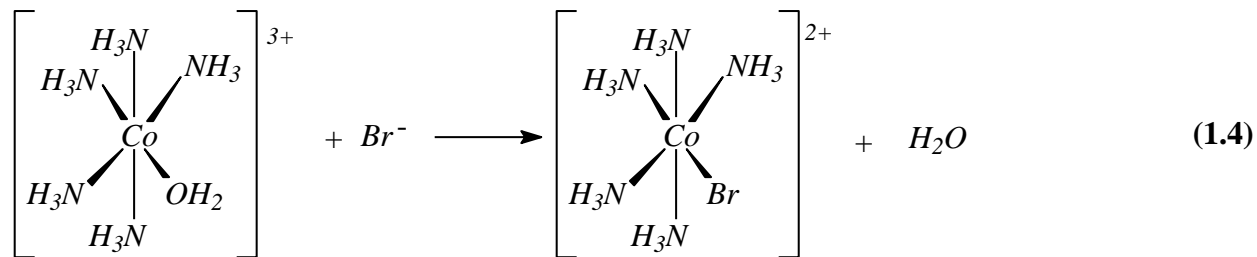
alloys used for prosthetics and also in radiology (Planinsek & Newkirk, 1979:481 and Morral, 1979:495).

The largest use of cobalt is in its metallic form as magnetic alloys, cutting and wear-resisting alloys and superalloys. Cobalt-molybdenum alloys are used for the desulfurization of high-sulfur bituminous coal and cobalt-iron alloys in the hydrocracking of crude oil shale and in coal liquefaction. The second largest use of cobalt is in the form of salt as electroplaters and it is also highly effective as driers for lacquer, enamels and varnishes. Another interesting use of cobalt oxide is the colouring of glass as was earlier indicated. Colours such as pink or blue can be obtained depending upon how the  $\text{CoO}_x$  molecules are arranged/bonded within the glass (Planinsek & Newkirk, 1979:481 and Morral, 1979:495).

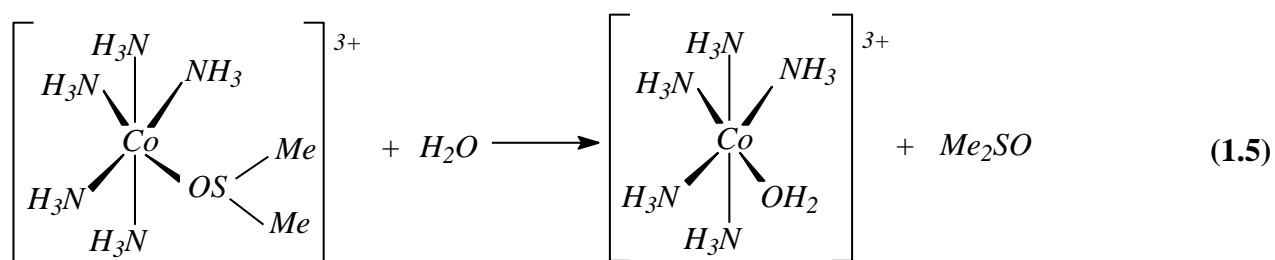
Cobalt(III) complexes of 1-(2-carboxyphenyl)azo-2-naphthol are most commonly used in dyestuff for polyamide fibers and leather due to the kinetic inertness and the stability of these complexes towards acid. The importance of such metal complexes stems principally from their very high degree of light fastness, which can be attributed to the protection of the azo group, which normally is associated with dyes (Lučka & Holeček, 2003:115).

The substitution reactions of octahedral complexes of cobalt(III) have been under investigation for many years (Morral, 1967:70). The reasons for this are that a great variety of these complexes can easily be prepared and the substitution reactions of these complexes are slow enough to be followed by conventional means (Purcell & Kotz, 1980:412). Hence it is not surprising that one finds a large number of publications and review articles on the substitution reactions of these metal complexes (Hay, 1984:1). Two well-known reactions, namely the anation of  $[\text{Co}(\text{NH}_3)_5(\text{OH}_2)]^{3+}$  and the hydrolysis of  $[\text{Co}(\text{NH}_3)_5\text{Me}_2\text{SO}]^{3+}$  is given by Purcell and Kotz (1980:412) in **Eq. 1.4** and **1.5**.

*Anation:*



*Hydrolysis:*



***The significance of cobalt(III) complexes containing tripod type ligands***

Complexes of cobalt(III) with ligands that simulate binding sites on protein chains have many applications and are of significant scientific value. According to Smith *et al.* (1993:7365) the cobalt-protoporphyrin (CoPP)-hemopexin may have an important role to play in cell growth and division. By effectively competing for the hemopexin receptor with heme-hemopexin, which supports and stimulates proliferation of human acute T-lymphoblastic cells, it will diminish its growth stimulatory effect. Cobalt(III) complexes containing tripod type ligand, such as bis-*N,N*-carboxymethyl-phenylalanine (bcmpa) is also of large scientific interest. This complex allows for the coordination of a bidentate amino acid (aa) through weak non-covalent interaction. This interaction is mainly between the coordination positions of bcmpa and aa ligands (not a metal–ligand interaction) which are important as molecular recognition models for the enzyme (bcmpa)-substrate (aa) complex formation (Jitsukawa *et al.*, 1994:249).

A large number of different tripod type ligands are known and their coordination to Co(III) and their subsequent reactions yielded interesting results. Nitrilotriacetic acid (nta) (**Figure 1.1**) is one of these tripod type ligands, which act as a tetradentate ligand in most metal chelation compounds, binding with nitrogen and three carboxylate oxygens to the metal ion. *l*-Leucine-*N,N*-diacetic acid (lda) (**Figure 1.2**) and *l*-phenylalanine-*N,N*-diacetic acid (pda) (**Figure 1.3**) are also examples of tripod ligands which have the possibility to react with cobalt(III) ions. Lda differs from nta by having a longer 4-methyl pentionate chain  $(\text{CH}_3)_2\text{CHCH}_2\text{CH}_2\text{C}(\text{O})\text{OH}$ , while pda differs by having a longer a 3-phenylpropionate chain  $(\text{C}_6\text{H}_5)\text{CH}_2\text{CH}_2\text{C}(\text{O})\text{OH}$  in place of the acetate groups.

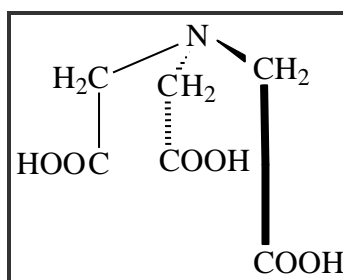


**Figure 1.1:** Nitrilotriacetic acid (nta).

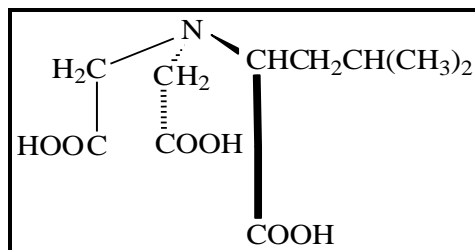


**Figure 1.2:** *l*-Leucine-*N,N*-diacetic acid (lda).

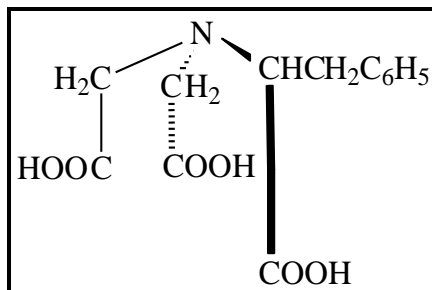
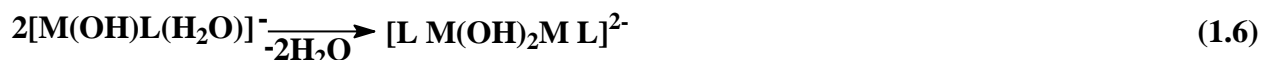


**Figure 1.3:** *l*-Phenylalanine-*N,N*-diacetic acid (pda).

Uehara *et al.* (1971:1548) emphasized that although these ligands all contain a similar structural framework, their coordinating behaviour can differ from each other due to the slight differences in their physical arrangement. It was pointed out that the ligands forming three, five-member chelate rings such as nta and lda, could act as a tridentate ligands of O<sub>3</sub> or N-O<sub>2</sub>-type as well as tetradentate ligands of N-O<sub>3</sub> type toward metals (Uehara *et al.* 1971:1548). If one hydrogen atom in a methylene group in nta is replaced by a substrate such as a benzyl group (pda), it is expected that the coordinated behaviours should differ considerably from nta and lda due to the larger steric demand of such a ligand.

It was postulated by Uehara *et al.* (1971:1548) that both nta and lda in their respective complexes act mainly as tetradentate ligands (N-O<sub>3</sub>) in solid state and as a tridentate ligands (O<sub>3</sub>) in aqueous solution. The possible explanation for such behaviour was not presented by the authors. Although pda also has three five-member chelate rings and can also act as a tetradentate toward the metal centre, its coordinating manner does not change as extensively as that in nta and lda. This was due to the stronger steric hindrance by a larger radical (benzyl radical) in pda.

Uehara and his co-workers (1971:1548) further noted that when nta, lda and pda ligands act as tetradentate ligands toward metal ions, the remaining *cis* coordination sites of their respective complexes can be occupied by H<sub>2</sub>O and/or OH<sup>-</sup> in an aqueous medium. They also postulated that under certain experimental conditions the aqua ligands can be converted to hydroxo ligands with the subsequent formation of diol complexes as indicated in **Eq. 1.6**.



Co(III) complexes containing tripod ligand, such as bis-*N,N*-carboxymethyl-leucine (bcmle) and bis-*N,N*-carboxymethyl-phenylalanine (bcmpa) were synthesised by Kumita *et al.* (1998:160) in which both bcmle and bcmpa act as tetradentate ligands. They characterised the Co(III)-lda and-pda complexes, [Co(III)(bcmle)(aa)] (**Figure 1.4**) and [Co(III)(bcmpa)(aa)] (**Figure 1.5**), on the basis of X-ray crystallography. The coordination structures around the metal ion in the Co(III) complexes studied by them were presumed to be the same, all octahedrally coordinated with NO<sub>3</sub>-type ligand and amino acid.

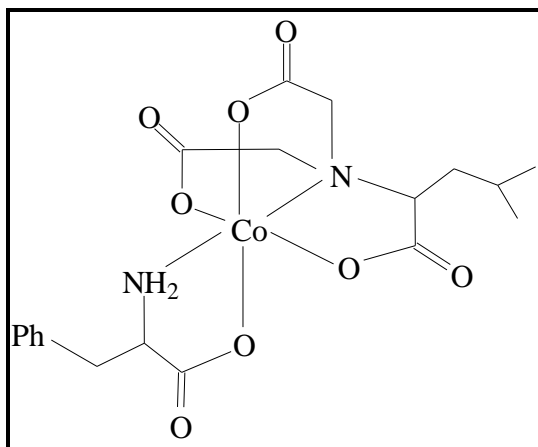


**Figure 1.4:** Structure of  $[(\text{Co}(\text{bcmlle})(l\text{-phen}))]$

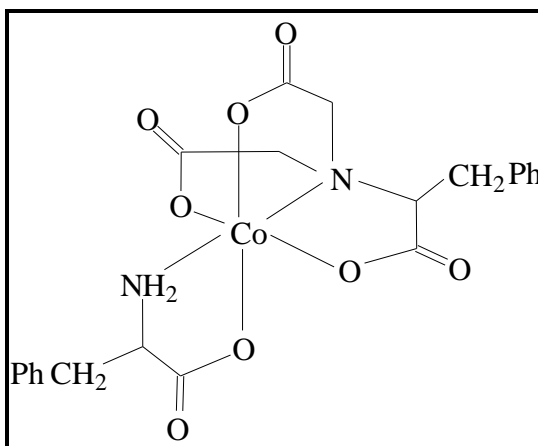


**Figure 1.5:** Structure of  $[(\text{Co}(\text{bcmpa})(l\text{-phen}))]$

Bocarsly *et al.* (1990:4898) prepared several chromium-nta derivatives. The crystal structures of  $[\text{Cr}((S)\text{-lda})(\text{Im})_2]$  (**Figure 1.6**) and  $[\text{Cr}((S)\text{-pda})(\text{Im})_2]$  (**Figure 1.7**) were determined and are the only data in the literature where *cis* positions of Cr(III) complexes with a nta derivative are occupied by monodentate ligands. The side chains on both complexes are located on a ring in the equatorial coordination plane. It was concluded from these studies that both lda and pda act as tetradentate ligands.

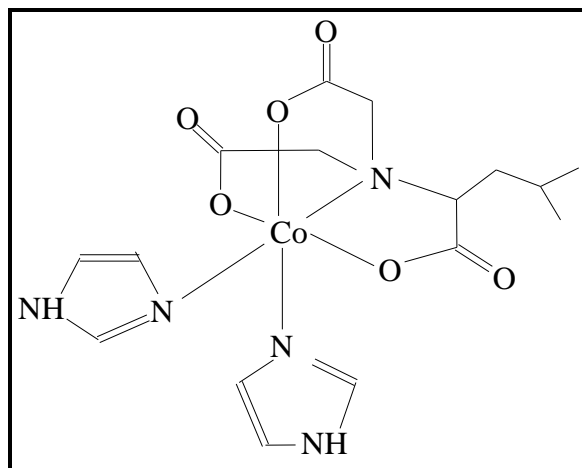


**Figure 1.6:** Structure of  $[\text{Cr}((S)\text{-lda})(\text{Im})_2]$

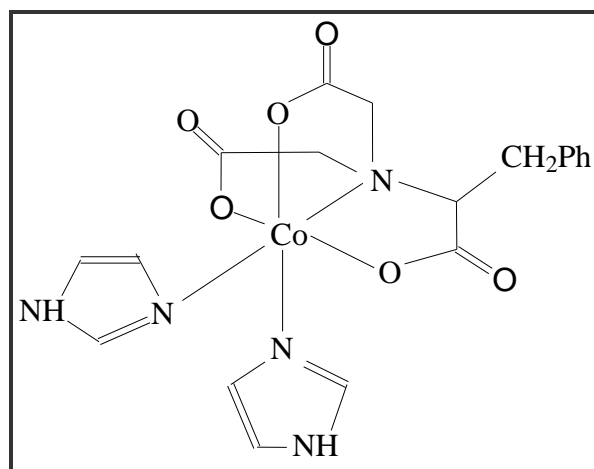


**Figure 1.7:** Structure of  $[\text{Cr}((S)\text{-pda})(\text{Im})_2]$

Some of the structural data for the different metal-lda and-pda complexes are shown in **Table 1.1**. The most obvious results are that the bidentate amino acid, *l*-phen, formed *trans*-N bonds in both cases reported. There are not enough reported structures in order to be able to discuss other structural tendencies.

**Table 1.1:** Different bond lengths and angles in metal-lda and-pda complexes.

Complexes	M-N (Å)	O-M-O (°)	O-M-N (°)	lda and pda Coordination mode	Reference
K[(Co(bcmlc)( <i>l</i> -phen)]	1.907(4)	171.9(1)	89.3(1)	Tetradentate	Kumita <i>et al.</i> (1998:160)
K[(Co(bcmlc)( <i>l</i> -phen)]	1.90(1)	171.6(5)	89.0(3)	Tetradentate	Jitsukawa <i>et al.</i> (1994:249)
[Cr((S)-lda)(Im) <sub>2</sub> ]	2.070(3)	164.4(5)	83.5(1)	Tetradentate	Bocarsly <i>et al.</i> (1990:4898)
[Cr((S)-pda)(Im) <sub>2</sub> ]	2.086(14)	164.9(1)	83.2(5)	Tetradentate	Bocarsly <i>et al.</i> (1990:4898)

- M-N bond refers to the bonding between M and N of lda and pda, O-M-O refers to angle between *trans*-O atoms of the lda and pda moiety, O-M-N refers to the angle between the atoms in the same plane as the other chelating ligand e.g. Imidazole/amino acid etc.

The tabulated bond lengths and angles found for the Co(III)-lda and-pda complexes in which lda and pda act as a tetradentate ligand compare very well to the values found for the Co(III)-nta complexes with nta acting as a tetradentate ligand (see **Table 1.2**, p. 13).

Co(III)-nta complexes were intensely studied in the last couple of years. A number of different aspects led to the revisitation of these systems. Uncertainty with regards to the accurate identification of these complexes was one of the main concerns. Questions such as bonding mode of the nta as well as the structures of different isomers in solution were unanswered.

Mori and co-workers (1958:940) were the first to prepare and identify different cobalt(III)-nta complexes. According to their study two monomeric hydroxo-aqua cobalt(III)-nta isomers,  $\alpha$ -[Co(nta)(H<sub>2</sub>O)(OH)]<sup>-</sup> and  $\beta$ -[Co(nta)(H<sub>2</sub>O)(OH)]<sup>-</sup> complexes, as well as a dimeric  $\mu$ -hydroxo bridged species [Co(nta)( $\mu$ -OH)]<sub>2</sub><sup>2-</sup> could be isolated. Close inspection of Mori's work revealed that their conclusion was made from chemical analyses of these different Co-nta complexes which all proved to be almost identical, thereby raising more questions about the existence of these different complexes.

A new study was undertaken by Visser *et al.* (1997:2851) to try and clarify the uncertainty with regards to the identity of the Co(III)-nta complexes. The significant result obtained by this research group was the isolation and the structure determination of  $\text{Cs}_2[\text{Co}(\text{nta})(\mu\text{-OH})]_2 \cdot 4\text{H}_2\text{O}$  (**Figure 1.8**).

Results obtained from this structural determination clearly indicate that the two Co metals are bonded to two-hydroxo ligands which also act as bridging ligands between the two Co centers. This structure determination also clearly indicated the tetradentate nature of the nta ligand which binds *via* the nitrogen and three oxygen atoms to the Co centers.

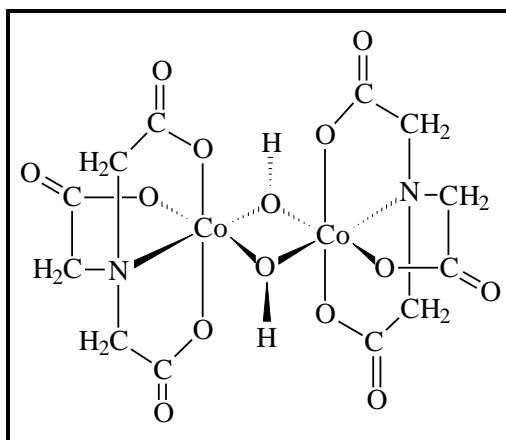


**Figure 1.8:** Structure of  $[\text{Co}(\text{nta})(\mu\text{-OH})]_2^{2-}$ .

Visser *et al.* (1997:2851) also performed a UV/VIS study (**Figure 1.9**) on the isolated complex to determine the effect of pH on the Co(III)-nta complex in solution and try to identify other Co(III)-nta species with this technique.  $\text{Cs}_2[\text{Co}(\text{nta})(\mu\text{-OH})]_2 \cdot 4\text{H}_2\text{O}$  crystals were dissolved in water (pH *ca* 6) and the UV/VIS spectrum was recorded. From their study it appears that the hydroxo bridges in the  $[\text{Co}(\text{nta})(\mu\text{-OH})]_2^{2-}$  were broken in the first protonation step during the addition of acid (pH 1) to form the diaqua complex,  $[\text{Co}(\text{nta})(\text{H}_2\text{O})_2]$ . It was also found that an aqua-hydroxo complex,  $[\text{Co}(\text{nta})(\text{H}_2\text{O})(\text{OH})]^-$ , is formed during the addition of base to  $[\text{Co}(\text{nta})(\text{H}_2\text{O})_2]$  (pH 5-7). These results were summarised by the following reaction:

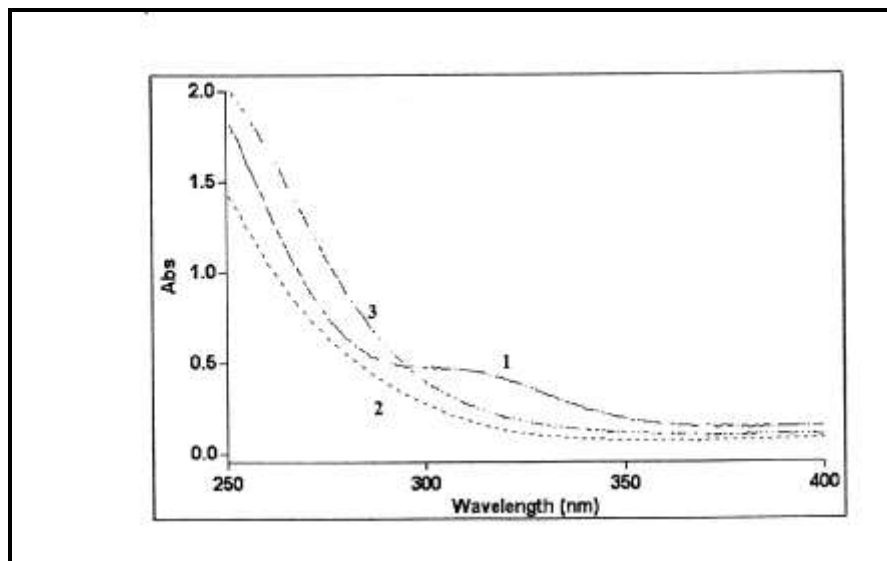
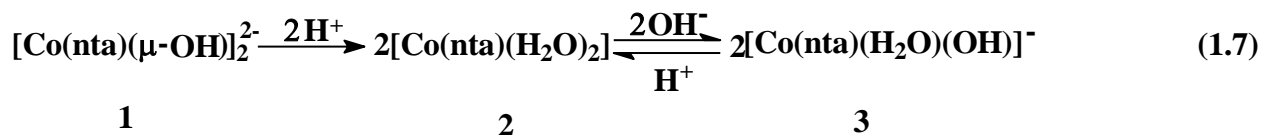


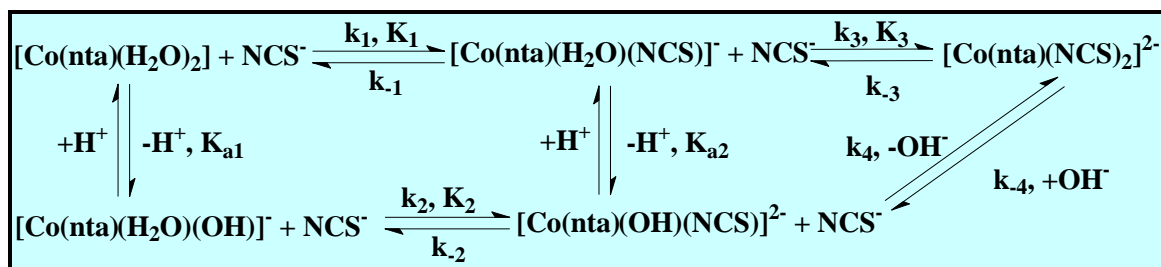
**Figure 1.9:** UV/VIS spectra of different Co(III)-nta species in solution.

1  $[\text{Co}(\text{nta})(\mu\text{-OH})_2]^{2-}$ , pH 5-7 ; 2  $[\text{Co}(\text{nta})(\text{H}_2\text{O})_2]$ , pH ~1;  
 3  $[\text{Co}(\text{nta})(\text{H}_2\text{O})(\text{OH})]^-$ , pH 5-7 (Visser *et al.*, 1997:2851).

The acid dissociation constant of  $[\text{Co}(\text{nta})(\text{H}_2\text{O})_2]$ ,  $K_{a1}$  (**Eq. 1.8**), for these observed changes in UV/VIS spectra was spectrophotometrically determined as 6.52(2) at pH = 2.

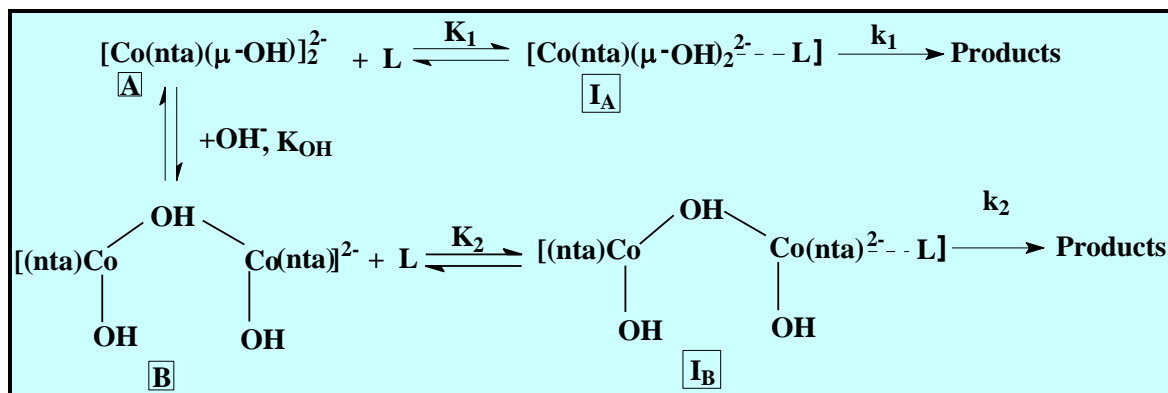


In a continuous study Visser *et al.* (2002:461) investigated the substitution reactions of  $[\text{Co}(\text{nta})(\text{H}_2\text{O})_2]/[\text{Co}(\text{nta})(\text{H}_2\text{O})(\text{OH})]^-$  with  $\text{NCS}^-$  ions at pH values between 2 and 7. The following mechanism (**Scheme 1.1**) was constructed from the experimental results they obtained.



**Scheme 1.1:** Reactions of  $[\text{Co}(\text{nta})(\text{H}_2\text{O})_2]/[\text{Co}(\text{nta})(\text{H}_2\text{O})(\text{OH})]^-$  with  $\text{NCS}^-$  ions.

Visser *et al.* (2003:235) also investigated the substitution reactions of  $[\text{Co}(\text{nta})(\mu\text{-OH})]_2^{2-}$  with different ligands such as dimethylaminopyridine (dmap) and pyridine (py) at pH 9.0–11.5. The following mechanism (**Scheme 1.2**) was constructed from the experimental results they obtained.



**Scheme 1.2:** Mechanism for the reaction between  $[\text{Co}(\text{nta})(\mu\text{-OH})]_2^{2-}$  and L (L = dmap, py).

Another cobalt(III)-nta complex,  $[\text{Co}(\text{nta})(N,N\text{-Et}_2\text{en})]$ , was synthesised by Visser and co-workers (2001:175). They characterised this complex on the basis of IR spectra,  $^1\text{H}$  NMR spectra and three-dimensional X-ray diffraction data. The results showed that the cobalt centre has a distorted octahedral geometry and is surrounded by three oxygen atoms and the nitrogen atom of the nta ligand and the two nitrogen atoms of the ethylenediamine molecule. The substituted nitrogen of *N,N*-diethylethylenediamine is bonded *trans* to the nta nitrogen (**Figure 1.10**).

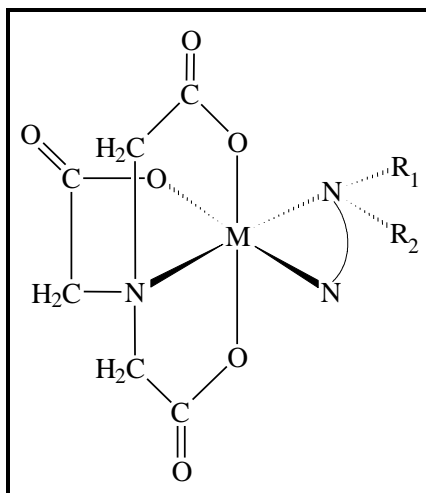


**Figure 1.10:** Structure of  $[\text{Co}(\text{nta})(\text{enR}_1\text{R}_2)]^{2-}$  ( $\text{enR}_1\text{R}_2$  = substituted ethylenediamines).

Visser and co-workers (2001:185) also characterised  $[\text{Co}(\text{nta})(\text{CO}_3)]^{2-}$  (**Figure 1.11**), on the basis of UV/VIS, IR spectra,  $^1\text{H}$  NMR spectrometry and X-ray crystallography. The cobalt centre has a distorted octahedral geometry and is surrounded by three oxygen atoms and the nitrogen atom of the nta ligand and the two oxygen atoms of the carbonato ligand. The fact that  $[\text{Co}(\text{nta})(\text{H}_2\text{O})_2]$  can be obtained by acidifying  $[\text{Co}(\text{nta})(\text{CO}_3)]^{2-}$  (Dasgupta & Harris, 1974:1275), provides an alternative route for the synthesis of different Co(III)-nta species.

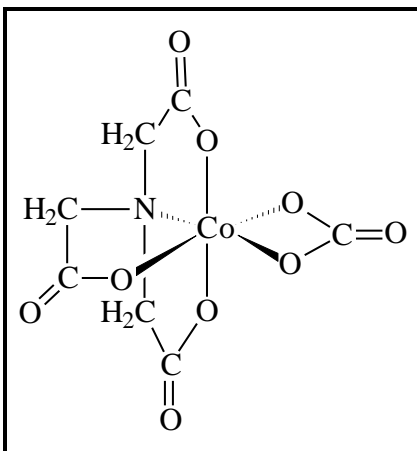


**Figure 1.11:** Structure of  $[\text{Co}(\text{nta})(\text{CO}_3)]^{2-}$ .

The  $\text{Co-N}_{\text{nta}}$  bond lengths,  $\text{O-Co-O}$  and  $\text{O-Co-N}$  angles of different cobalt(III)-nta complexes, with nta acting as a tetradentate ligand, are shown in **Table 1.2**.

The results in **Table 1.2** show that the Co-N<sub>nta</sub> bond distances vary between 1.962(3) and 1.920(2) Å for all the tabulated complexes. The O-Co-O angles vary between 170.5(3) and 173.62(9) ° while the O-Co-N angles vary between 86.3(3) and 89.3(3) ° for all the tabulated complexes.

All the tabulated bond lengths and angles are considered normal and agree well with those found in previous studies on [Ca(nta)]2H<sub>2</sub>O and Hnta (Hnta = monoprotonated form of nitrilotriacetic acid) (Whitlow S., 1972:1914 and Skrzypczak-Jankun *et al.*, 1994:1097).

Other cobalt(III)-nta complexes, K<sub>2</sub>[Co(nta)(ox)]xH<sub>2</sub>O, Ba[Co(nta)(*l*-leu)]<sub>2</sub>xH<sub>2</sub>O, Cs[Co(nta)(*l*-val)]xH<sub>2</sub>O, [Co(nta)(dmap)<sub>2</sub>]6H<sub>2</sub>O and (NEt<sub>4</sub>)<sub>2</sub>[Co(nta)(NCS)<sub>2</sub>]xH<sub>2</sub>O (reason for x is that the number of water molecules per mole were not determined), was synthesised and characterised by Visser and co-workers (2001:175) using different analytical techniques.

**Table 1.2:** Different bond lengths and angles in cobalt(III)-nta complexes.

Complex	Co-N (Å)	O-Co-O (°)	O-Co-N (°)	Reference
K[Co(H <sub>2</sub> Vi)(nta)]2H <sub>2</sub> O	1.942(7)	172.8(3)	86.3(3)	Almazan <i>et al.</i> (1990:2565)
[Co(nta)(pd)]H <sub>2</sub> O	1.962(3)	170.5(1)	86.8(1)	Swaminathan & Sinha (1989:566)
[Co(nta)(en)]H <sub>2</sub> O	1.946(3)	172.6(1)	87.6(1)	Gladkikh <i>et al.</i> (1992:1231)
Ba[Co(nta)(gly)]ClO <sub>4</sub> 3H <sub>2</sub> O	1.928(8)	172.5(3)	89.3(3)	Gladkikh <i>et al.</i> (1992:908)
Cs <sub>2</sub> [Co(nta)(μ-OH)] <sub>2</sub> 4H <sub>2</sub> O	1.922(6)	172.0(2)	88.1(2)	Visser <i>et al.</i> (1997:2851)
[Co(nta)(N,N-Et <sub>2</sub> en)]	1.953(4)	170.6(2)	87.9(2)	Visser <i>et al.</i> (2001:175)
Cs <sub>2</sub> [Co(nta)(CO <sub>3</sub> )]	1.920(2)	173.62(9)	88.52(9)	Visser <i>et al.</i> (2001:185)

- Co-N bond refers to the bonding between Co and N of nta, O-Co-O refers to angle between *trans*-O atoms of the nta moiety, O-Co-N refers to the angle between the atoms in the same plane as the other chelating ligand e.g. en/pd etc.

N-(2-carboxyethyl)iminodiacetic acid (apda) (**Figure 1.12**) is another tripod type ligand which can act as either a tridentate or tetradentate ligand. Apda differs from nta by having a longer propionate chain in place of one of the acetate groups.

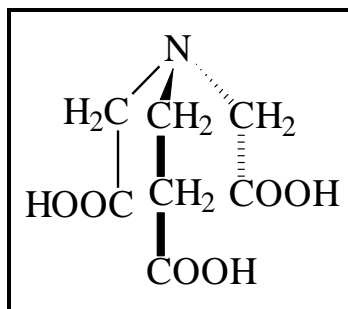


**Figure 1.12:** N-(2-carboxyethyl)iminodiacetic acid (apda).

Cobalt(III)–N-(2-carboxyethyl)iminodiacetic acetato (Co(III)–apda) complexes were first prepared by Tsuchiya and co-workers (1969:1886). According to their study a Co(III)-apda species with a tridentately coordinated apda could be isolated. The complex was formulated as  $[\text{Co}(\text{OH})(\text{apda})(\text{H}_2\text{O})_2]$  on the basis of chemical analysis and IR spectra. Tsuchiya and co-workers had difficulty explaining some characteristics of the apda-coordinating mode of this Co(III) complex.

The Co(III)-apda complex synthesised by Tsuchiya *et al.* (1969:1886) was also prepared by Gladkikh and co-workers (1997:1346). They performed X-ray crystal structure determination studies on the cobalt(III)- and chromium(III)-apda complexes and an iron(III) analogue. These complexes were found to be iso-structural. The structure for the Co(III)-apda complex was determined as  $[\text{Co}(\text{apda})(\text{H}_2\text{O})_2]$  with apda acting as a tetradentate ligand (**Figure 1.13**).

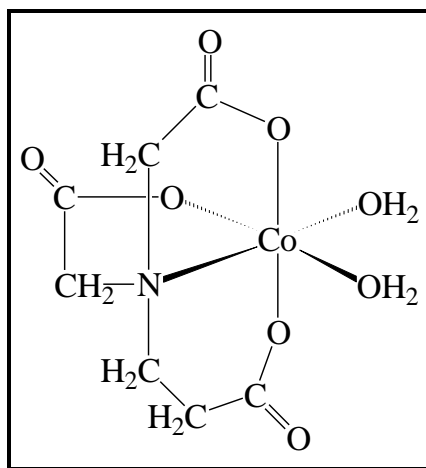


**Figure 1.13:** Structure of the  $[\text{Co}(\text{apda})(\text{H}_2\text{O})_2]$  complex.

Potgieter *et al.* (2005:1968) succeeded in isolating the  $[\text{Co}(\text{H}_2\text{O})_6][\text{Co}(\text{Hapda})_2]_2\text{H}_2\text{O}$  complex and characterised it with a three-dimensional X-ray structure determination. According to Potgieter and co-workers (2005:1968) in both the anionic units (**Figure 1.14**),  $[\text{Co}(\text{Hapda})_2]^-$ , the Co(III) centre is surrounded by two apda ligands which bind tridentately *via* one nitrogen and two oxygen atoms with the propionate group remaining uncoordinated in both the anionic units.

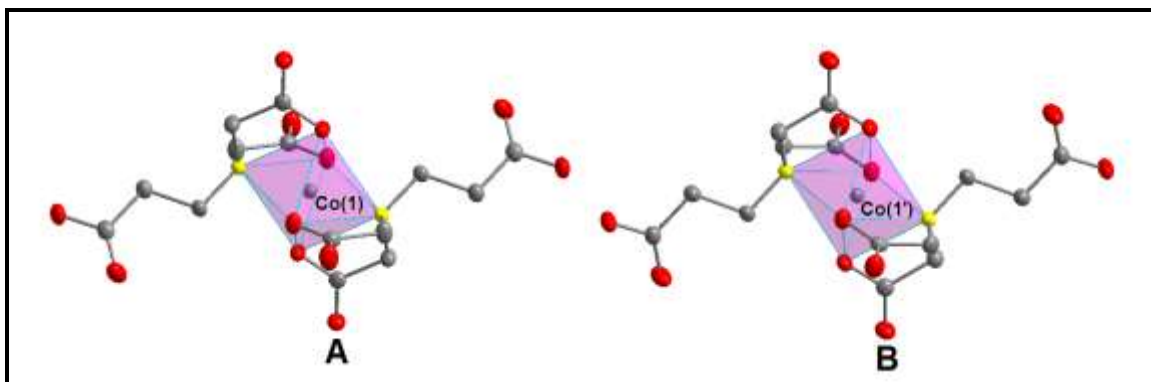


**Figure 1.14:** Octahedral distortion around cobalt(III) centres of anionic units,  $[\text{Co}(\text{Hapda})_2]$ , A and B (Potgieter *et al.*, 2005:1968).

Potgieter *et al.* (2005:1968) also synthesised the  $[\text{Co}(\text{apda})(\text{H}_2\text{O})_2]$  and recorded the UV/VIS spectrum of this complex at different pH values in **Figure 1.15** to determine the possible existing Co(III)-apda species at these pH values. These studies also showed that different species are formed in solution at different pH values, for example  $[\text{Co}(\text{apda})(\text{H}_2\text{O})(\text{OH})]^-$  and  $[\text{Co}(\text{apda})(\text{H}_2\text{O})_2]$  at pH 7 and 2, respectively.

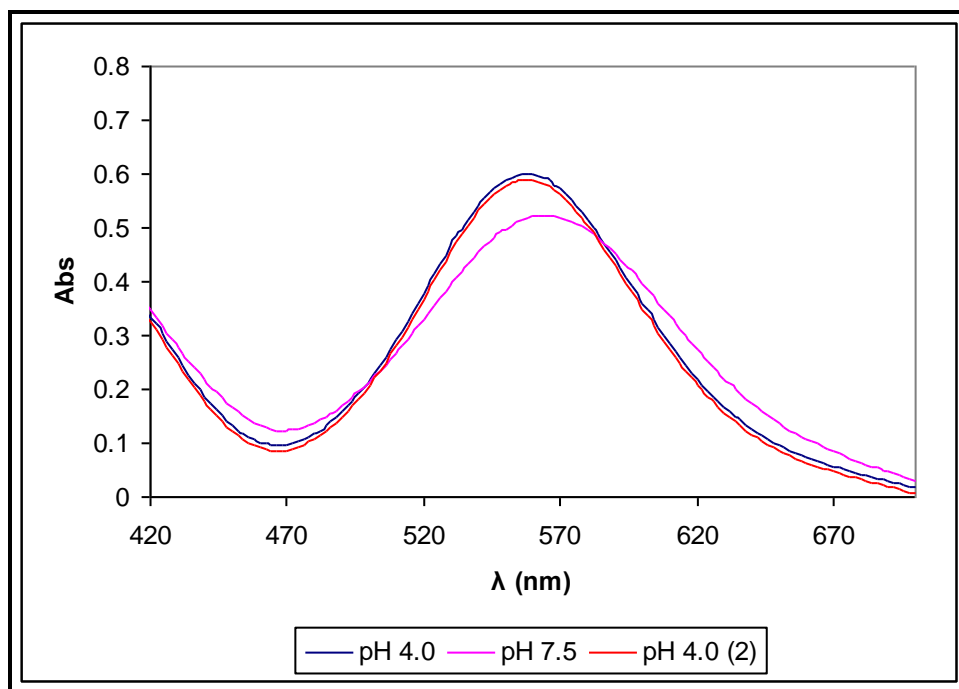


**Figure 1.15:** UV/VIS spectra of different Co(III)-apda species in solution (Potgieter *et al.*, 2005:1968).

At a  $\text{pH} > 7$ , a continuous change in spectrum was observed by Potgieter *et al.* (2005:1968), possibly due to dimer formation. It was therefore decided to keep the reaction conditions between  $\text{pH} 2\text{--}7$  in order to avoid complication by competitive reactions. Visser and co-workers (2002:461) also observed a continuous change in spectrum for their  $[\text{Co}(\text{nta})(\text{H}_2\text{O})_2]$  complex at a  $\text{pH} > 7$ . They attributed these changes to the formation of the Co(III)-nta dimer.

A possible explanation for these observed changes in UV/VIS spectra is an acid dissociation reaction presented in **Eq. 1.9**. The acid dissociation constant of  $[\text{Co}(\text{apda})(\text{H}_2\text{O})_2]$ ,  $K_{a1}$ , was determined spectrophotometrically as 6.23(2).

A similar reaction to that of Co(III)-nta (see **Eq. 1.8**) was postulated for this complex.



Kinetic studies for the substitution reactions of  $[\text{Co}(\text{apda})(\text{H}_2\text{O})_2]/[\text{Co}(\text{apda})(\text{H}_2\text{O})(\text{OH})]^-$  with  $\text{NCS}^-$  ions were investigated at pH values between 2 and 7 by Potgieter *et al.* (2005:1968). On the basis of the experimental results obtained by them a similar mechanism as presented in **Scheme 1.1** by Visser and co-workers (2002:461) for the substitution reactions of  $[\text{Co}(\text{nta})(\text{H}_2\text{O})_2]/[\text{Co}(\text{nta})(\text{H}_2\text{O})(\text{OH})]^-$  with  $\text{NCS}^-$  ions was constructed.

## 1.2 AIM OF THIS STUDY

Metal complexes of cobalt(III) containing lda and pda (see **Figure 1.2** and **1.3**) as possible multidentate or tripod ligands are rarely mentioned in the literature and little information on their structure and chemistry are available. A large number of complexes containing cobalt(III)-nta have been isolated and more information on their structures is available in the literature, although there is a lot of uncertainty regarding the synthesis, characterisation and reactions of these complexes. No kinetic studies on cobalt(III)-lda and-pda complexes have been published.

In an effort to obtain more information about the chemical behaviour and physical properties of these tripod ligands the research was now also extended to investigate the kinetics and mechanism of substitution reactions of Co(III)-lda and-pda systems.

The aim of this study was to:

- a) synthesise suitable Co(III)-lda and-pda complexes that can be used as biological models in future studies,
- b) characterise these complexes with especially  $^1\text{H}$  NMR so that they could be used as starting material in kinetic studies,
- c) determine the mechanism of the substitution reactions of cobalt(III)-lda and-pda complexes at different pH levels by means of a kinetic study and isolation and characterisation of the final products in these reactions.

# 2

## Literature overview

---

*A theoretical overview of reaction kinetics as well as octahedral substitution reactions will be discussed in this chapter.*

---

### 2.1 REACTION KINETICS

#### *Introduction*

Capellos and Bielski (1972:1) defined chemical reactions as processes in which a substance or substances (reactants) are transformed into other substances (products). In some processes the change occurs directly and the complete description of the mechanism of the reaction presents few difficulties. However, complex processes in which the substances undergo a series of stepwise changes, each constituting a reaction in its own right, are much more common. The overall mechanism is then made up of contributions from all such reactions and is far too complex to determine from the knowledge of only the reactants and products alone. In these complex cases chemical kinetics can often provide the only feasible approach toward the unraveling of the reaction mechanism.

Chemical kinetics is defined by Espenson (1995:1) as the study of rates of chemical reactions, which involves the precise measurements of the variation of concentration of the reacting species with time. Measurements are usually done to investigate the effects of temperature, pressure, pH, solvent, concentrations of additional species, salt concentration, and so forth in order to determine the mechanism and the rate constants of the reaction under investigation.

In essence chemical kinetics is a study of the dynamics of a chemical reaction. The data collected, indicates the measurement of a reaction rate and is used to explain this rate in

terms of a complete reaction mechanism. According to Capellos and Bielski (1972:1) chemical kinetics provides no information on the energy of the stereo-chemical states of individual molecules, but it does have the valuable potential to break down complex mechanisms into sequences of simple reactions. Complex mechanisms can be explained by sequence of elementary reactions, which combine together to give overall reactions.

### *Rate law and rate constants*

Espenson (1995:15) and Sykes (1966:43) defined the rate of a reaction as the change in the concentration of a reactant or product per unit time. For a general reaction in **Eq. 2.1**,



the reaction rate is given by:

$$\mathbf{Rate = \frac{-d[A]}{dt} = \frac{-d[B]}{dt} = \frac{d[C]}{dt} = k[A]^a[B]^b} \quad (2.2)$$

with  $k$  as a proportional constant (rate constant) that relates the rate of change to the reagent concentrations while the negative sign indicates the disappearance of A and B with the formation of C. The values  $a$  and  $b$  represent the order of the reaction with respect to the concentrations of A and B respectively, with the sum of  $a$  and  $b$  equal to the total order of the reaction. The order is the way in which the rate varies with a change in concentration of one or both of the reacting species and the units of the rates constant depend on the overall reaction order. These values can be determined experimentally but this is often difficult. This problem can be overcome by using pseudo first-order conditions, which implies that, the condition  $[B] \gg [A]$  in **Eq. 2.1**. The implication of this arrangement is that  $[B] \sim \text{constant}$  for the duration of the reaction and it allows for the simplification of the rate constants.

Eq. 2.2 is reduced to,

$$\text{Rate} = k_{\text{obs}}[\text{A}]^a \quad (2.3)$$

with the observed pseudo-first order rate constant being

$$k_{\text{obs}} = k[\text{B}]^b \quad (2.4)$$

Pseudo-first order conditions (with [B] at least ten times in excess of [A]) resulting in Eq. 2.4, also serve to obtain the rate constant by determining  $k_{\text{obs}}$  at different concentrations of B (Jordan, 1991:1). It can also be used to simplify second order reactions. If the value of  $b = 1$ , then the reaction is first order in B and a graph of  $k_{\text{obs}}$  vs. [B] will be a straight line with a zero intercept to indicate that there is no second reaction occurring.

The second order-rate constant,  $k$  (Eq. 2.1) is given by the slope of the graph. If the graph has a positive intercept it means that there is a second reaction with a rate constant,  $k_2$ , that is independent of the concentration of B. This leads to a rate law with more than one term as in Eq. 2.5

$$\text{Rate} = k_1[\text{A}][\text{B}] + k_2[\text{A}] \quad (2.5)$$

The pseudo-first order rate constant for the rate law in Eq. 2.5 would be given by Eq. 2.6.

$$k_{\text{obs}} = k_1 [\text{B}] + k_2 \quad (2.6)$$

For the following reaction (Eq. 2.7), the rate would be given in Eq. 2.8.



$$\text{Rate} = \frac{-d[B]}{dt} = k_1[B] \quad (2.8)$$

From the integration of (Eq. 2.8) between time = 0 and t respectively, the following equation (expressed in terms of B) is obtained:

$$\ln \frac{[B]_0}{[B]_t} = k_1 t \quad (2.9)$$

According to Beer-Lambert law:

$$A = \epsilon cl \quad (2.10)$$

with A = absorbance,  $\epsilon$  = molar absorptivity, c = concentration and l = light path length.

When Eq. 2.10 is incorporated into Eq. 2.9 and then manipulated, the following equation is obtained:

$$\ln \left[ \frac{A_0 - A_\infty}{A_t - A_\infty} \right] = k_1 t \quad (2.11)$$

with  $A_0$ ,  $A_t$  and  $A_\infty$  absorbance after time  $t = 0$ ,  $t = t$  seconds and infinite time respectively. Infinity is the time at which the reaction is complete for all practical purposes, and the value of  $k_1$  can then be determined by the least-squares fit using the absorbance vs. time data for the first-order reaction using Eq. 2.11.

### *Activation Parameters*

The activation parameters can be calculated from these kinetic results and can be used to gain important insight into the mechanism of subsequent substitution reactions. The

equation for the calculation of the enthalpy of activation,  $\Delta H^\ddagger$ , and entropy of activation,  $\Delta S^\ddagger$ , can be derived out of the absolute transition state theory.

According to Frost and Pearson (1953:74) this theory predicts that an activated complex or transition state is in equilibrium ( $K^\ddagger =$  equilibrium constant) with the reagents before the reaction proceed to give the final product. The rate of the reaction is given by the decomposition rate ( $k$ ) of the activated complex to yield the products:



The rate of which is given by:

$$k = \frac{k_B T}{h} K^\ddagger \quad (2.13)$$

where  $k_B =$  Boltzmann's,  $h =$  Planck's constants respectively,  $T =$  absolute temperature.

The free energy of activation,  $G^\ddagger$ , can be determined according to Barrow (1973:190) by normal thermodynamics, as shown in **Eq. 2.14**,

$$\Delta G^\ddagger = -RT \ln K^\ddagger = \Delta H^\ddagger - T\Delta S^\ddagger \quad (2.14)$$

and it follows that:

$$K^\ddagger = e^{\frac{-\Delta G^\ddagger}{RT}} \quad (2.15)$$

$\Delta G^\ddagger$  = standard free energy change,  $R$  = universal gas constant and  $T$  = absolute temperature.

Substituting **Eq. 2.15** into **Eq. 2.13** yields **Eq. 2.16**, which is known as the Eyring-Polanyi equation:

$$k = T \frac{k_B}{h} e^{\left(\frac{\Delta S^\ddagger}{R}\right) - \left(\frac{\Delta H^\ddagger}{RT}\right)} \quad (2.16)$$

where  $\Delta H^\ddagger$  = enthalpy of activation,  $\Delta S^\ddagger$  = entropy of activation. **Eq. 2.16** is generally written in its logarithmic form as shown below in **Eq. 2.17**:

$$\ln\left(\frac{k}{T}\right) = \ln\left(\frac{k_B}{h}\right) + \left(\frac{\Delta S^\ddagger}{R}\right) - \left(\frac{\Delta H^\ddagger}{RT}\right) \quad (2.17)$$

A graph of  $\ln \frac{k}{T}$  vs.  $\frac{1}{T}$  gives a linear relationship with the slope  $-\frac{\Delta H^\ddagger}{R}$  and the Y-intercept yielding  $\frac{\Delta S^\ddagger}{R} + \ln\left(\frac{k_B}{h}\right)$ . **Eq. 2.17** can be used to calculate both the enthalpy of activation,  $\Delta H^\ddagger$ , and entropy of activation,  $\Delta S^\ddagger$ .

The enthalpy of activation,  $\Delta H^\ddagger$ , provides little information regarding the mechanism of the reaction. A small positive or negative enthalpy of activation,  $\Delta H^\ddagger$ , which usually indicates more than one reaction, is seldom found.

The entropy of activation,  $\Delta S^\ddagger$ , on the other hand, gives much more information regarding the specific mechanism that has been followed during the reaction. Negative values for  $\Delta S^\ddagger$  show that there is a decrease in entropy during the formation of the transition state (rate limiting step). A negative entropy of activation is therefore

associated with bond formation. This is a good indication of an associative mechanism. Positive values for  $\Delta S^\ddagger$  are usually an indication of bond breaking in the activated complex and therefore indicative of a dissociative activation.

## 2.2 OCTAHEDRAL SUBSTITUTION REACTIONS

### *Introduction*

A substitution reaction is a reaction where existing metal-ligand bonds are broken and a new metal-ligand bond is formed between the metal and the entering group. In general substitution reactions are presented in **Figure 2.1** where the labile ligand, X, is replaced by the new entering ligand, Y.

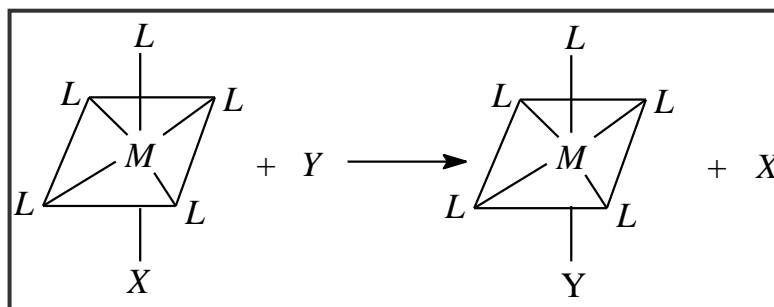
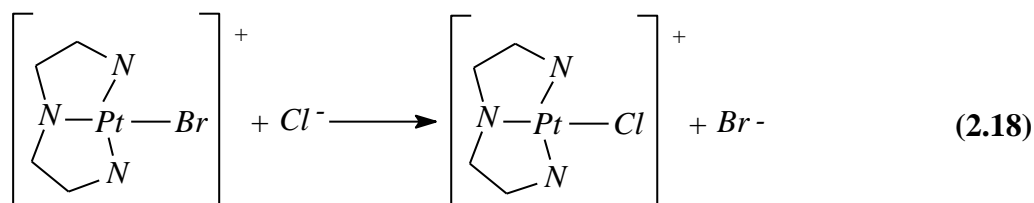


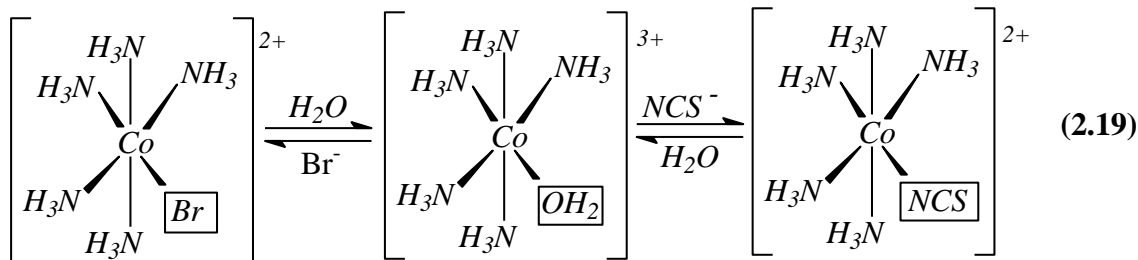
**Figure 2.1:** General substitution reactions of octahedral complexes.

The ligand substitution in metal complexes can occur in two ways, namely:

- (a) The replacement of one ligand by another without the direct intervention of solvent in **Eq. 2.18** (Wilkins, 1974:181)

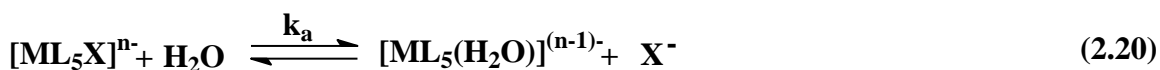


(b) Indirect substitution with the involvement of a water molecule (anation) as indicated in **Eq. 2.19** (Purcell and Kotz, 1980:412)



Solvolysis in aqueous medium can be divided into two groups, namely acid hydrolysis and base hydrolysis. The reaction product is an aqua complex for acid hydrolysis while a hydroxo complex is usually isolated for base hydrolysis according to Basolo and Pearson (1967:158).

Acid hydrolysis can be presented as follows:



The rate of the reaction is given by in **Eq. 2.21**.

$$\text{Rate} = k_a[\text{ML}_5\text{X}] \quad (2.21)$$

Base hydrolysis however, is depicted in **Eq. 2.22**:



The rate of the reaction is given by:

$$\text{Rate} = k_b[\text{ML}_5\text{X}][\text{OH}^-] \quad (2.23)$$

Purcell and Kotz (1980:412) presented a typical base hydrolysis mechanism, involving the rapid formation of a conjugated base, **Figure 2.2**.

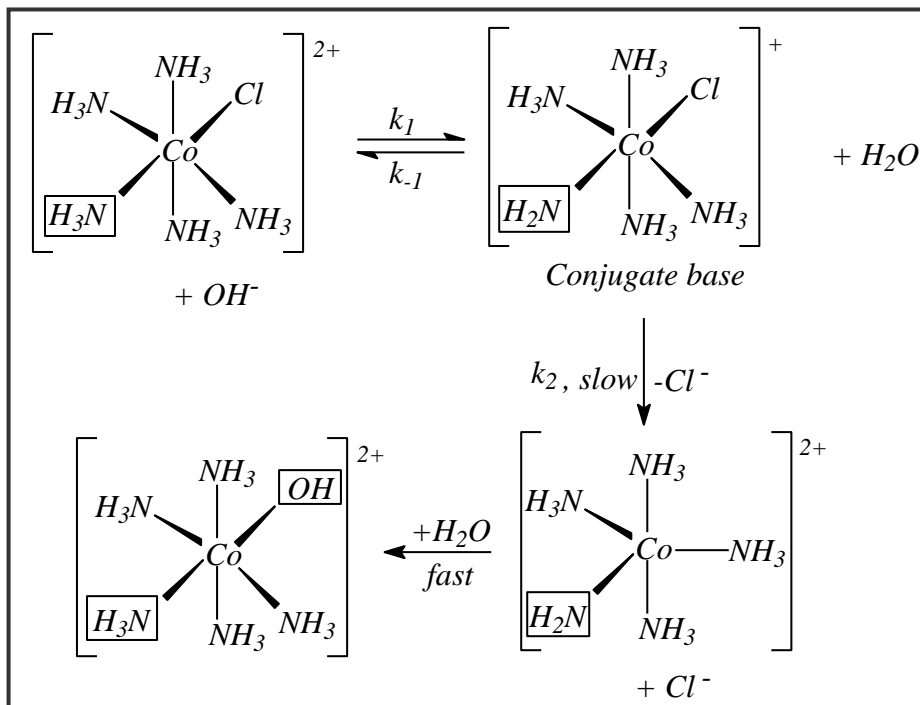


**Figure 2.2:** Base hydrolysis mechanism

Using the steady-state approximation, the observed rate law for the above-mentioned mechanism is as follows:

$$\text{Rate} = \frac{k_1 K [\text{Co}(\text{NH}_3)_5(\text{Cl})^{2+}] [\text{OH}^-]}{1 + K [\text{OH}^-]} \quad (2.24)$$

If, however, K is quite small, which result in the term  $K [\text{OH}^-] \ll 1$ , the rate expression reduces to the following equation:

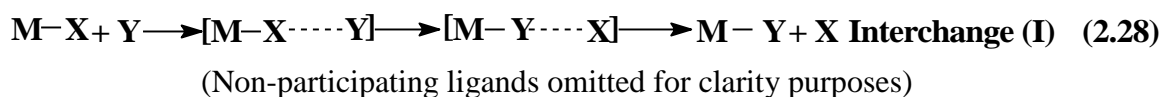
$$\text{Rate} = k_1 K [\text{Co}(\text{NH}_3)_5(\text{Cl})^{2+}] [\text{OH}^-] \quad (2.25)$$

Eq. 2.23 and 2.21 are of the same form and both show a first order dependence in  $[\text{OH}^-]$ .

*Mechanism of substitution reactions*

The mechanism of a reaction is an indication of the various steps that occur during the reaction to produce the final product. The mechanism describes the entire process of individual elementary processes involved in the reaction. These steps can take place either simultaneously or consecutively to produce the observed overall reaction.

Three main reaction mechanisms are considered by Cotton and Wilkinson (1988:1285) as well as by Langford and Gray (1966:7) and are illustrated in the following equations:



The main difference between the three possible mechanisms is the status of the entering and the leaving group in the transition state. The rate-determining step in the dissociative mechanism involves the complete dissociation of the leaving group, which result in the lowering of the coordinated number of the complex. In contrast, during an associative mechanism the entering group in the rate-determining step increases the coordination number due to bond formation. The interchange mechanism involves the simultaneous formation and the breaking of bonds in the rate-determining step.

It is not always easy to determine the kind of mechanism which was followed during the reaction. One useful way to try and elucidate the mechanism of substitution reactions is to study the reaction and consequent rate constants under different conditions. The three different reaction mechanisms will be discussed in more detail in the following paragraphs.

*Dissociative mechanism (D)*

The complete dissociation of one of the bonded ligands is the rate-determining step for the reaction that follows a dissociative mechanism. The reaction can be illustrated by:



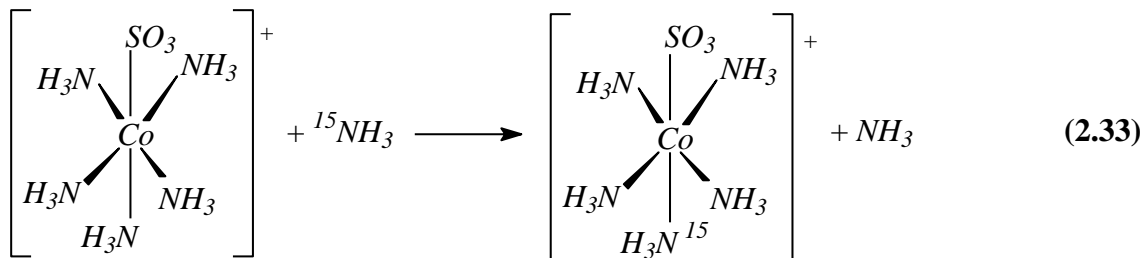
By employing the steady-state approximation for the intermediate,  $\text{ML}_5$ , the rate of reaction is given by:

$$\text{Rate} = \frac{k_1 k_2 [\text{ML}_5\text{X}][\text{Y}]}{k_{-1}[\text{X}] + k_2[\text{Y}]} \quad (2.31)$$

According to **Eq.2.29** the reaction rate depends on the concentration of entering ligand,  $[\text{Y}]$ , as well as on the concentration of complex,  $\text{ML}_5\text{X}$ , and non-linear kinetics is expected from this rate law. If, however, the  $[\text{Y}]$  is quite large so that  $k_2[\text{Y}] \gg k_{-1}[\text{X}]$ , this leads to the following rate expression:

$$\text{Rate} = k_1[\text{ML}_5\text{X}] \quad (2.32)$$

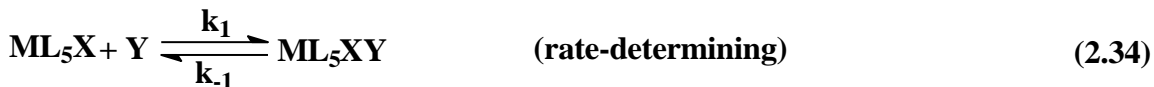
The rate of the reaction according to **Eq. 2.32** is independent of the concentration of entering ligand,  $\text{Y}$ . An example of a dissociative reaction is given by Halpern *et al.* (1966:2877) in **Eq. 2.33**.



It was found that the above-mentioned reaction shows a non-linear relationship between  $k_{\text{obs}}$  and  $[{}^{15}\text{NH}_3]$  (Halpern *et al.*, 1966:2877). Further it was found that the rate of the reaction is independent of the  $[{}^{15}\text{NH}_3]$  when the concentration of  ${}^{15}\text{NH}_3$  is high, resulting in non-linear kinetics as indicated by **Eq. 2.31**.

*Associative mechanism (A)*

Bond formation is the predominant factor in the reaction that follows an associative mechanism. The reaction can be illustrated as follows:



By employing the steady-state approximation for the intermediate,  $\text{ML}_5\text{XY}$ , the rate of reaction is given by the following equation:

$$\text{Rate} = \frac{k_1 k_2}{k_{-1} + k_2} [\text{ML}_5\text{X}][\text{Y}] \quad (2.36)$$

Under pseudo first-order conditions with ( $[\text{Y}] \gg [\text{ML}_5\text{X}]$ ), **Eq. 2.36** can be simplified to:

$$\text{Rate} = k_{\text{obs}}[\text{Y}] \quad (2.37)$$

According to **Eq. 2.37** a linear relationship exists between the observed rate constant and the concentration of entering ligand, [Y].

*Interchange mechanism (I)*

The interchange mechanism (I) entails a concerted exchange of the leaving (X) and entering (Y) ligand in which bond breaking and bond formation occurs nearly simultaneously. The reaction can be illustrated by:



The rate expression for the above reaction scheme is given in **Eq. 2.40**,

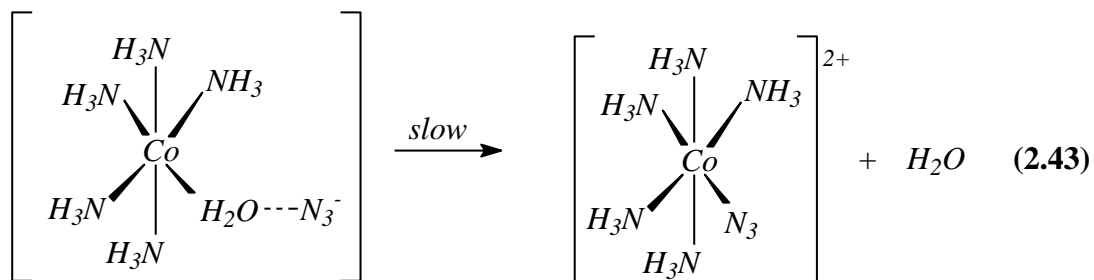
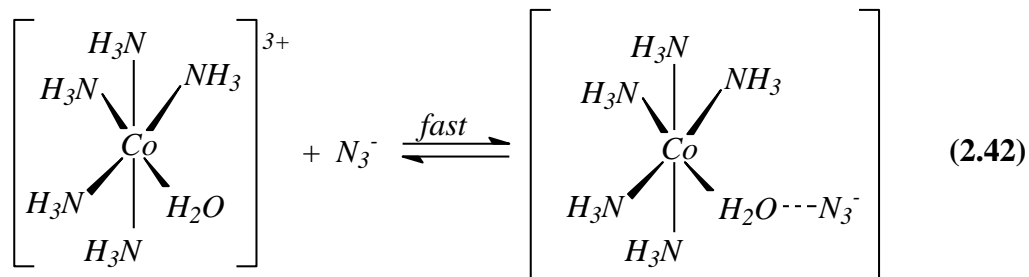
$$\text{Rate} = \frac{k_2 \text{K}[\text{M}]_{\text{tot}}[\text{Y}]}{1 + \text{K}[\text{Y}]} \quad (2.40)$$

where  $[\text{M}]_{\text{tot}}$  is the total metal ion concentration.

Under conditions where  $\text{K}[\text{Y}] \ll 1$  the rate of the reaction is directly proportional to the concentration of the entering ligand, [Y], and non-linear kinetics is expected from this rate law, but under conditions where  $\text{K}[\text{Y}] \gg 1$  the rate of reaction is independent from [Y], meaning linear kinetics and **Eq. 2.40** is simplified to **Eq. 2.41**.

$$\text{Rate} = k_2[\text{M}]_{\text{tot}} \quad (2.41)$$

The rate of the reaction according to **Eq. 2.41** is independent of the concentration of incoming ligand, Y. An example of a reaction that follows interchange mechanism is given by Swaddle and Gustalla (1969:1604) in **Eq. 2.42** and **2.43** below.



Swaddle and Gustalla (1969:1604) observed two reactions during the study of the above-mentioned substitution reaction. They postulated that the first reaction is the fast formation of the outside sphere -ion pair and the second reaction is the slower inner sphere substitution of H<sub>2</sub>O with N<sub>3</sub>.

From the above paragraphs it was clear that the rate law for an associative mechanism (Eq. 2.37) at all times show linear relationships between rate of reaction and the concentrations of entering ligands, [Y]. For dissociative and interchange mechanisms (Eq. 2.31 and Eq. 2.40) the rate law of the reaction is dependent of the ligand concentration and non-linear kinetics will be expected, but under certain conditions the rate law of the reaction (Eq. 2.32 and Eq. 2.41) is independent from [Y] meaning, linear kinetics.

Theoretically it is possible to distinguish between an associative, dissociative and interchange mechanism by means of different rate laws. It is seldom however practically possible to increase the concentration of the incoming ligand to such an extent that the rate of the reaction is independent of [Y]. It is therefore not always possible or advisable to allocate a mechanism to a reaction solely from the type of graph that is obtained from the kinetics of one set of reactions.

### *Factors that influence the reactivity of octahedral complexes*

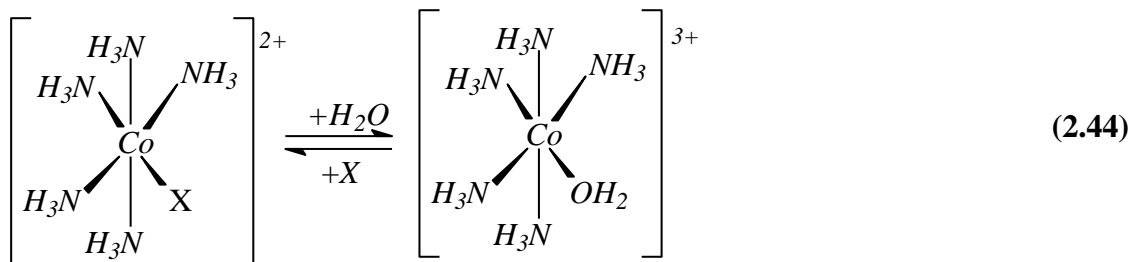
Fortunately there are various other factors that give important information concerning the type of mechanism followed during the reactions of octahedral complexes. Factors such as the influence of the central metal ion, leaving, entering and non-labile ligand as well as activation parameters (refer to paragraph 2.1) and linear relationships. These factors all give additional information with regards to the mechanism which is followed during the reaction. These important factors will be discussed in the following paragraphs.

#### *Influence of the leaving ligand*

The effect of the leaving ligand is according to Candlin *et al.* (1968:12) related to the strength of the M - X (metal-ligand bond, where X = the leaving ligand). A weaker M - X bond strength implies that X can more easily be replaced in the substitution rate. A stronger M - X bond however, makes it more difficult for X to be substituted by another ligand, causing the reaction to progress more slowly.

An increase in the negative charge of the leaving ligand will also cause stronger M - X bonds and make it difficult to break. The higher negative charge of the leaving ligand will decrease the rate of substitution reactions that follows a dissociative mechanism. The higher charge of the ligand will also decrease the positive charge of the central metal ion and therefore delay the reaction which follows an associative activation.

An increase in size of the leaving ligand will cause steric repulsion in the metal ion coordination sphere. Steric repulsion between the non-labile and leaving ligand will favor a dissociative activation. Bond formation will be hindered by steric repulsion and this will not favor an associative mechanism. An example of a substitution reaction where the influence of change of the leaving ligand is clearly illustrated is the acid hydrolysis reaction (Basolo & Pearson, 1967:164) which is given in **Eq. 2.44**.



The substitution rate constants of the acid hydrolysis reactions between  $[\text{Co}(\text{NH}_3)_5\text{X}]^{2+}$  and different ions are reported in **Table 2.1** below.

**Table 2.1:** Rate constants for the acid hydrolysis reaction of  $[\text{Co}(\text{NH}_3)_5\text{X}]^{2+}$  with different ions at 25.0 °C.

$\text{X}^-$	$k \text{ (s}^{-1}\text{)}$
$\text{NO}_3^-$	$2.7 \times 10^{-5}$
$\text{NCS}^-$	$5.0 \times 10^{-5}$
$\text{I}^-$	$8.3 \times 10^{-6}$
$\text{Cl}^-$	$1.8 \times 10^{-6}$
$\text{F}^-$	$8.6 \times 10^{-8}$
$\text{N}_3^-$	$2.1 \times 10^{-9}$

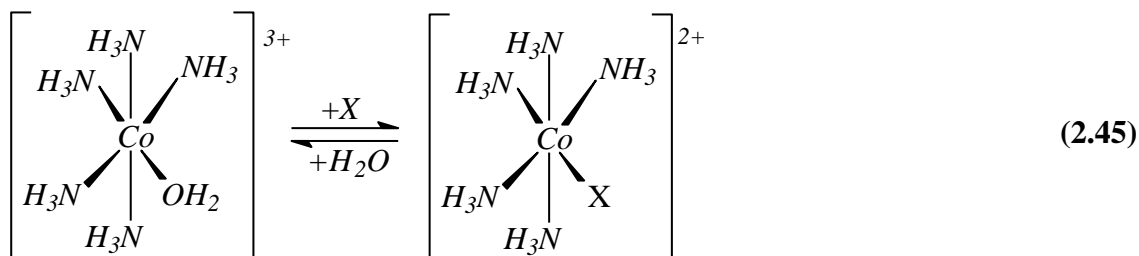
The rate constants for the above reactions differ by a factor of almost 4 and clearly illustrate the effect of the leaving group. These results are easily understood on the basis of a dissociative mechanism.

#### *Influence of the entering ligand*

Important information concerning the mechanism which is followed during the reaction can be obtained through the variation of the entering ligand. For a dissociative activated mechanism, bond breaking, with the formation of a five-coordinated intermediate, is the

rate-determining step. Varying the nature of the entering ligand should have a very small influence on the rate of substitution in such a reaction.

An example of a substitution reaction where the variation of the entering ligand has a small influence on the rate of substitution was reported by Wilkins (1974:181) for the following reaction



The substitution rate constants of the acid hydrolysis reactions between  $[\text{Co}(\text{NH}_3)_5(\text{H}_2\text{O})]^{3+}$  and different ions are reported in **Table 2.1** below.

**Table 2.2:** Rate constants for the acid hydrolysis reactions of  $[\text{Co}(\text{NH}_3)_5(\text{H}_2\text{O})]^{3+}$  with different ions at 45.0 °C.

$\text{X}^-$	$k \text{ (s}^{-1}\text{)}$
$\text{N}_3^-$	$1.0 \times 10^{-4}$
$\text{Cl}^-$	$2.1 \times 10^{-5}$
$\text{NCS}^-$	$1.6 \times 10^{-5}$

The rate constants of the reactions differ only by a factor of 1. The rate of the forward reaction is for all practical purpose thus independent of the nature of the entering ligand. These results were clearly upon a dissociative mechanism for the forward reaction in **(Eq. 2.45)**.

The equilibrium constant of the above-mentioned reaction can be defined as:

$$K_1 = \frac{k_1}{k_{-1}} \quad (2.46)$$

Any change in equilibrium constant,  $K_1$ , for the sequence of ligands can be explained in terms of a variation of the backward rate constant,  $k_{-1}$ . The application of equilibrium constant will be discussed further under linear free-energy relationship.

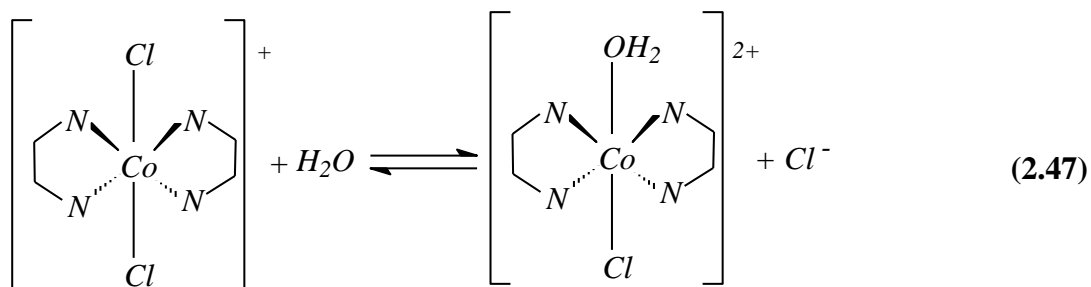
### *Effect of the non-labile ligand*

The bonded ligands in an octahedral complex also have a significant influence on the rate of substitution reactions. These ligands influence the rate of substitution *via* the *cis* or *trans*-labilization of ligands in the coordinated sphere or by steric intervention within the coordination sphere or interaction with entering groups. The effect of the *cis* ligand is mainly sterically in nature, whereas the *trans* ligand can influence the rate electronically. It occurs *via* the labilization of the leaving group in the ground state, or *via* the electronic stabilization of the transitional state.

### Steric effect

The variation in size of the non-labile ligand normally provides valuable information with regard to the mechanism of the substitution reaction. The increase in steric bulk (Langford and Gray 1966:59) of the non-labile ligands can favor dissociative activation due to steric demand within the coordination sphere. Bond breaking releases this large steric demand between different bonded ligands, which favors a dissociative mechanism. For a reaction, which follows an associative mechanism, steric hindrance of the non-ligands will result in the delay of bond formation between the metal ion and the incoming group in the rate-determining step.

A typical example of a study of the effect of steric repulsion of non-labile ligand on the rate of reaction was illustrated by Porterfield (1993:703) and is given in **Eq. 2.47**.



The substitution rate constants of the acid hydrolysis reactions between  $[\text{Co}(\text{N-N})_2\text{Cl}_2]^+$  and different diamine chains are being given in **Table 2.3**

**Table 2.3:** Rate constants for the acid hydrolysis reactions of  $[\text{Co}(\text{N-N})_2\text{Cl}_2]^+$  with different diamine chains at 25.0°C.

Diamine	Structure	k (s <sup>-1</sup> )
Ethylenediamine	H <sub>2</sub> N-CH <sub>2</sub> -CH <sub>2</sub> -NH <sub>2</sub>	3.2 × 10 <sup>-5</sup>
Propylenediamine	H <sub>2</sub> N-CH <sub>2</sub> -CH(CH <sub>3</sub> )-NH <sub>2</sub>	6.2 × 10 <sup>-5</sup>
<i>d l</i> -Butylenediamine	<i>d l</i> -H <sub>2</sub> N-CH(CH <sub>3</sub> )-CH(CH <sub>3</sub> )-NH <sub>2</sub>	1.5 × 10 <sup>-4</sup>
<i>meso</i> -Butylenediamine	<i>meso</i> -H <sub>2</sub> N-CH(CH <sub>3</sub> )-CH(CH <sub>3</sub> )-NH <sub>2</sub>	4.2 × 10 <sup>-3</sup>
Tetramethylethylenediamine	H <sub>2</sub> N-C(CH <sub>3</sub> ) <sub>2</sub> -C(CH <sub>3</sub> ) <sub>2</sub> -NH <sub>2</sub>	3.3 × 10 <sup>-2</sup>

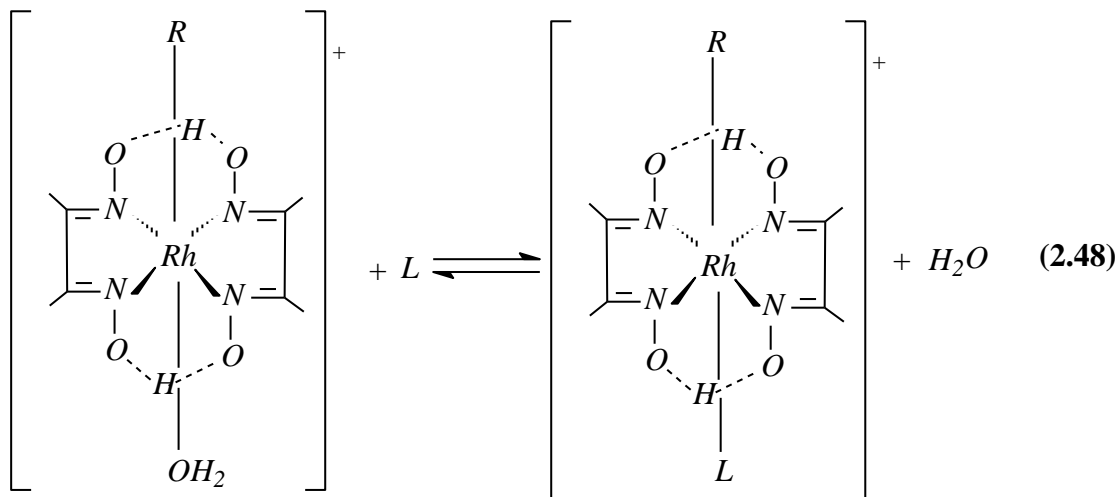
These results clearly show that there is an increase in the substitution reaction rate of the Cl<sup>-</sup> ligand with an increase in steric repulsion within the complex. These results are easily understood on the basis of a dissociative mechanism.

### Trans- labilization

The nature of the ligand *trans* to the leaving group has a significant influence on the rate of substitution reaction according to Jordan (1991:57). The *trans*-effect can be defined as the ability of the ligand *trans* with respect to the leaving group to decrease the activation energy of the reaction and the stabilization of transition state through delocalization of the

electron density. If a ligand has a large *trans*-effect, it will weaken the metal-ligand bond *trans* to it which will increase the rate of substitution of the reaction that follows the dissociative mechanism. On the other hand *trans*-ligands with strong electron withdrawing properties can cause the incoming ligands with strong electron donating property to bind easily on the metal ions. This implies that the reactions that follow an associative activated mechanism will experience an increase in rate of reaction making it difficult to distinguish between D and A mechanism using this method of investigation.

An example of the reaction where the non-labile ligand has on the influence of the rate of substitution of the aqua ligand was illustrated by Garlatti *et al.* (1986:27) in **Eq. 2.48**,



where (R = CH<sub>3</sub>CH<sub>2</sub>, ClCH<sub>2</sub> and CF<sub>3</sub>CH<sub>2</sub>) and L = thiourea. The different rate constants for the reaction was determined as 3.6 × 10<sup>4</sup>, 3.1 × 10<sup>2</sup> and 15 dm<sup>3</sup>mol<sup>-1</sup>s<sup>-1</sup> for R = CH<sub>3</sub>CH<sub>2</sub>, ClCH<sub>2</sub> and CF<sub>3</sub>CH<sub>2</sub> respectively. The rate constants for the above-mentioned reactions increase by a factor of more than 10<sup>3</sup> due to the labilization effect of CH<sub>3</sub>CH<sub>2</sub> > ClCH<sub>2</sub> > CF<sub>3</sub>CH<sub>2</sub>. These results are easily understood on the basis of a dissociative mechanism. Due to the inertness and strong electron donating property, the CF<sub>3</sub>CH<sub>2</sub> has the largest *trans*-effect according to the authors.

Cis- labilization

Non-labile ligand *cis* with respect to the coordinated leaving ligand can also play a significant role in the rate of octahedral substitution reaction due to change of the electronic environment around the metal center.

Douglas *et al.* (1983:341) followed the acid hydrolysis reactions of  $[\text{Co}(\text{cyclam})\text{Cl}_2]^+$ ,  $[\text{Co}(\text{DMG})_2\text{Cl}_2]^-$  and  $[\text{Co}(\text{tet-}b)\text{Cl}_2]^+$  ions (where cyclam = 1,4,8,11-tetraazacyclotetradecane, DMG = dimethylglyoximate and *tet-b* = d,1-1,4,8,11-tetraaza-5,5,7,12,12,14-hexamethylcyclotetradecane) in order to investigate the effect of the *cis*-ligand on the rate of substitution.

A reaction which clearly illustrates the *cis*-labilization effect of bonded ligand is given by acid hydrolysis reactions of  $[\text{Co}(\text{N}_4)\text{LCl}]^{n+}$  and which is given in **Table 2.4**

**Table 2.4:** Rate constants for the acid hydrolysis reactions of  $[\text{Co}(\text{N}_4)\text{LCl}]^{n+}$  at 25.0°C.

Complex	k (s <sup>-1</sup> )
$[\text{Co}(\text{cyclam})\text{Cl}_2]^+$	$1.1 \times 10^{-6}$
$[\text{Co}(\text{DMG})_2\text{Cl}_2]^-$	$2.7 \times 10^{-4}$
$[\text{Co}(\text{tet-}b)\text{Cl}_2]^+$	$9.3 \times 10^{-4}$

The system of ligands was chosen in such a way that the steric effect of the above-mentioned ligands were almost equal, indicating that any effects on the rate of the reactions could be contributed to the electron donating ability of cyclam, DMG and *tet-b* ligands.

### *Influence of the central metal ion*

The nature of the central metal ion should also be taken into consideration when deciding the type of mechanism favored by the substitution reaction. Basolo and Pearson (1967:124) confirmed that the charge, the size as well as electron configuration of the metal ion could influence the rate as well as the intimate mechanism of substitution reactions.

An increase in positive charge of the central metal ion would make bond breaking between the ligand and the metal more difficult. Hence it is expected that the rate will decrease with increasing positive charge of the metal ions if the reaction is dissociative activation. A large positive charge on the metal ion will enhance the rate of substitution for an associative mechanism (greater electrostatic attraction between the positively charged metal ion and the entering ligand).

An increase in size of the central metal ion will weaken the bond between the metal ion and the leaving ligand (due to weaker orbital overlap). The weakened metal-ligand bonds will favor the dissociation of the ligand. At the same time, this will also promote the forming of the bond between the metal ion and the entering ligand because of an increase in primary coordination sphere and these will thus favor an associative activation resulting in an increase in the rate of substitution from these reaction.

Wilkins (1974:181) reported that the lowering of the charge and the greater the size of either the central atom or the leaving group, will lead to weakening of metal-ligand bond strengths. The above factors according to the author will enhance the reactions that follow a dissociative type of mechanism. Based on the radius of the central ion, it was pointed out by the author that  $\text{Fe}(\text{H}_2\text{O})_6^{2+}$  will be expected to exchange water more rapidly than  $\text{Fe}(\text{H}_2\text{O})_6^{3+}$  and  $\text{Co}(\text{NH}_3)_5\text{Br}^{2+}$  to react more rapidly than  $\text{Co}(\text{NH}_3)_5\text{Cl}^{2+}$  based on the radius of the central ion. In addition the author also pointed out to the above factors, such as smaller size and the greater charge of the entering group, the faster the

reaction would be. The expected nucleophilic efficiency according to the order of anions in the reaction that follows via a dissociative mechanism is  $F^- > Cl^- > Br^- > I^-$ .

The electron configuration of the metal ion can also play an important part in the rate of substitution, which will determine whether the metal ion is labile or inert. The ligand field stabilization energy theory, predicts that the contribution of the ligand field to the activation energy of the reaction can be determined. An increase in ligand field stabilization energy will lead to the decrease in energy of activation due to the change in the geometry of the octahedral complex during the reaction. For an example, formation of a five- or seven-coordinated transition state is characterised by a dissociative or associative mechanism. A transitional state with a low ligand field stabilizing energy such as the starting materials will generally lead to an increase in the activation energy with a decrease in rate of substitution. It was found experimentally by Llewellyn *et al.* (1964:196) as well as by Plumb and Harris (1964:542) that the complexes of  $Cr(III)d^3$ ,  $Co(III)d^6$  and  $Rh(III)d^8$  are relatively inert towards substitution reactions.

*Linear free-energy relationship*

The relationship between the equilibrium constant and the rate constants for a sequence of reactions can also provide valuable information concerning the mechanisms which is followed during the substitution reactions. Consider the following reaction:



where  $H_2O$  is the leaving ligand,  $X$  the entering ligand,  $K_1$  the equilibrium constant for the reaction,  $k_1$  the forward rate constant and  $k_{-1}$  the backward rate constant.

The equilibrium constant of the above-mentioned reaction can be defined as:

$$K_1 = \frac{k_1}{k_{-1}} \quad (2.50)$$

Any change in equilibrium constant,  $K_1$ , for the sequence of ligands can be explained in terms of a variation of the backward rate constant,  $k_{-1}$ . **Eq. 2.50** is generally written in its logarithmic form as shown below in **Eq. 2.51**:

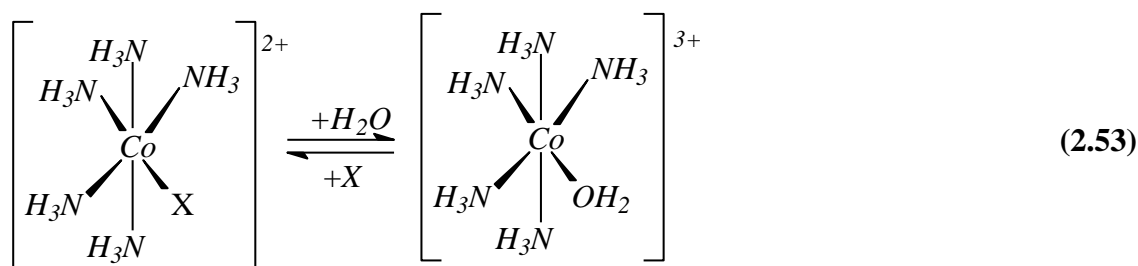
$$\ln k_{-1} = -\ln K_1 + \ln k_1 \quad (2.51)$$

For a reaction associated with a dissociative mechanism the rate constant,  $k_1$ , is independent and it can be considered as constant and **Eq. 2.51** can be simplified to:

$$\ln k_{-1} = -\ln K_1 + \text{constant} \quad (2.52)$$

Following **Eq. 2.52** a linear relationship between  $\ln k_{-1}$  and  $-\ln K_1$  should be observed and the slope of the graph of  $\ln k_1$  vs.  $\ln K$  should be equal to minus one.

A typical example where the linear free-energy relationship is applied can be illustrated by the acid hydrolysis reaction of  $[\text{Co}(\text{NH}_3)_5\text{X}]^{2+}$  and different ions (Basol & Pearson, 1967:164) below,



where  $\text{X}^- = \text{NCS}^-, \text{N}_3^-, \text{HC}_2\text{O}_4^-, \text{F}^-, \text{Cl}^-, \text{H}_2\text{PO}_4^-, \text{Br}^-, \text{I}^-$  and  $\text{NO}_3^-$  ions. A graph of  $\ln k_{-1}$  vs.  $\ln K_1$  for the above-mentioned reactions was linear with a slope of minus one. The interpretation of this linear relationship for the sequence of reactions is that the state of

## Chapter 2

the starting material and the entering ligand remains the same before the reaction and during the transition state, meaning that the reaction thus follow *via* a dissociative mechanism.







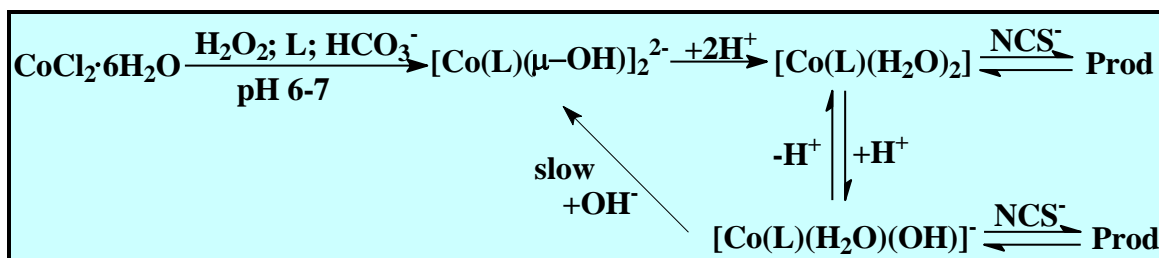
### 3 Synthesis and identification of cobalt(III)-lda and-pda complexes

*This chapter deals mainly with the synthesis of cobalt(III)-lda and-pda complexes. The characterisation of these complexes by means of <sup>1</sup>H NMR, infrared (IR) and UV/VIS spectroscopy is also discussed in this chapter.*

#### 3.1 Introduction

It was pointed out in Chapter 1 that the synthesis and identification of cobalt(III)-lda and-pda complexes have not yet been conclusively documented. The identification of the starting complexes and final products in this study is also vitally important to the determination of the mechanism of the substitution reactions, which will be discussed in the next chapter.

**Scheme 3.1** provides a general illustration of the formation of different cobalt(III)-L complexes investigated in this study.



**Scheme 3.1:** Synthesis and reactions of  $[\text{Co}(\text{L})(\mu\text{-OH})]_2^{2-}$  (L = lda, pda).

The IR spectra of complexes containing lda, pda, nta and apda are complicated and not always conclusive. It has been shown by Nakamoto (1963:206) that the stretching frequencies for  $\text{COO}^-$  groups are affected by coordination as well as by intermolecular interaction. According to the author,  $\text{COO}^-$  groups exhibit stretching frequencies at

1650–1620  $\text{cm}^{-1}$  when coordinated to metals such as cobalt(III) and 1750–1700  $\text{cm}^{-1}$  when un-ionised or uncoordinated.

$^1\text{H}$  NMR can provide important structural information, especially by investigating the signals of the protons of the acetate rings of these tripod ligands (Potgieter *et al.*, 2005:1968). This chapter also includes very interesting results which are related to the identification of Co(III)-lda and-pda complexes by means of  $^1\text{H}$  NMR spectra.

Previous studies of  $[\text{Co}(\text{nta})(\mu\text{-OH})]_2^{2-}$  (Visser *et al.*, 2002:461, Thacker & Higginson 1975:704) have shown that different species are formed in solution at different pH values. It has been shown for example that the  $\mu$ -hydroxo bridges of  $[\text{Co}(\text{nta})(\mu\text{-OH})]_2^{2-}$  is cleaved by  $\text{H}^+$  ions upon acidifying solutions of the above-mentioned complex from pH 7 to 2 to form the corresponding  $[\text{Co}(\text{nta})(\text{H}_2\text{O})_2]$  complex. When the pH of solutions of this diaqua complex at pH 2 were re-adjusted to 7, an aqua-hydroxo complex,  $[\text{Co}(\text{nta})(\text{H}_2\text{O})(\text{OH})]^-$  formed. Solutions of this last complex again formed the dimer upon standing for several days. This work is continued in this Chapter with the similar lda and pda complexes.

During this study, Co(III)-lda and-pda complexes were synthesised and the formation of the different species in solution were investigated by all physical techniques available.

## **3.2 Chemicals and Instrumentation**

All common laboratory reagents were of analytical grade. pH measurements were all performed on a HI 8520 microprocessor bench pH/ $^{\circ}\text{C}$  meter, calibrated with pH 7.01 (H17007) and pH 4.01 (H17004) buffer solutions, all obtained from Hannan instruments. UV/VIS spectra were recorded in 1.00  $\text{cm}^3$  quartz cells on a Varian Cary 50 (Conc.) spectrophotometer equipped with constant temperature cell holder (accurate with 0.1  $^{\circ}\text{C}$ ). Infrared spectra recorded on a DIGILAB Merlin f.t.i.r spectrophotometer in the range of 4000-500  $\text{cm}^{-1}$  as a powder. The  $^1\text{H}$  NMR spectra were recorded on a 300 MHz Bruker

spectrometer and all chemical shifts are reported in parts ppm (with *s* = singlet, *d* = doublet, *m* = multiplet, *t* = triplet and *q* = quartet).

### 3.3 Synthesis and isolation

#### 3.3.1 *l*-Leucine-*N,N*-diacetic acid (lda)

*l*-Leucine-*N,N*-diacetic acid (lda) was synthesised according to the procedure developed by Bocarsly *et al.* (1990:4898). ClCH<sub>2</sub>COOH (18.90 g, 0.20 mol) was dissolved in water and the solution was neutralised by adding NaHCO<sub>3</sub> (16.81 g, 0.20 mol). The pH of the solution stabilised at pH 6.3 after stirring for several minutes. *l*-Leucine (13.12 g, 0.10 mol), neutralised with NaOH (4.0 g, 0.10 mol), was added to the ClCH<sub>2</sub>COOH solution. The solution was heated (80-85 °C) on a water bath and after 20 minutes of heating NaOH (8.01 g, 0.20 mol) was added over a period of 40 minutes with heating (87-91 °C). Heating was continued for a further 10 minutes and the second solution of ClCH<sub>2</sub>COOH (9.45 g, 0.10 mol) and NaHCO<sub>3</sub> (8.40 g, 0.10 mol) was added drop-wise for 10 minutes, while the temperature was maintained at 87-91 °C for 20 minutes. The solution was cooled to room temperature and the pH was adjusted to ~ 2 with HCl (6 M). After 1 hour a waxy white precipitate was filtered off and it was washed several times with cold water. The precipitate was then re-dissolved in hot water for purification. The solution was stored overnight at room temperature to allow the product to form. The white precipitate was filtered and washed several times with cold water and dried.

**Yield:** 7.22 g (29 %)

**IR (ν-coo(cm<sup>-1</sup>)):** 1708 (shoulder), 1613 (strong)

**<sup>1</sup>H NMR (Acetone) δ:** 0.94 (6H *d*), 1.65 (2H *m*), 1.85 (1H *m*),  
3.60-3.75 (5H *overlapped*)

### 3.3.2 *l*-Phenylalanine-*N,N*-diacetic acid (pda)

*l*-Phenylalanine-*N,N*-diacetic acid (pda) was synthesised according to the procedure developed by Bocarsly *et al.* (1990:4898). ClCH<sub>2</sub>COOH (18.90 g, 0.20 mol) solution was dissolved in water and the solution was neutralised by adding KHCO<sub>3</sub> (20.03 g, 0.20 mol). The pH of the solution stabilised at pH 7.5 after stirring for several minutes. *l*-Phenylalanine (16.52 g, 0.10 mol), neutralised with KOH (5.61 g, 0.10 mol), was added to the ClCH<sub>2</sub>COOH solution. The solution was heated (*ca.* 70 °C) on a water bath and after 10 minutes of heating KOH (11.23 g, 0.20 mol) was added over a period of 45 minutes with heating (88-92 °C). Heating was continued for 15 minutes and the second solution of ClCH<sub>2</sub>COOH (9.45 g, 0.10 mol) and KHCO<sub>3</sub> (10.01 g, 0.10 mol) was added drop-wise over 8 minutes, while the temperature was maintained at *ca.* 70 °C for 22 minutes. The solution was cooled to room temperature and the pH was adjusted to ~ 1.5 with HCl (6 M). The solution was stored covered overnight at room temperature to allow the product to form. The white precipitate was filtered and washed several times with water. Re-crystallised was carried out in acetone: water solution.

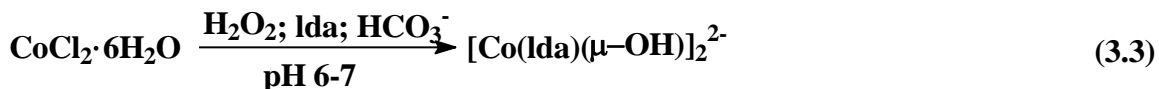
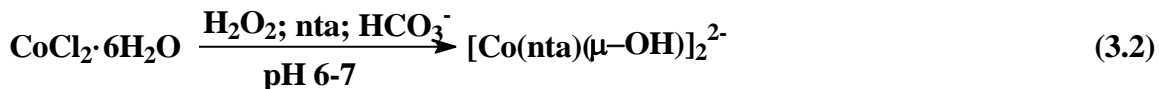
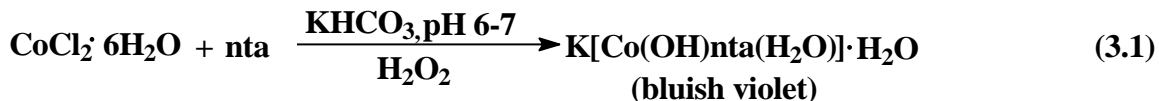
**Yield:** 9.56 g (34 %)

**IR (ν-coo(cm<sup>-1</sup>)):** 1719 (strong)

**<sup>1</sup>HNMR (Acetone) δ:** 3.05 (2H *t*), 3.25 (2H *q*), 3.82 (2H *q*), 4.25 (1H *s*),  
7.25-7.35 (5H *m*)

### 3.3.3 Complexes of *l*-leucine-*N,N*-diacetic acid (lda)

Uehara *et al.* (1971:1552) prepared several Co(L)-type complexes (L = nta, lda *etc.*). One of these complexes was K[Co(OH)nta(H<sub>2</sub>O)]·H<sub>2</sub>O according to them, see **Eq. 3.1**. It has since been proven by X-ray, UV/VIS and <sup>1</sup>H NMR in a recent study (Visser *et al.* 2002:461) that this final product was in fact a dimer, [Co(L)(μ-OH)]<sub>2</sub><sup>2-</sup>, for L = nta (**Eq. 3.2**). The lda dimer, [Co(lda)(μ-OH)]<sub>2</sub><sup>2-</sup>, was prepared by the method used by Visser and co-workers for [Co(nta)(μ-OH)]<sub>2</sub><sup>2-</sup>, see **Eq. 3.3**.



$\text{CoCl}_2 \cdot 6\text{H}_2\text{O}$  (2 g, 0.008 mol) and *l*-leucine-*N,N*-diacetic acid (2.08 g, 0.008 mol) was added to a  $\text{KHCO}_3$  solution (5 g, 0.05 mol) and heated on a water bath. The pH of the solution was adjusted to 6-7 and this solution was placed on an ice bath.  $\text{H}_2\text{O}_2$  (1 cm<sup>3</sup>, 30 %) was added to the solution and after a few hours a bluish violate precipitate separated out. The precipitate was filtered and dried. Re-crystallisation was carried out in water and blue/purple crystals were obtained after 24 hours. The structure of this product is confirmed as  $\text{K}_2[\text{Co}(\text{lda})(\mu\text{-OH})]_2 \cdot 2\text{H}_2\text{O}$  by the physical evidence presented in later paragraphs.

**Yield:** 0.24 g (3.9 %)

**IR (ν-coo-co(cm<sup>-1</sup>)):** 1625.7 (strong)

**UV/VIS :** λ<sub>max</sub>, 400 nm; λ<sub>max</sub>, 565 nm

**<sup>1</sup>H NMR (D<sub>2</sub>O) δ:** 0.95 (6H *d*), 1.65 (1H *m*), 1.90 (2H *m*), 3.56 (1H *d*) and 3.85 (1H *d*),  
3.82(1H *d*) and 4.44 (1H *d*), 4.44 (1H *t*)

### 3.3.4 *In situ* synthesis of $[\text{Co}(\text{lda})(\text{H}_2\text{O})_2]$

Solutions of  $[\text{Co}(\text{lda})(\mu\text{-OH})]_2^{2-}$  were acidified to pH = 2 (HCl, 1.0 M) and left to stand for 1 hour to form  $[\text{Co}(\text{lda})(\text{H}_2\text{O})_2]$ . This is similar to the synthesis of  $[\text{Co}(\text{nta})(\text{H}_2\text{O})_2]$  (Visser *et al.* 2002:461). Unfortunately this complex can not be obtained in the solid state due to its high solubility and hygroscopic nature. The formation of  $[\text{Co}(\text{lda})(\text{H}_2\text{O})_2]$  complex is supported by the UV/VIS results presented in paragraph 3.4.3.

### 3.3.5 Isolation of [Co(lda)(H<sub>2</sub>O)(NCS)]<sup>-</sup>

[Co(lda)(μ-OH)]<sub>2</sub><sup>2-</sup> (0.15 g) was dissolved in water (25 cm<sup>3</sup>) and the pH was adjusted to 2 (HCl, 1.0 M). An aqueous (25 cm<sup>3</sup>) solution containing NaSCN (0.034 g) was added. The reaction mixture was allowed to react at 25 °C for 30 minutes until the completion of the reaction. Ethanol was added to the mixture until precipitation occurred under reduced pressure at 70 °C. The solid was dried under vacuum in a dessicator in the presence of P<sub>2</sub>O<sub>5</sub>.

**IR (ν-COO-CO(cm<sup>-1</sup>)):** 1640.1 (strong)

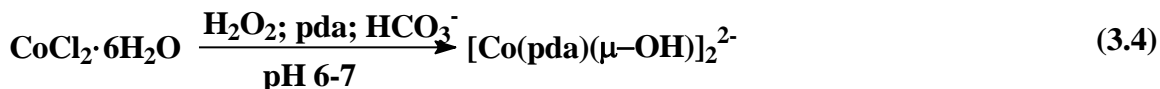
**IR (ν-SCN(cm<sup>-1</sup>)):** 2092.1 (strong)

**UV/VIS :** λ<sub>max</sub>, 400 nm; λ<sub>max</sub>, 565 nm

**<sup>1</sup>H NMR (D<sub>2</sub>O) δ:** 0.65 (6H *d*), 1.50-1.65 (3H *m*), 3.65-3.80 (5H *overlapped*)

### 3.3.6 Complexes of *l*-phenylalanine-*N,N*-diacetic acid (pda)

This complex was also prepared according to the method used to synthesis a dimer, [Co(L)(μ-OH)]<sub>2</sub><sup>2-</sup>, for L= nta by Visser *et al.* (2002:461), see **Eq. 3.4**.



CoCl<sub>2</sub>·6H<sub>2</sub>O (2 g, 0.008 mol) and *l*-phenylalanine-*N,N*-diacetic acid (2.36 g, 0.008 mol) was added to a KHCO<sub>3</sub> solution (5 g, 0.05 mol) and heated on a water bath. The pH of the solution was adjusted to 6-7 and this solution was placed on an ice bath. H<sub>2</sub>O<sub>2</sub> (1 cm<sup>3</sup>, 30 %) was added to the solution and after some few hours a bluish violet precipitate separated out. The precipitate was filtered and dried. Re-crystallisation was carried out in water and blue/purple crystals were obtained after 24 hours. The structure of this product is confirmed as K<sub>2</sub>[Co(pda)(μ-OH)]<sub>2</sub>·2H<sub>2</sub>O by the physical evidence presented in later paragraphs.

**Yield:** 0.67 g (10 %)

**IR ( $\nu$ -COO-CO( $\text{cm}^{-1}$ )):** 1632.7 (strong)

**UV/VIS :**  $\lambda_{\text{max}}$ , 400 nm;  $\lambda_{\text{max}}$ , 565 nm

**$^1\text{H NMR (D}_2\text{O)}$   $\delta$ :** 2.65 (1H *d*) and 3.85 (1H *d*), 3.45 (1H *d*) and 4.15 (1H *d*), 3.25 (1H *t*), 4.9(2H *m*), 7.30-35(5H *m*)

### 3.3.7 *In situ* synthesis of [Co(pda)(H<sub>2</sub>O)<sub>2</sub>]

Solutions of [Co(pda)( $\mu$ -OH)]<sub>2</sub><sup>2-</sup> were acidified to pH = 2 (HCl, 1.0 M) and left to stand for 1 hour to form [Co(pda)(H<sub>2</sub>O)<sub>2</sub>]. This is similar to the synthesis of [Co(lda)(H<sub>2</sub>O)<sub>2</sub>], see Paragraph 3.3.4. Unfortunately this complex also can not be obtained in the solid state due to its high solubility and hygroscopic nature. The formation of this complex is also confirmed later under the UV/VIS spectral studies discussion. The formation of [Co(pda)(H<sub>2</sub>O)<sub>2</sub>] complex is supported by the UV/VIS results presented in paragraph 3.4.4.

### 3.3.8 Isolation of [Co(pda)(H<sub>2</sub>O)(NCS)]<sup>-</sup>

[Co(pda)( $\mu$ -OH)]<sub>2</sub><sup>2-</sup> (0.15 g) was dissolved in water (25 cm<sup>3</sup>) and the pH was adjusted to 2 (HCl, 1.0 M). An aqueous (25 cm<sup>3</sup>) solution containing NaSCN (0.031 g) was added. The reaction mixture was allowed to react at 25 °C for 30 minutes until the completion of the reaction. Ethanol was added to the mixture until precipitation occurred under reduced pressure at 70 °C. The solid was dried under vacuum in a dessicator in the presence of P<sub>2</sub>O<sub>5</sub>.

**IR ( $\nu$ -COO-CO( $\text{cm}^{-1}$ )):** 1587.7 (strong)

**IR ( $\nu$ -SCN( $\text{cm}^{-1}$ )):** 2096.9 (strong)

**UV/VIS :**  $\lambda_{\text{max}}$ , 400 nm;  $\lambda_{\text{max}}$ , 565 nm

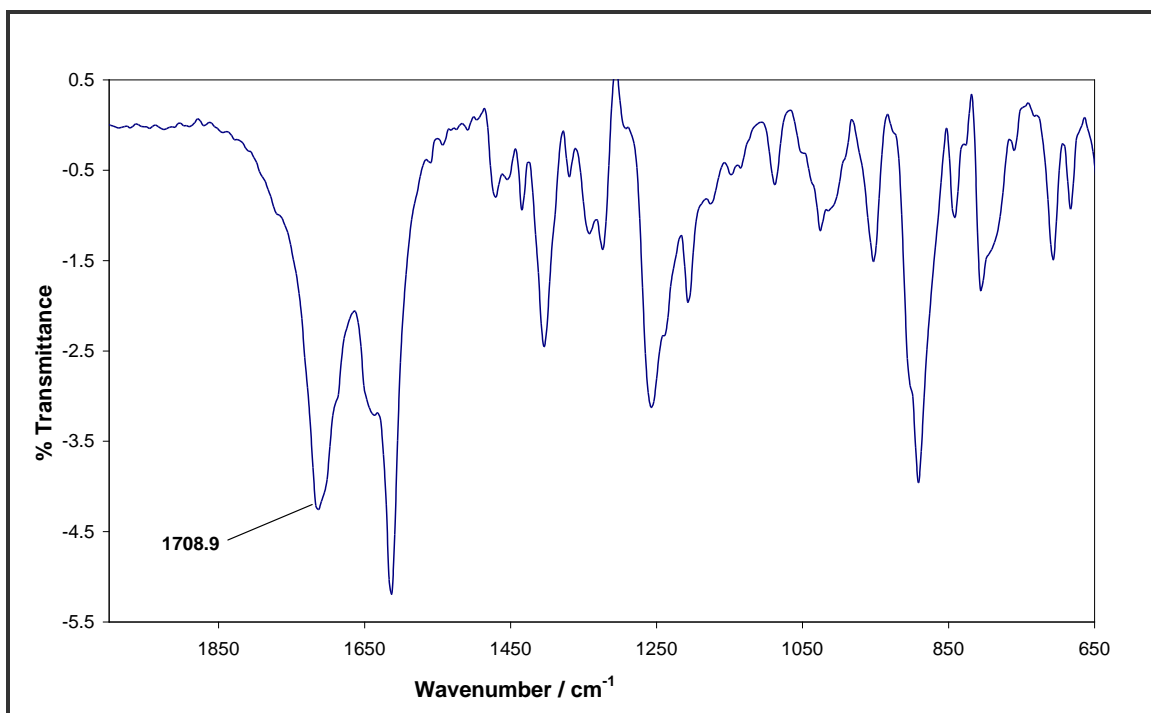
**$^1\text{H NMR (D}_2\text{O)}$   $\delta$ :** 2.75-3.00 (3H *m*), 3.60 (2H *m*), 3.90-4.10 (2H *m*), 7.05 (5H *m*)

### 3.4 Results and discussion

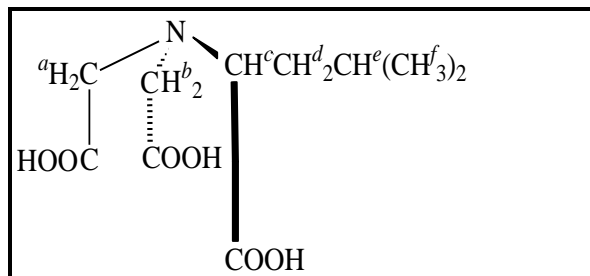
#### 3.4.1 *l*-Leucine-*N,N*-diacetic acid (lda)

##### *IR spectrum of l-leucine-N,N-diacetic acid (lda)*

The IR spectra of the free *l*-leucine-*N,N*-diacetic acid (lda) show a characteristic COO<sup>-</sup> stretching frequency at 1708 cm<sup>-1</sup>. This is indicative of un-ionised or uncoordinated COO<sup>-</sup> groups which have stretching frequencies of 1750–1700 cm<sup>-1</sup> as was stated by Nakamoto (1963:206). The IR spectrum for the free *l*-leucine-*N,N*-diacetic acid (lda) is shown in **Figure 3.1**.



**Figure 3.1:** IR spectrum of lda ligand.

*<sup>1</sup>H NMR spectrum of l-leucine-N,N-diacetic acid (lda)*

**Figure 3.2:** The structure of *l*-leucine-*N,N*-diacetic acid (lda).

The two-methylene groups between the carboxylic acids and nitrogen are equivalent and resonate at 3.60-3.75 ppm (overlapped) integrating for four protons (H<sup>a</sup> and H<sup>b</sup>). The methine proton (H<sup>c</sup>) attached to the nitrogen also resonates at 3.60-3.75 ppm (overlapped). Due to the positive inductive effect the remaining methylene protons (H<sup>d</sup>) are slightly shielded and resonate as a multiplet at 1.65 ppm integrating for two protons. The methine proton (H<sup>e</sup>) between the two methyl groups resonates as a multiplet at 1.85 ppm, while the two methyl groups resonate as doublets at 0.94 ppm integrating for six protons (H<sup>f</sup>).

The <sup>1</sup>H NMR spectrum of *l*-leucine-*N,N*-diacetic acid (lda) is presented in **Figure 3.3**.

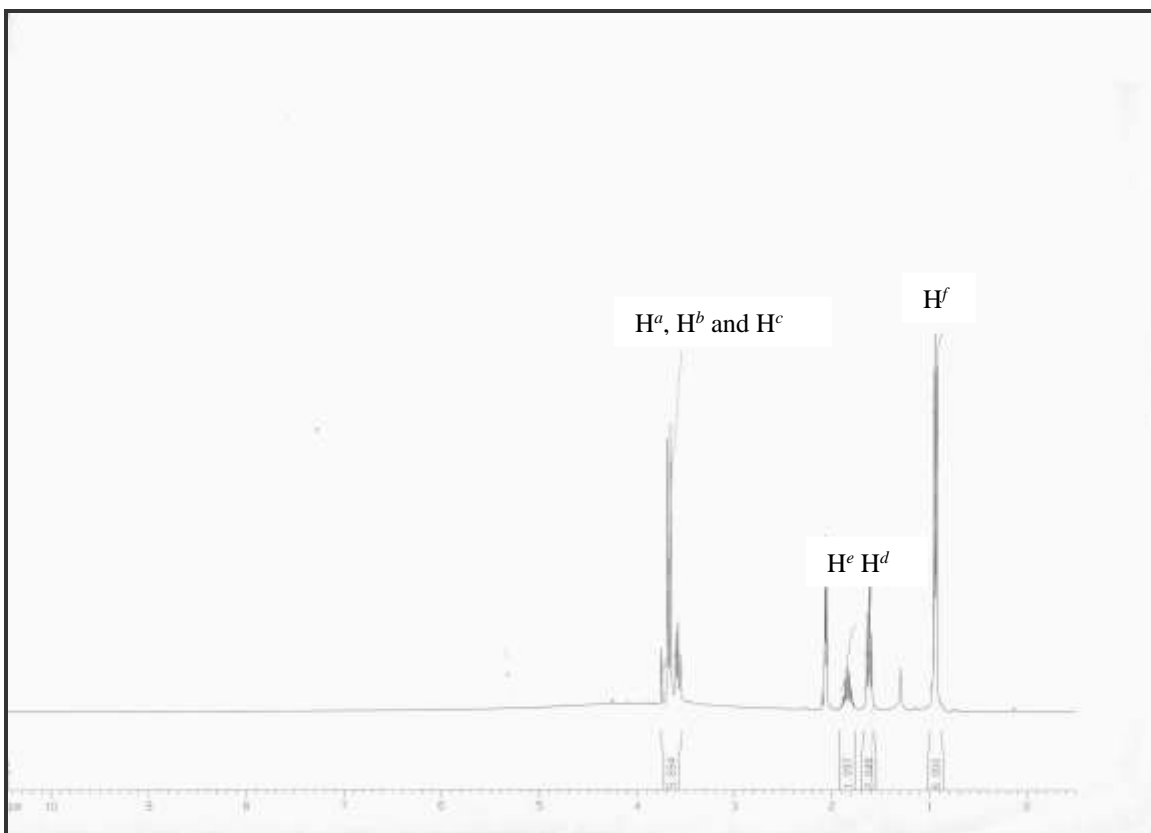


**Figure 3.3:**  $^1\text{H}$  NMR spectrum of lda in acetone.

The IR and the  $^1\text{H}$  NMR spectra presented in **Figure 3.1** and **3.3**, respectively, provide substantial evidence that the ligand was successfully synthesised.

### 3.4.2 *l*-Phenylalanine-*N,N*-diacetic acid (pda)

#### *IR spectrum of l-phenylalanine-N,N-diacetic acid (pda)*

The IR spectra of the free *l*-phenylalanine-*N,N*-diacetic acid (pda) show a characteristic  $\text{COO}^-$  stretching frequency at  $1719\text{ cm}^{-1}$ . This is indicative of un-ionised or uncoordinated  $\text{COO}^-$  groups which have stretching frequencies of  $1750\text{--}1700\text{ cm}^{-1}$  as was stated by Nakamoto (1963:206). The IR spectrum for the free *l*-phenylalanine-*N,N*-diacetic acid (pda) is shown in **Figure 3.4**.

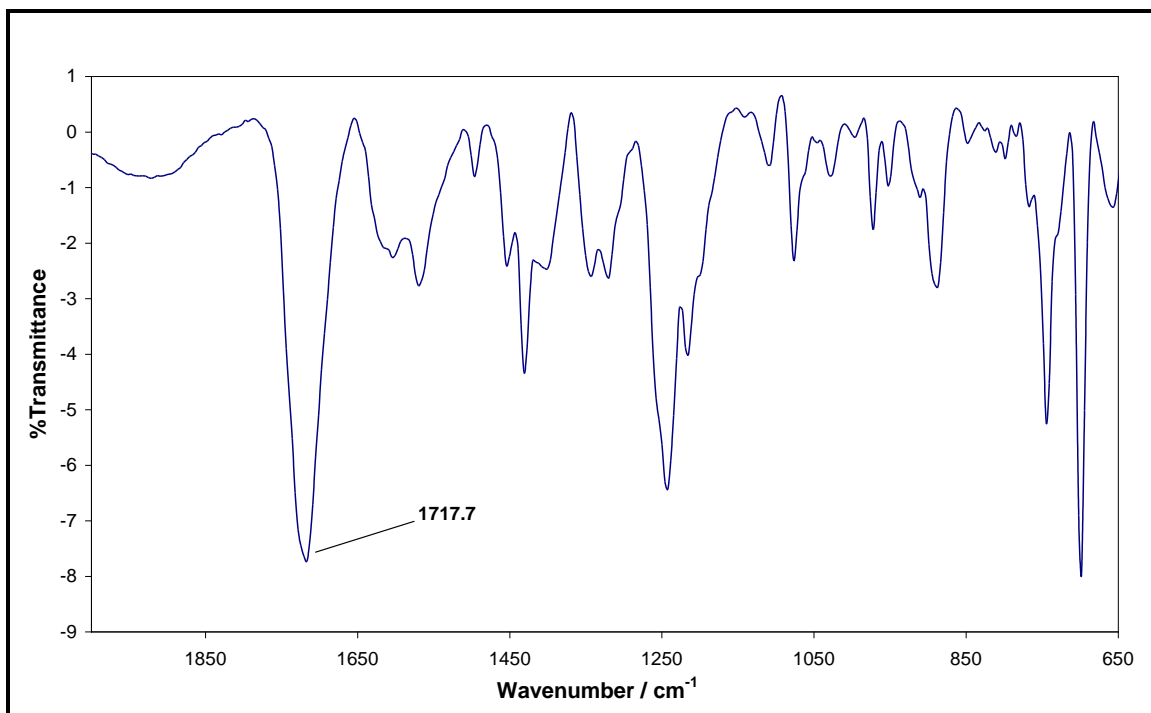


**Figure 3.4:** IR spectrum of pda ligand.

*<sup>1</sup>H NMR spectrum of l-phenylalanine-N,N-diacetic acid (pda)*

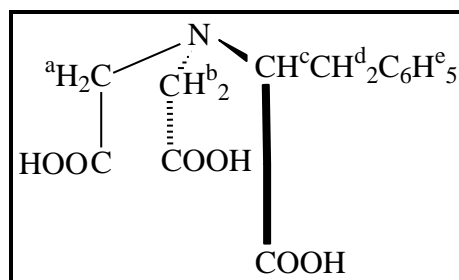


**Figure 3.5:** The structure of *l*-phenylalanine-*N,N*-diacetic acid (pda).

The five aromatic protons (H<sup>e</sup>) allocated to the phenyl group resonate as a multiplet between 7.25 and 7.35 ppm. A singlet assigned to the methine proton (H<sup>c</sup>) attached to the nitrogen shows at 4.25 ppm. The benzylic methylene protons (H<sup>d</sup>) are observed at 3.82 ppm integrating for two protons. The remaining methylene protons (H<sup>a</sup> and H<sup>b</sup>) between the carboxylic acids and nitrogen are equivalent and resonate at 3.05 ppm and 3.25 ppm integrating for four protons.

The  $^1\text{H}$  NMR spectrum of *l*-phenylalanine-*N,N*-diacetic acid (pda) is presented in **Figure 3.6**.

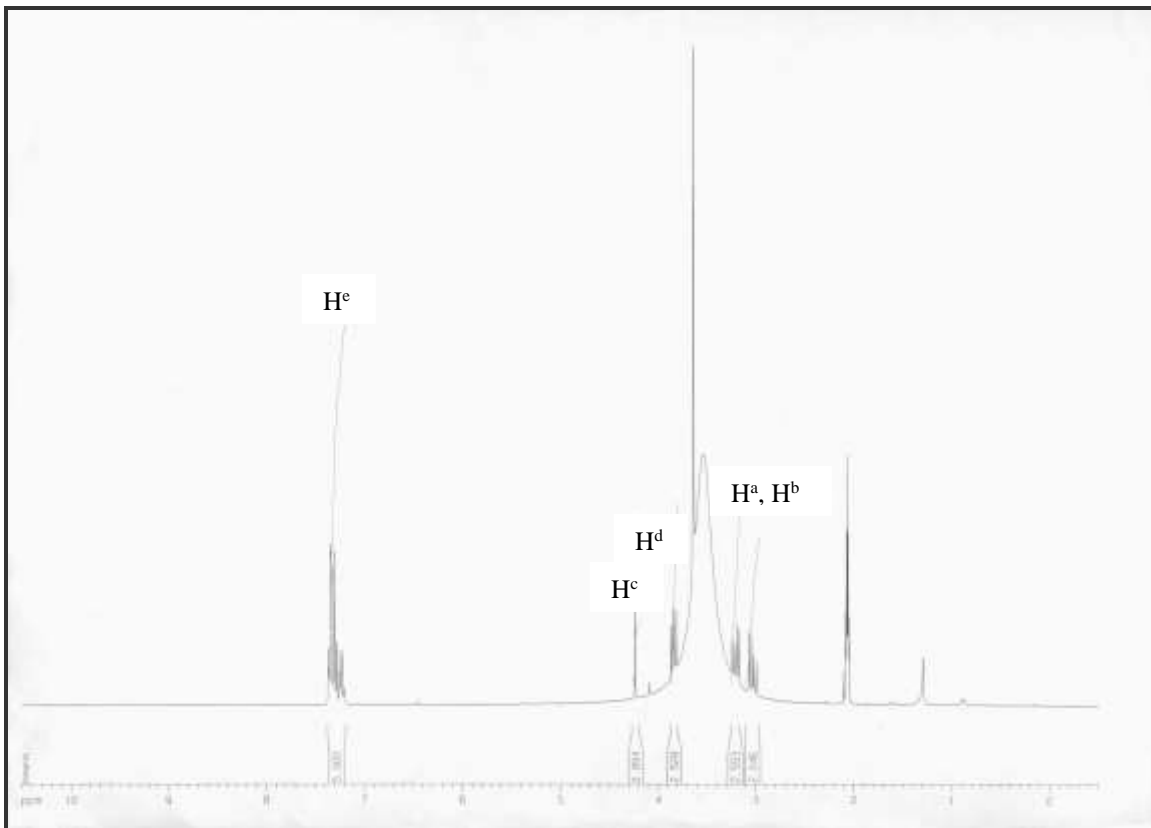


**Figure 3.6:**  $^1\text{H}$  NMR spectrum for pda in acetone.

The IR and the  $^1\text{H}$  NMR spectra presented in **Figure 3.4** and **3.6**, respectively, provide substantial evidence that the ligand was successfully synthesised.

### 3.4.3 Complexes of *l*-leucine-*N,N*-diacetic acid (lda)

#### *IR spectra of $[\text{Co}(\text{lda})(\mu\text{-OH})]_2^{2-}$*

The identification of this type of complex by IR techniques is complicated and not always conclusive as mentioned earlier in Paragraph 3.1. The IR spectra of  $[\text{Co}(\text{lda})(\mu\text{-OH})]_2^{2-}$  (**Figure 3.7**) show a strong carboxylate peak at  $1631\text{ cm}^{-1}$ . This value is indicative of  $\text{COO}^-$  groups coordinated to a metal centre such as Co(III) (Nakamoto 1963:206).

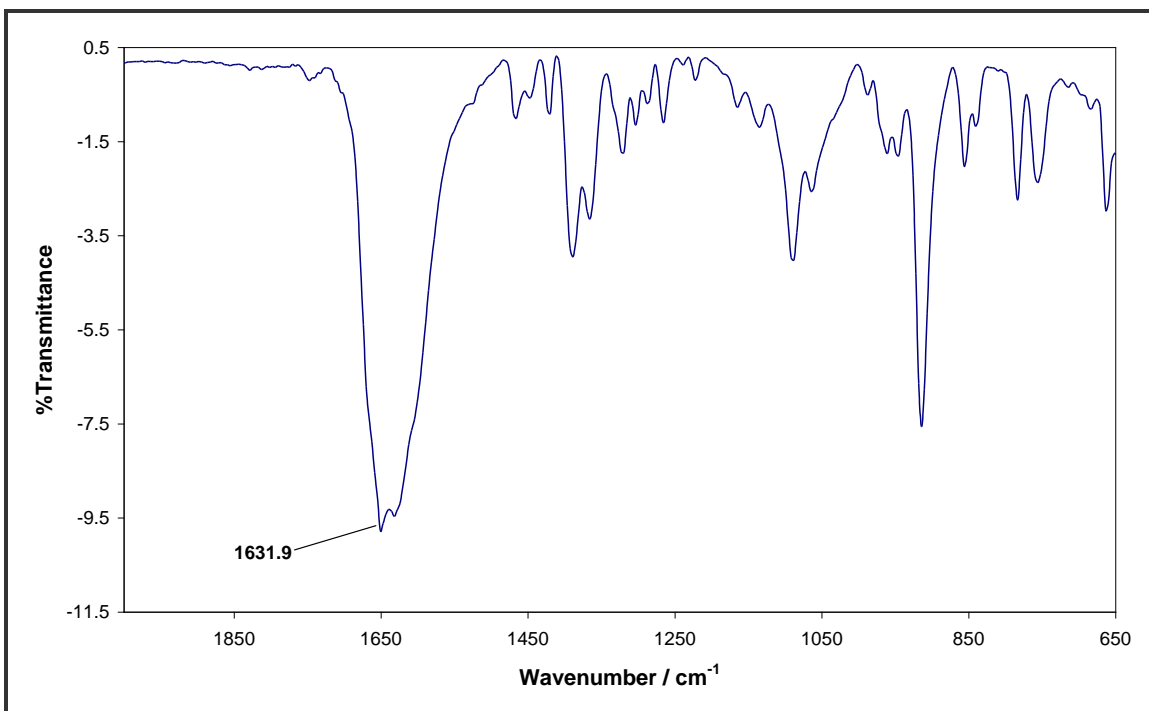


**Figure 3.7:** IR spectrum of  $[\text{Co}(\text{lda})(\mu\text{-OH})]_2^{2-}$ .

*<sup>1</sup>H NMR spectra of  $[\text{Co}(\text{lda})(\mu\text{-OH})]_2^{2-}$*

The <sup>1</sup>H NMR spectrum (see **Figure 3.8**) obtained for  $[\text{Co}(\text{lda})(\mu\text{-OH})]_2^{2-}$  integrates for fourteen lda protons. All fourteen protons of lda are non-equivalent, leading to four distinguishable doublets, each integrating for one proton; one triplet, integrating for one proton; two multiplets, each integrating for one proton and two protons respectively; and one doublet, integrating for six protons; all occurring in the 0.85–4.55 ppm region. The <sup>1</sup>H NMR spectrum for  $[\text{Co}(\text{lda})(\mu\text{-OH})]_2^{2-}$  is shown in **Figure 3.8**. The possible structure for this complex is illustrated in **Figure 3.10**.

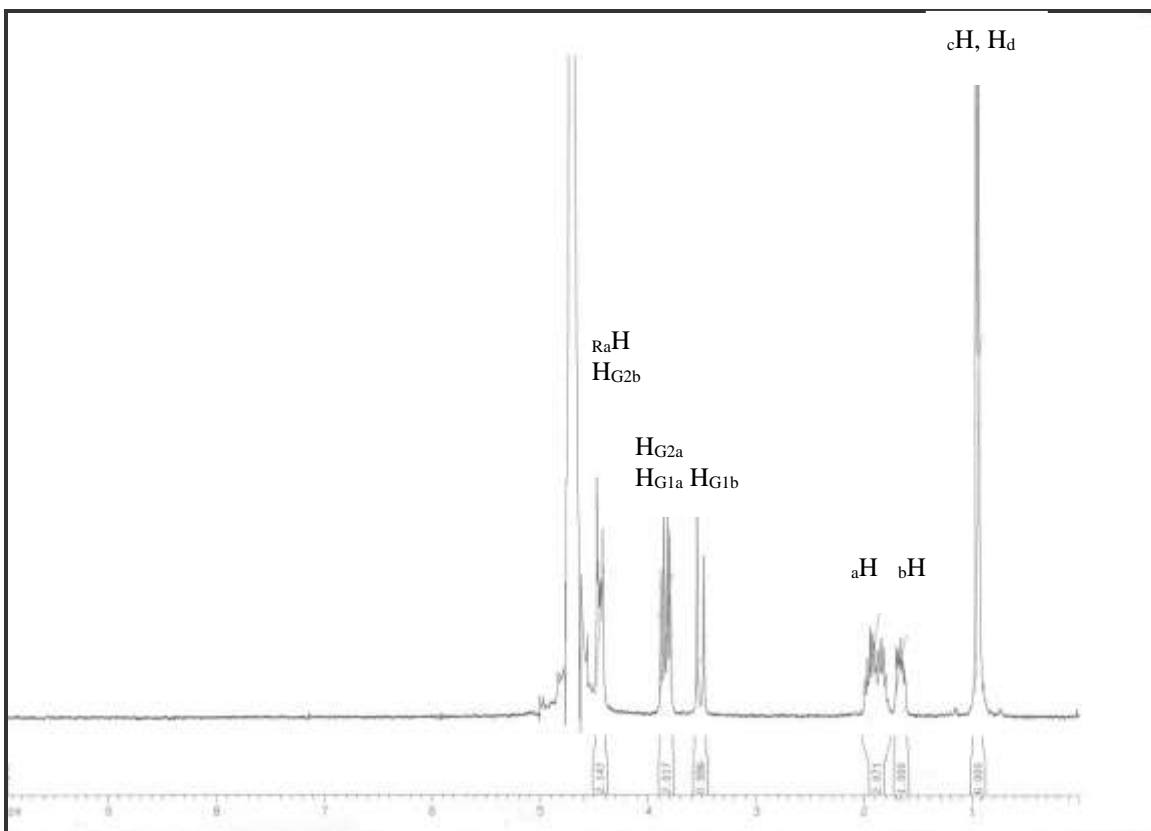


**Figure 3.8:**  $^1\text{H}$  NMR spectrum for  $[\text{Co}(\text{lda})(\mu\text{-OH})]_2^{2-}$  in  $\text{D}_2\text{O}$ .

The investigation of  $[\text{Co}(\text{nta})(N\text{-Eten})]$  with  $^1\text{H}$  NMR by Visser *et al.* (2001:175) provided new possibilities to the identification of Co(III)-nta and related complexes.

The  $^1\text{H}$  NMR spectra can be used as follows to gain evidence regarding the structures of  $[\text{Co}(\text{nta})(N\text{-Eten})]$ . The acetate protons of the two G rings of nta ( $\text{H}_{\text{G}2\text{a}}$  and  $\text{H}_{\text{G}1\text{a}}$  in **Figure 3.9**) are non-equivalent if  $L \neq L'$ , while the protons of specific G ring ( $\text{H}_{\text{G}2\text{a}}$  and  $\text{H}_{\text{G}1\text{a}}$  in **Figure 3.9**) are also non-equivalent under the same conditions for L and L'. This will result in two distinguishable doublets in the 3.9 and 4.4 ppm region as explained by Visser *et al.* (2001:175). A multiplet in the same region was assigned to the non-equivalent protons of the remaining acetate ring (R ring). Both doublets integrate for one proton each as expected for non-equivalent protons. Complexes with nta where the protons of a two glycinato G rings ( $\text{H}_{\text{G}2\text{a}}$  and  $\text{H}_{\text{G}1\text{a}}$ ) are equivalent where  $L = L'$  will exhibit totally different spectra than the above.

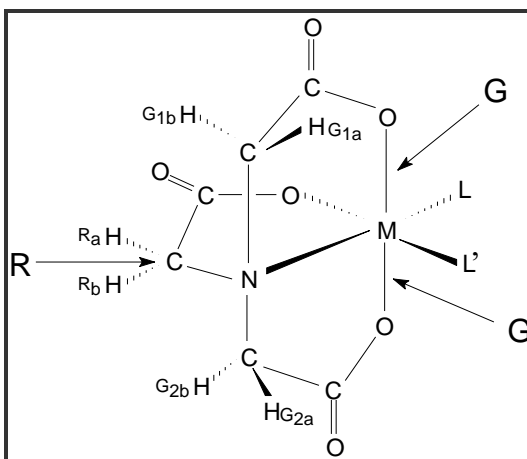


**Figure 3.9:** Glycinato rings in Co(III)-nta complexes.

The same method of identification discussed by Visser and co-workers can be applied to metal complexes with lda where the acetate protons of the two G rings ( $H_{G2a}$  and  $H_{G1a}$  in **Figure 3.10**) are non-equivalent and the longer 4-methyl pentionato ring is situated in the R position. The  $^1H$  NMR spectrum (see **Figure 3.8**) obtained for  $[Co(lda)(\mu-OH)]_2^{2-}$  is basically the same as for  $[Co(nta)(N-Eten)]$  (Visser *et al.* 2001:175) because the acetate protons of the two G rings of lda ( $H_{G2a}$  and  $H_{G1a}$  in **Figure 3.10**) are also non-equivalent. The only difference in their spectra is that the chemical shifts of these acetate protons vary slightly.

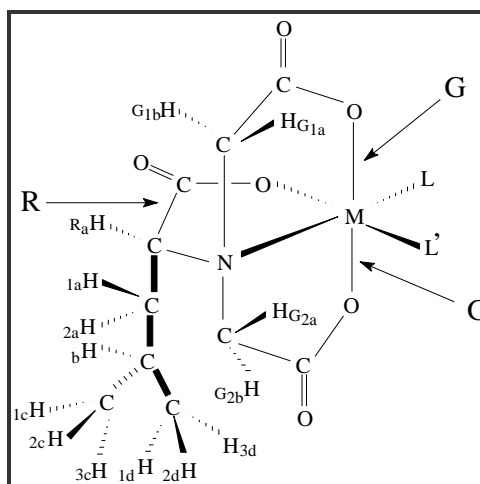


**Figure 3.10:** Glycinato and 4-methyl pentionato rings in Co(III) lda complexes.

The IR and the  $^1\text{H}$  NMR spectra presented in **Figure 3.7** and **3.8**, respectively, indicate the presence of lida ligand bonded to the metal center. Unfortunately the crystals obtained for this complex were not suitable for X-ray diffraction data collection. The existence of the hydroxo bridges is supported by the UV/VIS results presented in the paragraph below.

#### *UV/VIS spectral studies of $\text{K}_2[\text{Co}(\text{lida})(\mu\text{-OH})_2\cdot 2\text{H}_2\text{O}$*

##### *Effect of pH on different Co(III)-lida species in solution*

$\text{K}_2[\text{Co}(\text{lida})(\mu\text{-OH})_2\cdot 2\text{H}_2\text{O}$  complex were dissolved in water (pH *ca.* 6.5) and the UV/VIS spectrum was recorded in the UV region (205 (sh), 218 (s), 304 (w)).  $\text{NaHCO}_3$  was added to this solution (pH *ca.* 7.5) and the spectrum was again recorded. No change in absorption maxima at 218 and 304 nm was observed. The results indicate that the complex is not affected by pH in the 6.5-7.5 regions. Unfortunately no UV/VIS spectrum for the  $\text{K}_2[\text{Co}(\text{lida})(\mu\text{-OH})_2\cdot 2\text{H}_2\text{O}$  complex was published by Uehara *et al.* (1971:1552) to compare with these spectra.

A fresh solution of  $\text{K}_2[\text{Co}(\text{lida})(\mu\text{-OH})_2\cdot 2\text{H}_2\text{O}$  was again prepared and its spectrum recorded (200-400 nm), **(1)** in **Figure 3.11**. A few drops of HCl (1.0 M) were added to this solution (pH *ca.* 2) and the spectrum immediately changed with the disappearance of the peak at 304 nm **(2)** and a shift of the absorption maximum at 218 nm to 225 nm. The addition of base ( $\text{NaHCO}_3$ ) to this solution (pH *ca.* 7) resulted in the immediate change in the spectrum with absorption maxima at 225 nm **(3)**. The absorption maxima at 304 nm observed in solution **(1)** did not reappear, indicating that this observed pH dependency of  $[\text{Co}(\text{lida})(\mu\text{-OH})_2]^{2-}$  is not reversible, in other words not a normal acid/base equilibrium, but possibly an acid assisted cleavage of the hydroxo bridges as shown for  $[\text{Co}(\text{nta})(\mu\text{-OH})_2]^{2-}$  (Visser *et al.* 2002:461).

The spectrum (1) in **Figure 3.11** was only attained after the solutions of (3) were left to stand for several days, indicating that the species formed in (3) slowly regain the structure of (1).

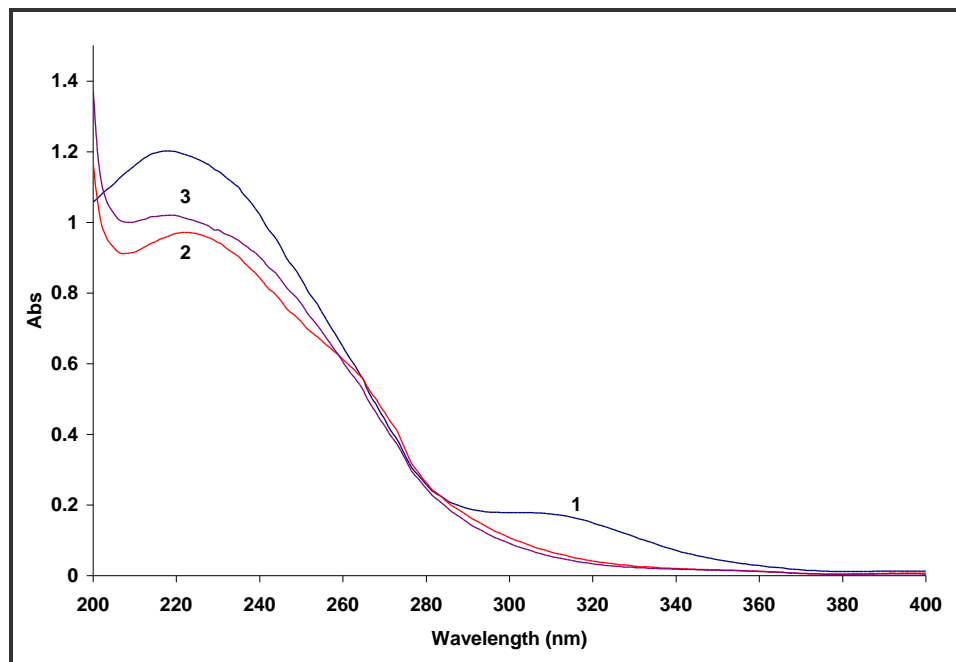


**Figure 3.11:** UV/VIS spectra of different Co(III)-lda species in solution.

- 1  $[\text{Co}(\text{lda})(\mu\text{-OH})]_2^{2-}$  ( $3.3 \times 10^{-4}$  M) pH 5-7 ; 2  $[\text{Co}(\text{lda})(\text{H}_2\text{O})_2]$ , pH ~ 2;  
3  $[\text{Co}(\text{lda})(\text{H}_2\text{O})(\text{OH})]^-$ , pH 5-7, T = 25.1 °C.

The experiment in **Figure 3.11** was also repeated in the visible region, giving the same results. A fresh solution of  $\text{K}_2[\text{Co}(\text{lda})(\mu\text{-OH})]_2 \cdot 2\text{H}_2\text{O}$  was prepared and dissolved in water (pH *ca.* 6.5). The UV/VIS spectrum was recorded (350-700 nm), (1) in **Figure 3.12**, which showed peaks at 370.0 (s) and 550.0 (w) nm and a shoulder at 400.0 (sh) nm. The pH of the solution was adjusted to ~ 2 (HCl, 1.0 M) and the spectrum was recorded (2) which shows an immediate decrease in absorption at 400 nm and a shift of the absorption maximum at 565 to 550. The pH was again adjusted to ~ 6.5 (KOH, 1.0 M) and the spectrum was recorded (3).

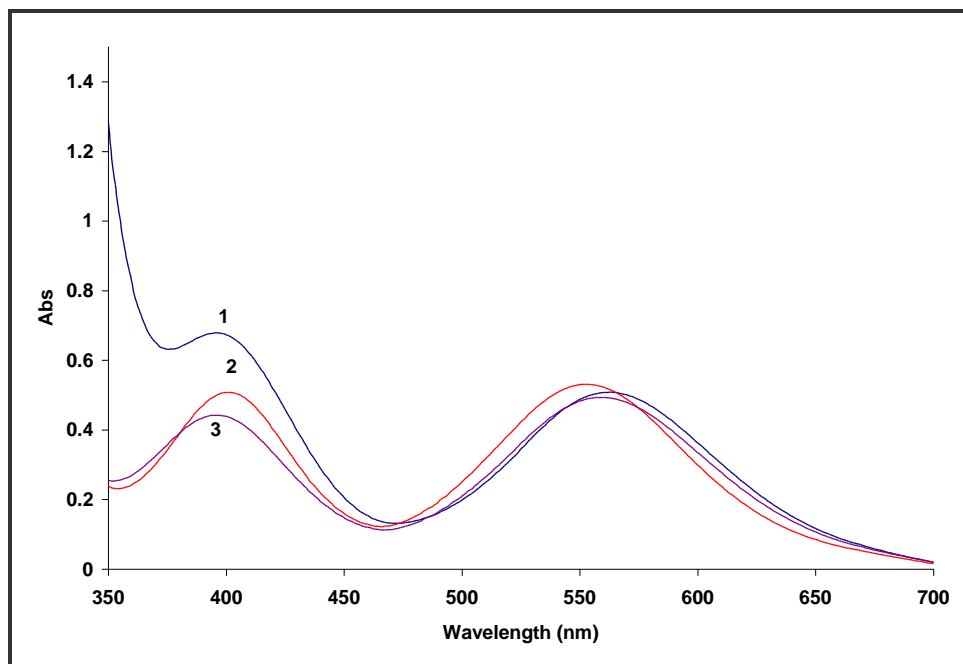
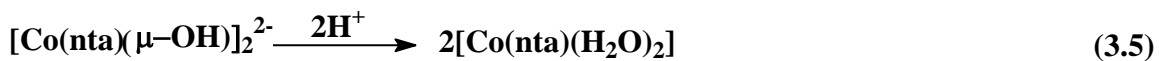


**Figure 3.12:** UV/VIS spectra of different Co(III)-lda species in solution.

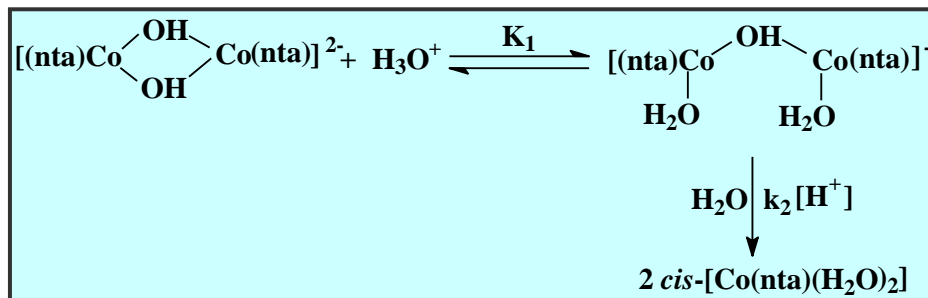
- 1**  $[\text{Co}(\text{lda})(\mu\text{-OH})]_2^{2-}$  ( $1.3 \times 10^{-3}$  M) pH 5-7 ; **2**  $[\text{Co}(\text{lda})(\text{H}_2\text{O})_2]$ , pH ~ 2;  
**3**  $[\text{Co}(\text{lda})(\text{H}_2\text{O})(\text{OH})]^-$ , pH 5-7,  $T = 25.1$  °C.

These results are similar to that found for the pH dependence of  $[\text{Co}(\text{nta})(\mu\text{-OH})]_2^{2-}$  (Visser *et al.* 2002:461). Visser and co-workers (2002:461) proposed that the hydroxo bridges are cleaved upon acidification of the dimer to form the *cis*-diaqua complex  $[\text{Co}(\text{nta})(\text{H}_2\text{O})_2]$  (see **Eq. 3.5**).



The acidic cleavage of the hydroxo bridges of  $[\text{Co}(\text{nta})(\mu\text{-OH})]_2^{2-}$  has been investigated by other workers (Thacker & Higginson, 1975:704 and Meloon & Harris, 1977:434). In both these studies a fast initial reaction was observed, followed by a second slower reaction upon allowing  $[\text{Co}(\text{nta})(\mu\text{-OH})]_2^{2-}$  to stand in moderately acidic solutions (*ca.* pH 4) for 20–30 minutes. It was observed that the aqueous solutions of  $[\text{Co}(\text{nta})(\mu\text{-OH})]_2^{2-}$  did not show any evidence of normal acidic or basic properties when titrated rapidly with dilute acid and back-titrated with a base. It was postulated that these two reactions

involved the formation of a mono-hydroxo-bridged species that dissociates to form *cis*-[Co(nta)(H<sub>2</sub>O)<sub>2</sub>] in the second, slower step (**Scheme 3.2**).



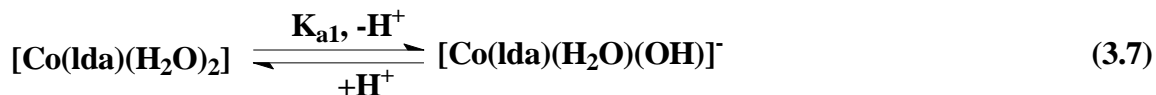
**Scheme 3.2:** Acidic cleavage of [Co(nta)(μ-OH)]<sub>2</sub><sup>2-</sup> (Thacker & Higginson, 1975:704 and Meloon & Harris, 1977:434).

We therefore propose the following:

1. Similar results was found by Visser *et al.* (2002:461) for the preparation of [Co(nta)(μ-OH)]<sub>2</sub><sup>2-</sup> and this was supported by the X-ray and UV/VIS data obtained for these complex. The complex prepared by Uehara *et al.* (1971:1552) was not [Co(OH)lda(H<sub>2</sub>O)] but rather [Co(lda)(μ-OH)]<sub>2</sub><sup>2-</sup>.
2. Acidification of the dimer (steps (1) to (2) in **Figure 3.11** and **3.12**) leads to the formation of a diaqua complex, [Co(lda)(H<sub>2</sub>O)<sub>2</sub>] as in **Eq. 3.6**. This is also supported by results obtained by Thacker & Higginson, (1975:704) as well as by Meloon & Harris, (1977:434) studies.



3. An acid dependency is observed for [Co(lda)(H<sub>2</sub>O)<sub>2</sub>] and is illustrated in **Eq. 3.7**. The determination of the acid dissociation constant, K<sub>a1</sub>, is discussed in Chapter 4.



Similar results were found by Visser and co-workers (2002:461) as well as by Potgieter *et al.* (2005:1968), for the pH dependence of  $[\text{Co}(\text{nta})(\text{H}_2\text{O})_2]$  and  $[\text{Co}(\text{apda})(\text{H}_2\text{O})_2]$ , respectively. The acid dissociation constants of  $[\text{Co}(\text{nta})(\text{H}_2\text{O})_2]$  and  $[\text{Co}(\text{apda})(\text{H}_2\text{O})_2]$ , were determined spectrophotometrically as 6.52(2) and 6.23(2), respectively.

### *IR spectra of $[\text{Co}(\text{lda})(\text{H}_2\text{O})(\text{NCS})]^-$*

The IR spectra obtained for this complex show a stretching frequency for  $\text{COO}^-$  at  $1640 \text{ cm}^{-1}$  corresponding to the presence of coordinated  $\text{COO}^-$  groups. The stretching frequency at  $2092 \text{ cm}^{-1}$  (**Figure 3.13**) correlates well with the stretching frequency of  $2082.0 \text{ cm}^{-1}$  that was assigned to  $\nu(\text{SCN})$  for the  $[\text{Cr}(\text{NCS})_3\text{py}_3]$  complex, reported by DasSarma *et al.* (1979:3618). The presence of SCN peak indicates the bonding of  $\text{NCS}^-$  ligand to the metal centre.

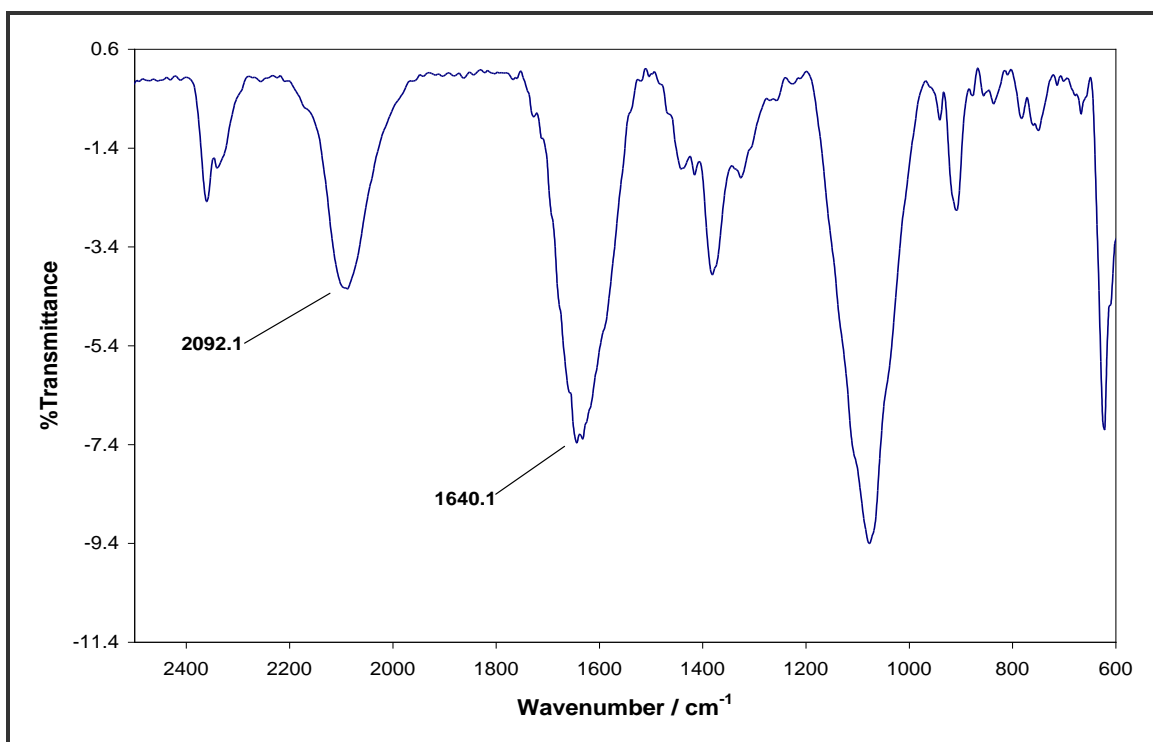


**Figure 3.13:** IR spectrum of  $[\text{Co}(\text{lda})(\text{H}_2\text{O})(\text{NCS})]^-$ .

*<sup>1</sup>H NMR spectra of [Co(lda)(H<sub>2</sub>O)(NCS)]<sup>-</sup>*

The <sup>1</sup>H NMR spectrum for [Co(lda)(H<sub>2</sub>O)(NCS)]<sup>-</sup> integrates for fourteen lda protons. All fourteen protons of lda are non-equivalent, leading to five protons that resonate at 365-380 ppm (overlapped); one multiplet, integrating for three protons and resonate at 1.50-1.65 ppm; and one doublet, integrating for six protons and resonate at 0.65 ppm. The <sup>1</sup>H NMR spectrum for [Co(lda)(H<sub>2</sub>O)(NCS)]<sup>-</sup> show the presence of lda ligand (see **Figure 3.2**) bonded to the metal center.

*UV/VIS spectra of [Co(lda)(H<sub>2</sub>O)(NCS)]<sup>-</sup>*

The UV/VIS spectral change of a solution of [Co(lda)(H<sub>2</sub>O)<sub>2</sub>] (pH = 2) upon the addition NaSCN (0.034 g) was recorded (**Figure 3.14**). The spectrum shows an increase in absorption with the peak formation at 400 nm. The kinetics of this reaction is discussed in Chapter 4.

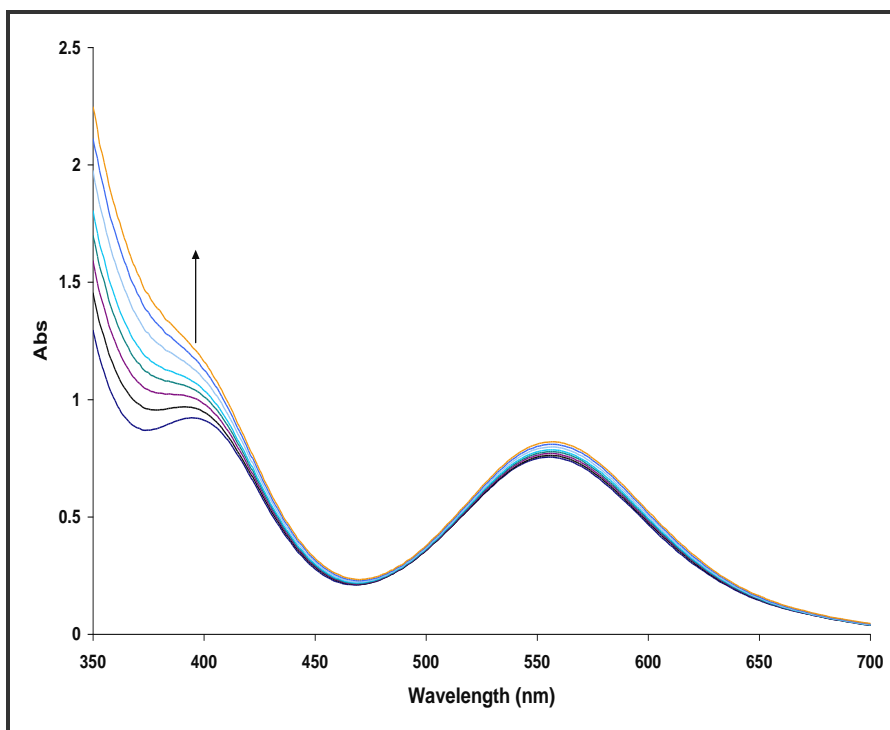


**Figure 3.14:** UV/VIS spectral changes for the reaction between [Co(lda)(H<sub>2</sub>O)<sub>2</sub>] ( $7.9 \times 10^{-3}$  M) with NCS<sup>-</sup> ions. T = 25.3 °C, [NCS<sup>-</sup>] =  $1.7 \times 10^{-2}$  M.

### 3.4.4 Complexes of *l*-phenylalanine-*N,N*-diacetic acid (pda)

#### *IR spectra of [Co(pda)(μ-OH)]<sub>2</sub><sup>2-</sup>*

The IR spectrum of  $[\text{Co}(\text{pda})(\mu\text{-OH})]_2^{2-}$  complex (**Figure 3.15**) show a strong carboxylate peaks at  $1633\text{ cm}^{-1}$ . This value is indicative of  $\text{COO}^-$  groups coordinated to metal centre such as Co(III). The stretching frequency at  $1633\text{ cm}^{-1}$  obtained for  $[\text{Co}(\text{pda})(\mu\text{-OH})]_2^{2-}$  correlates very well to the value of  $\sim 1640\text{ cm}^{-1}$  observed by Uehara *et al.* (1971:1548) for their Co(III)-pda complex.

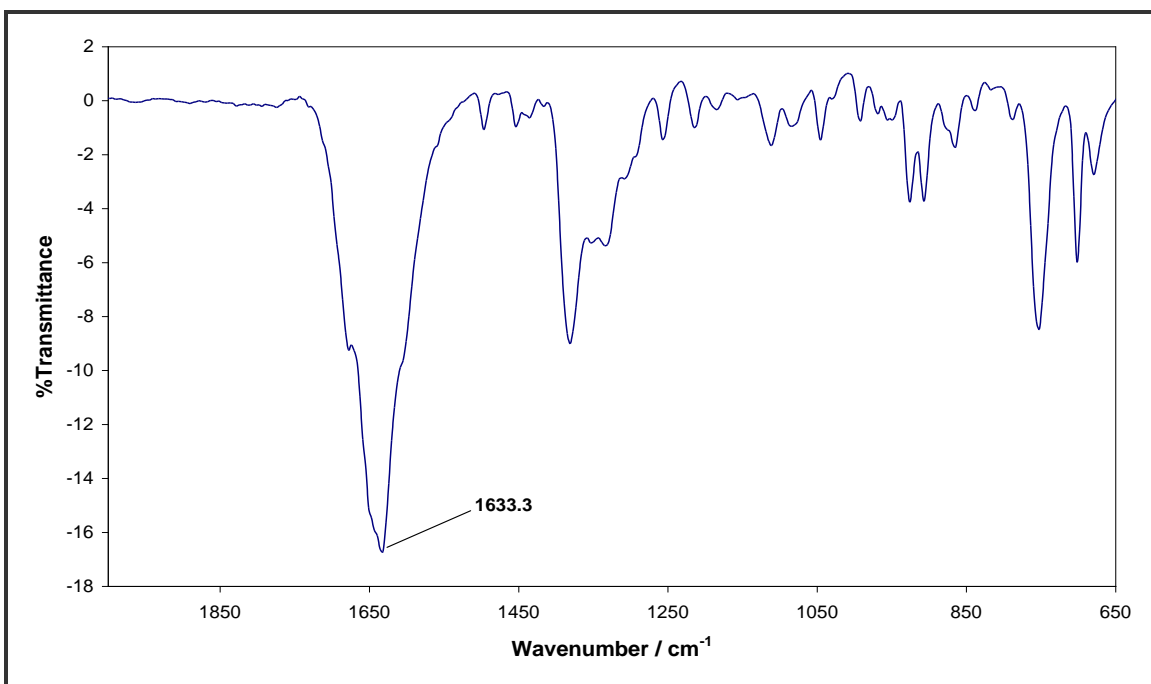


**Figure 3.15:** IR spectrum of  $[\text{Co}(\text{pda})(\mu\text{-OH})]_2^{2-}$ .

#### *<sup>1</sup>H NMR spectra of [Co(pda)(μ-OH)]<sub>2</sub><sup>2-</sup>*

The  $^1\text{H}$  NMR spectrum (see **Figure 3.16**) obtained for  $[\text{Co}(\text{pda})(\mu\text{-OH})]_2^{2-}$  integrates for twelve pda protons. All twelve protons of pda are non-equivalent, leading to four distinguishable doublets each integrating for one proton; one triplet, integrating for one proton; one multiplets, integrating for two protons; and the remaining multiplet, integrating for five phenyl protons; all occurring in the 2.6–7.5 ppm region. The

$^1\text{H}$  NMR spectrum for  $[\text{Co}(\text{pda})(\mu\text{-OH})]_2^{2-}$  is shown in **Figure 3.16**. The possible structure for this complex is illustrated in **Figure 3.17**.

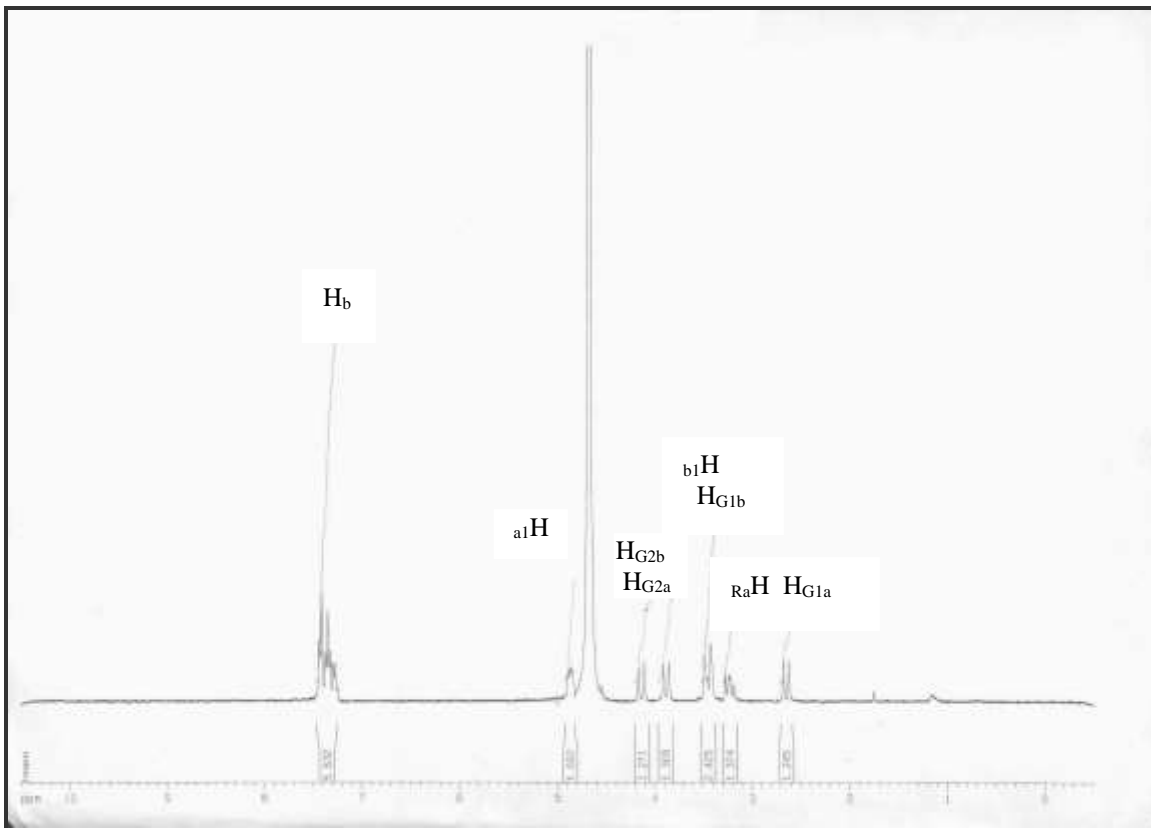


**Figure 3.16:**  $^1\text{H}$  NMR spectrum for  $[\text{Co}(\text{pda})(\mu\text{-OH})]_2^{2-}$  in  $\text{D}_2\text{O}$ .

Similar to complexes of *lda* the same method of identification discussed by Visser *et al.* (2001:175) can also be applied to metal complexes with *pda* because also with this complex the acetate protons of the two G rings ( $\text{H}_{\text{G}2\text{a}}$  and  $\text{H}_{\text{G}1\text{a}}$  in **Figure 3.17**) are non-equivalent and the longer 3-phenylpropionato ring is also situated in the R position. The  $^1\text{H}$  NMR spectrum (see **Figure 3.16**) obtained for  $[\text{Co}(\text{pda})(\mu\text{-OH})]_2^{2-}$  is also basically the same as for  $[\text{Co}(\text{nta})(N\text{-Eten})]$  (Visser *et al.* 2001:175) because the acetate protons of the two G rings of *pda* ( $\text{H}_{\text{G}2\text{a}}$  and  $\text{H}_{\text{G}1\text{a}}$  in **Figure 3.17**) are non-equivalent. The only difference with  $[\text{Co}(\text{lda})(\mu\text{-OH})]_2^{2-}$  is that the chemical shifts of the acetate protons of their spectra also vary slightly.

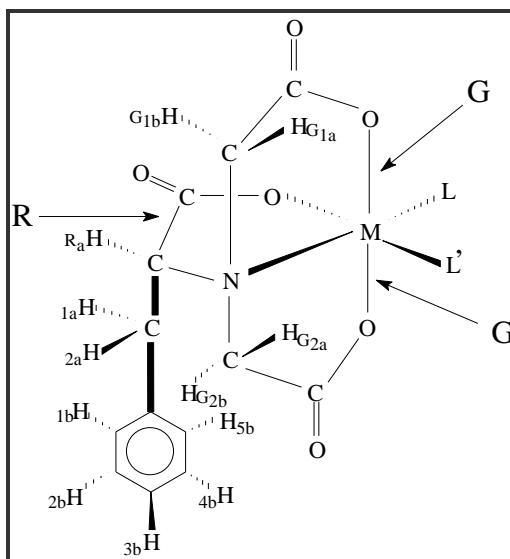


**Figure 3.17:** Glycinato and 3-phenylpropionato rings in Co(III)-pda complexes.

The IR and the  $^1\text{H}$  NMR spectra presented in **Figure 3.15** and **3.16**, respectively, indicate the presence of pda ligand bonded to the metal center. Unfortunately the same as Co(III)-lda the crystals obtained for this complex were also not suitable for X-ray diffraction data collection so that we can be able to demonstrate the geometric arrangement of the bonded ligand. Similar to Co(III)-lda the existence of the hydroxo bridges is supported by the UV/VIS results presented in the paragraph below.

#### *UV/VIS spectral studies of $\text{K}_2[\text{Co}(\text{pda})(\mu\text{-OH})_2]$*

##### *Effect of pH on different Co(III)-pda species in solution*

The UV/VIS spectra of  $\text{K}_2[\text{Co}(\text{pda})(\mu\text{-OH})_2]$  were recorded in the UV region (218 (sh), 228 (s), 305 (w)), see **Figure 3.18** and show similar behavior to that found for the pH dependence of  $\text{K}_2[\text{Co}(\text{lda})(\mu\text{-OH})_2]\cdot 2\text{H}_2\text{O}$  (**Figure 3.11**).

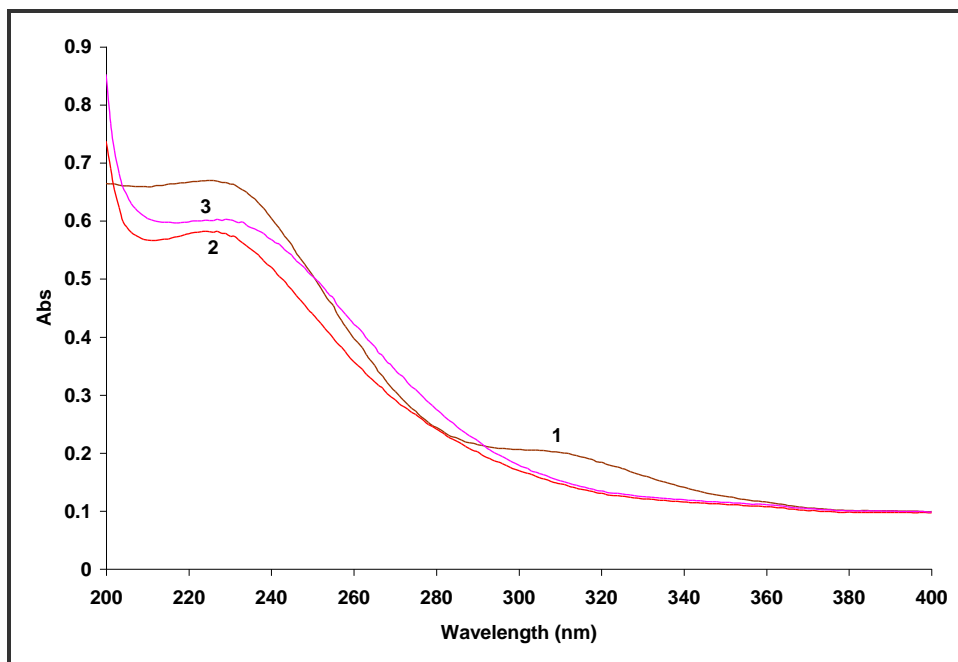


**Figure 3.18:** UV/VIS spectra of different Co(III)-pda species in solution.

- 1**  $[\text{Co}(\text{pda})(\mu\text{-OH})]_2^{2-}$  ( $3.0 \times 10^{-4}$  M) pH 5-7 ; **2**  $[\text{Co}(\text{pda})(\text{H}_2\text{O})_2]$ , pH ~ 2;  
**3**  $[\text{Co}(\text{pda})(\text{H}_2\text{O})(\text{OH})]^-$ , pH 5-7, T = 25.1 °C.

The UV/VIS spectra of  $\text{K}_2[\text{Co}(\text{pda})(\mu\text{-OH})]_2$  recorded in the visible region, see **Figure 3.19** also show similar behavior to that of  $\text{K}_2[\text{Co}(\text{lda})(\mu\text{-OH})]_2 \cdot 2\text{H}_2\text{O}$  complex (**Figure 3.12**) for the repeated experiment in **Figure 3.11**. From this study it also appears that the hydroxo bridges in the  $[\text{Co}(\text{pda})(\mu\text{-OH})]_2^{2-}$  (**1**) were cleaved in the first protonation step during the addition of acid (pH 2) to form the diaqua complex (**2**),  $[\text{Co}(\text{pda})(\text{H}_2\text{O})_2]$ . It was also found that an aqua-hydroxo complex (**3**),  $[\text{Co}(\text{pda})(\text{H}_2\text{O})(\text{OH})]^-$  is formed in the next deprotonation step during the addition of a base (pH 5-7). The absorption maxima at 304 nm observed in solution (**1**) also did not reappear, indicating that this observed pH dependency of  $[\text{Co}(\text{pda})(\mu\text{-OH})]_2^{2-}$  is also not reversible, as was observed for  $[\text{Co}(\text{lda})(\mu\text{-OH})]_2^{2-}$ .

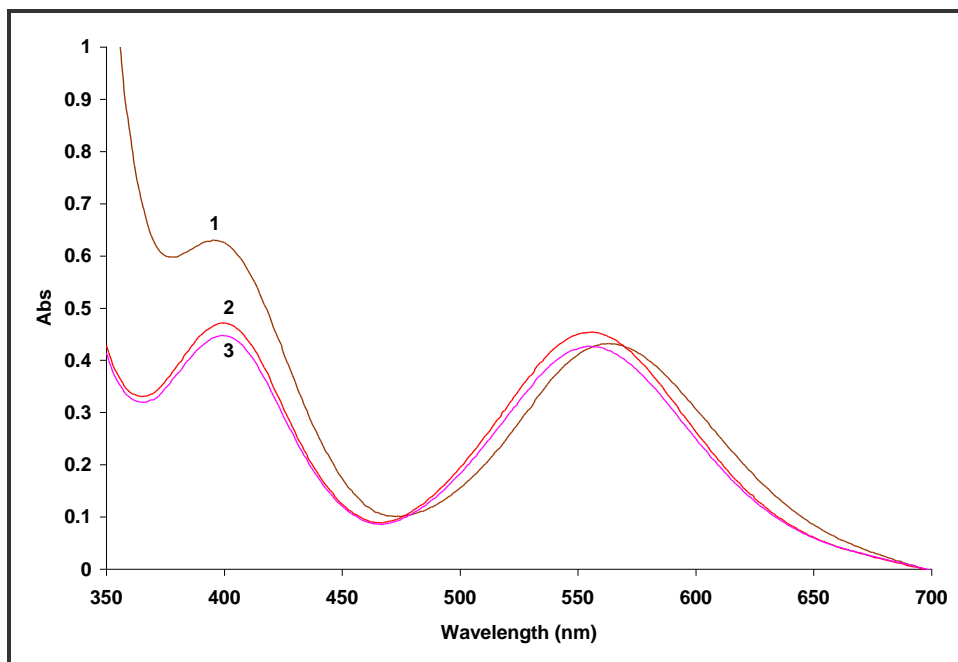


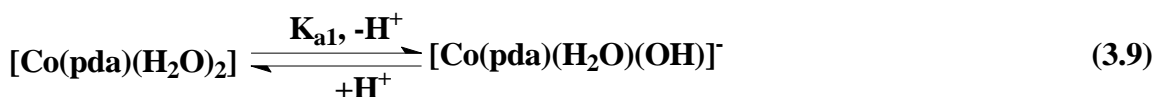
**Figure 3.19:** UV/VIS spectra of different Co(III)-pda species in solution.

- 1**  $[\text{Co}(\text{pda})(\mu\text{-OH})]_2^{2-}$  ( $1.2 \times 10^{-3}$  M) pH 5-7 ; **2**  $[\text{Co}(\text{pda})(\text{H}_2\text{O})_2]$ , pH ~ 2;  
**3**  $[\text{Co}(\text{pda})(\text{H}_2\text{O})(\text{OH})]^-$ , pH 5-7, T = 25.1 °C.

An acid assisted bridge cleavage reaction also takes place for the formation of *cis*-diaqua complex,  $[\text{Co}(\text{pda})(\text{H}_2\text{O})_2]$  and is illustrated in **Eq. 3.8**.



An acid dependency is also observed for  $[\text{Co}(\text{pda})(\text{H}_2\text{O})_2]$  and is illustrated in **Eq. 3.9**. The determination of the acid dissociation constant,  $K_{a1}$ , is discussed in Chapter 4.



Similar results were found by Visser and co-workers (2002:461) as well as by Potgieter *et al.* (2005:1968), for the pH dependence of  $[\text{Co}(\text{nta})(\text{H}_2\text{O})_2]$  and  $[\text{Co}(\text{apda})(\text{H}_2\text{O})_2]$ , respectively.

*IR spectra of [Co(pda)(H<sub>2</sub>O)(NCS)]<sup>-</sup>*

The IR spectra obtained for this complex show a stretching frequency for COO<sup>-</sup> at 1587 cm<sup>-1</sup> corresponding to the presence of coordinated COO<sup>-</sup> groups. The stretching frequency at 2096 cm<sup>-1</sup> (**Figure 3.20**) correlates well with the stretching frequency of 2082.0 cm<sup>-1</sup> that was assigned to  $\nu(\text{SCN})$  for the [Cr(NCS)<sub>3</sub>py<sub>3</sub>] complex, reported by DasSarma *et al.* (1979:3618). The presence of SCN peak indicates the bonding of NCS<sup>-</sup> ligand to the metal centre.

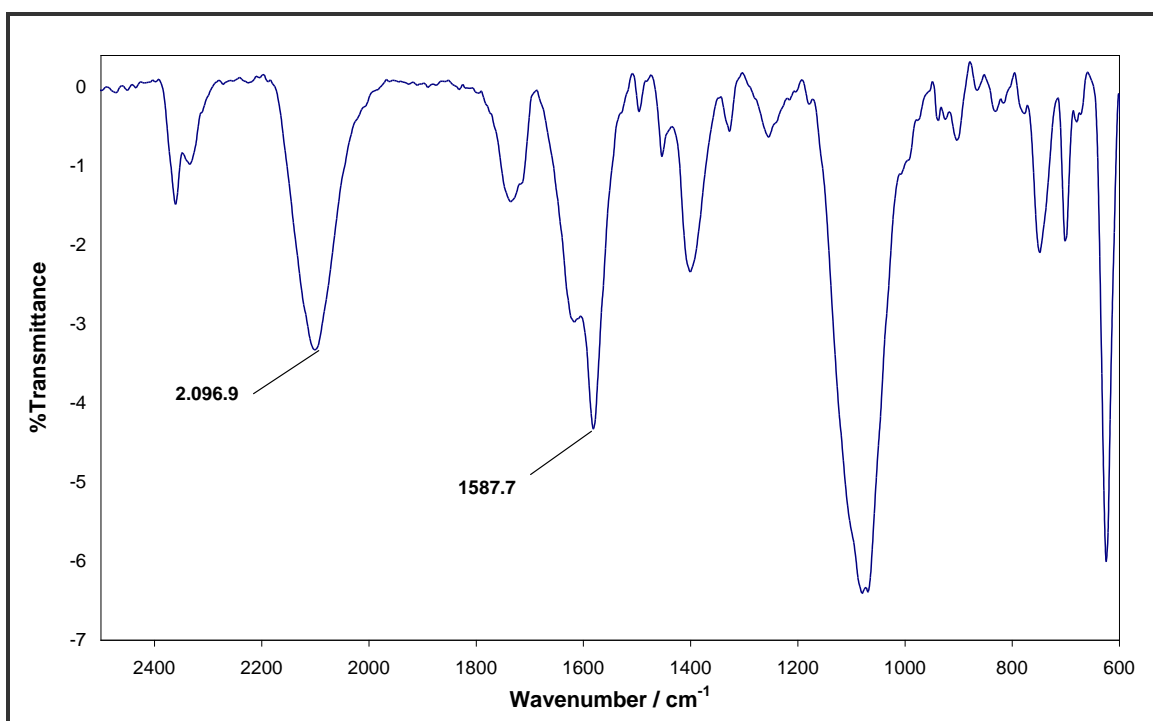


**Figure 3.20:** IR spectrum of [Co(pda)(H<sub>2</sub>O)(NCS)]<sup>-</sup>.

*<sup>1</sup>H NMR spectra of [Co(pda)(H<sub>2</sub>O)(NCS)]<sup>-</sup>*

The <sup>1</sup>H NMR spectrum for [Co(pda)(H<sub>2</sub>O)(NCS)]<sup>-</sup> integrates for twelve pda protons. All twelve protons of pda are non-equivalent, leading to four multiplets, the first multiplet integrating for three protons and resonate at 2.75-3.00 ppm; the second integrating for two protons and resonate at 3.60 ppm; third integrating for two protons and resonate at 3.90-4.10 ppm; and the remaining multiplet integrating for five phenyl protons and

resonate at 7.05 ppm. The  $^1\text{H}$  NMR spectrum for  $[\text{Co}(\text{pda})(\text{H}_2\text{O})(\text{NCS})]^-$  show the presence of pda ligand (see **Figure 3.5**) bonded to the metal center.

#### *UV/VIS spectra of $[\text{Co}(\text{pda})(\text{H}_2\text{O})(\text{NCS})]^-$*

The UV/VIS spectral change of a solution of  $[\text{Co}(\text{pda})(\text{H}_2\text{O})_2]$  (pH = 2) upon the addition NaSCN (0.031 g) was recorded (**Figure 3.21**). The spectrum shows an increase in absorption with the peak formation at 400 nm. The kinetics of this reaction is discussed in Chapter 4.

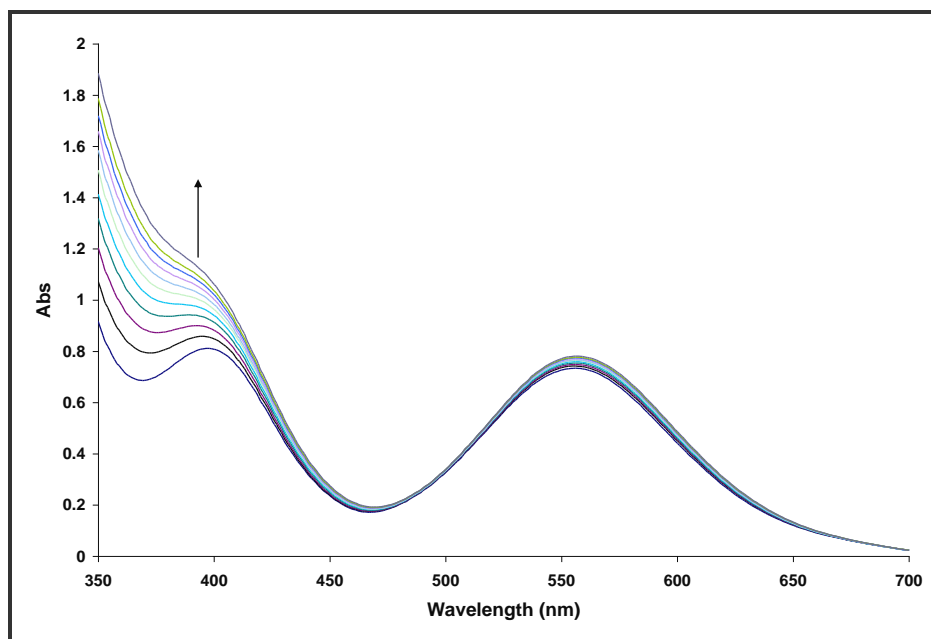


**Figure 3.21:** UV/VIS spectral changes for the reaction between  $[\text{Co}(\text{pda})(\text{H}_2\text{O})_2]$  ( $7.2 \times 10^{-3}$  M) with  $\text{NCS}^-$  ions.  $T = 25.3$  °C,  $[\text{NCS}^-] = 1.5 \times 10^{-2}$  M.

### 3.5 Conclusion

The Co-lda and-pda complexes presented in **Scheme 3.1** were successfully characterised by means of  $^1\text{H}$  NMR, IR, UV/VIS spectra. The  $^1\text{H}$  NMR spectra for both  $[\text{Co}(\text{lda})(\mu\text{-OH})_2]^{2-}$  and  $[\text{Co}(\text{pda})(\mu\text{-OH})_2]^{2-}$  are basically the same in that all the protons of lda and pda are non-equivalent, leading to four distinguishable doublets. The only

difference in these spectra is that the chemical shifts of these doublets vary slightly (see **Table 3.1**). The doublets for the spectrum of  $[\text{Co}(\text{lda})(\mu\text{-OH})]_2^{2-}$  are slightly deshielded and resonate at higher field as compared to the doublets of  $[\text{Co}(\text{pda})(\mu\text{-OH})]_2^{2-}$ .

**Table 3.1:** Summary of  $^1\text{H}$  NMR data for four distinguishable doublets of Co(III)-lda and-pda complexes.

Complexes	Chemical shift (number of protons, multiplicity) (ppm)
$[\text{Co}(\text{lda})(\mu\text{-OH})]_2^{2-}$	3.56 (1H, <i>d</i> ) and 3.85 (1H, <i>d</i> ); 3.82 (1H, <i>d</i> ) and 4.44 (1H, <i>d</i> )
$[\text{Co}(\text{pda})(\mu\text{-OH})]_2^{2-}$	2.65 (1H, <i>d</i> ) and 3.85 (1H, <i>d</i> ); 3.45 (1H, <i>d</i> ) and 4.15 (1H, <i>d</i> )

The UV/VIS studies on the Co-lda and-pda complexes first prepared by Uehara *et al.* (1971:1552) and (1971:1548), respectively, can prove very useful in the determination of the possible existence of Co(III)-lda and-pda species at different pH values.

It was shown that both  $[\text{Co}(\text{lda})(\mu\text{-OH})]_2^{2-}$  and  $[\text{Co}(\text{pda})(\mu\text{-OH})]_2^{2-}$  were easily prepared and that these complexes can prove to be very useful in the investigation of the mechanism of substitution reactions (Visser *et al.*, 2002:461). The kinetic study on Co(III)-lda and-pda complexes in the next Chapter can finally give more clarity about the findings in this Chapter.

# 4 Kinetic study of the reactions of [Co(lda)(H<sub>2</sub>O)<sub>2</sub>] and [Co(pda)(H<sub>2</sub>O)<sub>2</sub>] complexes

---

*The first part of this chapter deals with the pH dependence of [Co(lda)(H<sub>2</sub>O)<sub>2</sub>] and [Co(pda)(H<sub>2</sub>O)<sub>2</sub>], while the second part of this chapter focuses on the substitution reactions of [Co(L)(H<sub>2</sub>O)<sub>2</sub>]/[Co(L)(H<sub>2</sub>O)(OH)]<sup>-</sup> (L = lda, pda) with NCS<sup>-</sup> ions.*

---

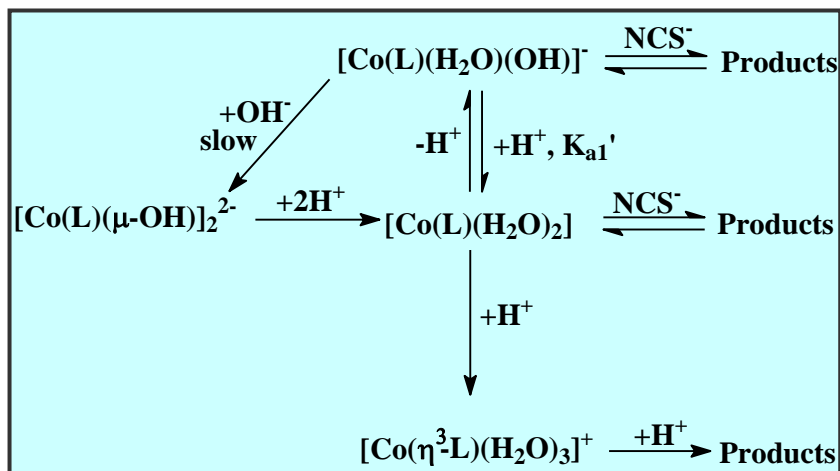
## 4.1 Introduction

The UV/VIS results reported earlier (Paragraph 3.4.3 and 3.4.4) show that the  $\mu$ -hydroxo bridges of [Co(L)( $\mu$ -OH)]<sub>2</sub><sup>2-</sup> (dimer) are cleaved by H<sup>+</sup> ions to form the corresponding *cis*-diaqua complex, [Co(L)(H<sub>2</sub>O)<sub>2</sub>] (L = lda, pda). These results also indicated that if the pH of solutions of this diaqua complex at pH 2 were re-adjusted to 7, resulted in the formation of aqua-hydroxo complex, [Co(L)(H<sub>2</sub>O)(OH)]<sup>-</sup>. It was also observed that the aqua-hydroxo complex change back to the dimer at pH 6-7 upon standing for several days.

This chapter deals with the influence of H<sup>+</sup> ions on the behaviour of the Co(III)-lda and-pda systems in aqueous medium (**Scheme 4.1**) as well as with the substitution reactions of [Co(L)(H<sub>2</sub>O)<sub>2</sub>]/[Co(L)(H<sub>2</sub>O)(OH)]<sup>-</sup> (L = lda, pda) with NCS<sup>-</sup> ions.

The influence of H<sup>+</sup> ions on the behaviour of the similar Co(III)-nta system in aqueous medium as well as the substitution reactions of [Co(nta)(H<sub>2</sub>O)<sub>2</sub>]/[Co(nta)(H<sub>2</sub>O)(OH)]<sup>-</sup> with NCS<sup>-</sup> ions have been investigated by other groups (Thacker & Higginson, 1975:704 and Visser *et al.*, 2002:461). They studied the pH dependence of the [Co(nta)(H<sub>2</sub>O)<sub>2</sub>] complex between pH 2 and 7 to avoid complications by competing reactions. The reactions of [Co(nta)(H<sub>2</sub>O)<sub>2</sub>]/[Co(nta)(H<sub>2</sub>O)(OH)]<sup>-</sup> with NCS<sup>-</sup> ions were studied at pH values between 2 and 7, which allow both Co(III)-nta species to react with NCS<sup>-</sup>. The

**Scheme 1.1** in Chapter 1 was proposed by Visser and co-workers (2002:461) for the pH dependence of the  $[\text{Co}(\text{nta})(\text{H}_2\text{O})_2]$  complex and the reactions of  $[\text{Co}(\text{nta})(\text{H}_2\text{O})_2]/[\text{Co}(\text{nta})(\text{H}_2\text{O})(\text{OH})]^-$  with  $\text{NCS}^-$  ions.



**Scheme 4.1:** Formation and reactions of  $[\text{Co}(\text{L})(\text{H}_2\text{O})_2]$  (L = lda, pda).

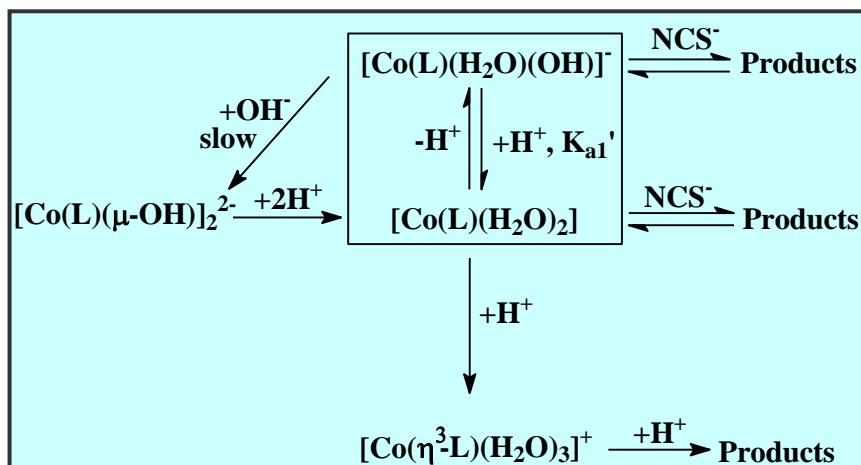
## 4.2 Experimental Procedures

All reagents and chemicals were of analytical grade and double distilled water was used in all experiments. All pH measurements were performed on a HI 8520 microprocessor bench pH/°C meter, calibrated with pH 7.01 (H17007) and pH 4.01 (H17004) buffer solutions, all obtained from Hannan instruments. Kinetic measurements were performed on a Cary 50 (Conc.) spectrophotometer equipped with constant temperature cell holders (accuracy within 0.1 °C). Scientist (Micromath, 1990) was used to fit the data. All the kinetic runs were performed under pseudo first-order conditions with the ligand in excess in each case. The ionic strength of all the reaction solutions was kept constant with the addition of  $\text{NaClO}_4$ . Linear plots of  $\log(A - A_t)$  vs. time were obtained for at least two half-lives under all conditions. The solid lines and the figures represent computer least squares fits of data, while the experimentally determined values are represented by dots. Detailed tables of the experimental values are given in Appendix A (Section I).

### 4.3 Kinetic Results

#### 4.3.1 Influence of H<sup>+</sup> ions on the Co(III)-lda and-pda system

*pH dependence of [Co(lda)(H<sub>2</sub>O)<sub>2</sub>] and [Co(pda)(H<sub>2</sub>O)<sub>2</sub>]*



**Scheme 4.2:** pH dependence of [Co(L)(H<sub>2</sub>O)<sub>2</sub>] (L = lda, pda).

It was observed in Chapter 3 that the aquahydroxo complexes of both lda and pda revert back to the dimer at pH 6-7 upon standing several days. Spectroscopic results indicated that these reactions become faster as the pH is increased and that competitive reactions, possibly dimer formation, occur at pH > 7.0. Therefore, it was decided to keep the reaction conditions between pH 2-7.

The protonation behaviour of a monoprotic complex such as [Co(L)(H<sub>2</sub>O)<sub>2</sub>] (as defined by Eq. 4.1) is given by Eq. 4.2 (Appendix A, Section II).



$$A_{\text{tot}} = \frac{A_{\text{HB}} + A_{\text{B}^-}(\text{K}_{a1}/[\text{H}^+])}{1 + (\text{K}_{a1}/[\text{H}^+])} \quad (4.2)$$

In **Eq. 4.2**,  $A_{\text{tot}}$  = absorbance at a specific  $[\text{H}^+]$ ,  $A_{\text{HB}}$  = absorbance of the  $[\text{Co}(\text{L})(\text{H}_2\text{O})_2]$  complex,  $A_{\text{B}^-}$  = absorbance of the  $[\text{Co}(\text{L})(\text{H}_2\text{O})(\text{OH})]^-$  complex and  $K_{\text{a1}}$  is the acid dissociation constant.

Both  $[\text{Co}(\text{lda})(\text{H}_2\text{O})_2]$  and  $[\text{Co}(\text{pda})(\text{H}_2\text{O})_2]$  complexes were obtained by respectively acidifying the solutions of  $[\text{Co}(\text{lda})(\mu\text{-OH})]_2^{2-}$  and  $[\text{Co}(\text{pda})(\mu\text{-OH})]_2^{2-}$  to  $\text{pH} = 2.0$  ( $\text{HClO}_4$ ). The acid dissociation constants,  $K_{\text{a1}}$ , of both complexes were determined spectrophotometrically at  $\lambda = 400 \text{ nm}$  and  $25.0 \text{ }^\circ\text{C}$  by separately adjusting the pH of their respective solutions ( $2 \times 10^{-3} \text{ M}$ ) with  $\text{KOH}$  ( $1.0 \text{ M}$ ) and immediately measuring the absorbance of each solution. The data of both complexes were fitted to **Eq. 4.2** and the results are illustrated in **Figures 4.1** and **4.2**, respectively.

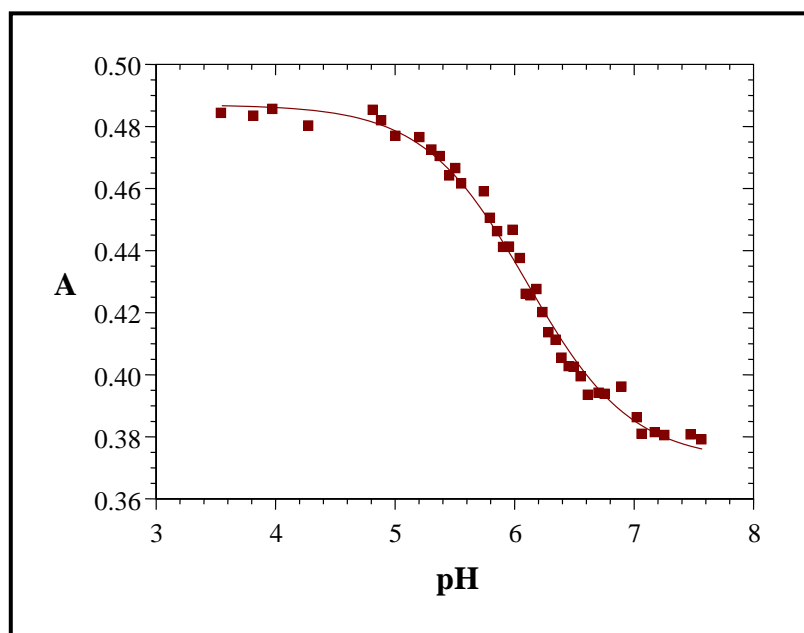


**Figure 4.1:** Plot of Abs ( $\lambda = 400 \text{ nm}$ ) vs. pH for  $[\text{Co}(\text{lda})(\text{H}_2\text{O})_2]$  ( $2 \times 10^{-3} \text{ M}$ ),  $25.1 \text{ }^\circ\text{C}$ ,  $\mu = 1.0 \text{ M}$  ( $\text{NaClO}_4$ ).

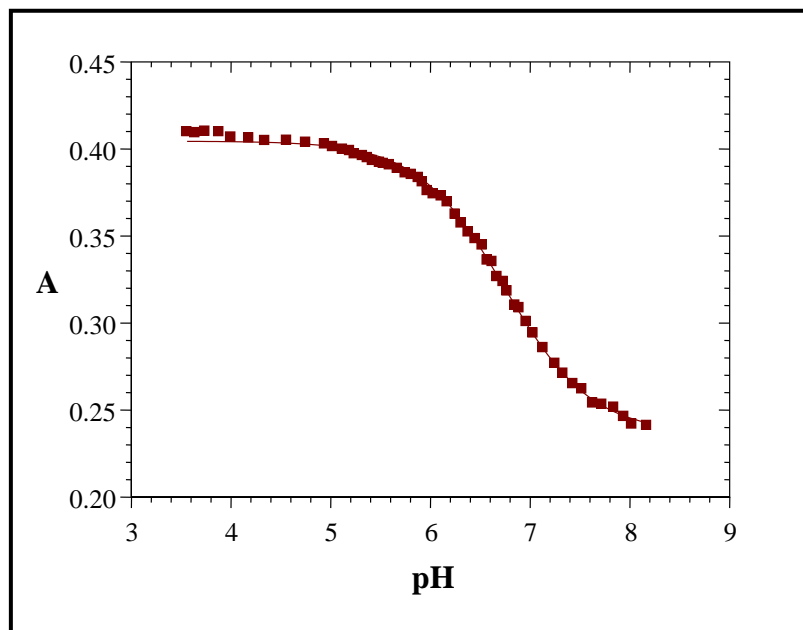
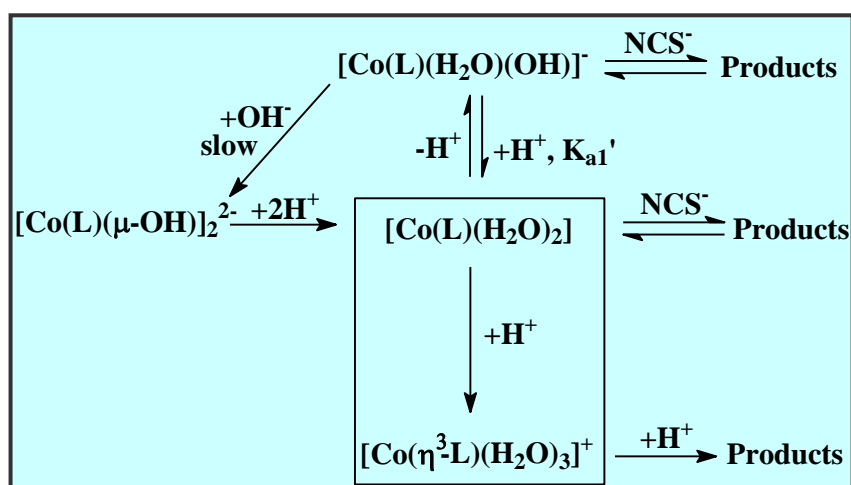


**Figure 4.2:** Plot of Abs ( $\lambda = 400$  nm) vs. pH for  $[\text{Co}(\text{pda})(\text{H}_2\text{O})_2]$  ( $2 \times 10^{-3}$  M),  $25.2$  °C,  $\mu = 1.0$  M ( $\text{NaClO}_4$ ).

The  $\text{pK}_{\text{a}1}$  values were determined as 6.11(2) and 6.74(1), respectively for  $[\text{Co}(\text{lda})(\text{H}_2\text{O})_2]$  and  $[\text{Co}(\text{pda})(\text{H}_2\text{O})_2]$  and are reported in **Table 4.2**.

*Reaction of  $[\text{Co}(\text{L})(\text{H}_2\text{O})_2]$  ( $\text{L} = \text{lda}, \text{pda}$ ) with  $\text{H}^+$  ions*



**Scheme 4.3:** Reaction of  $[\text{Co}(\text{L})(\text{H}_2\text{O})_2]$  ( $\text{L} = \text{lda}, \text{pda}$ ) with  $\text{H}^+$  ions.

A slow change in the spectrum was observed after lowering the pH of solutions of  $[\text{Co}(\text{lda})(\text{H}_2\text{O})_2]$  and  $[\text{Co}(\text{pda})(\text{H}_2\text{O})_2]$  ( $\text{pH} < 1.0$ ). This does not correspond to normal protonation reactions as observed in Chapter 3. These solutions of  $[\text{Co}(\text{lda})(\text{H}_2\text{O})_2]$  and  $[\text{Co}(\text{pda})(\text{H}_2\text{O})_2]$  were allowed to stand for a few days upon which the crystals of the free ligands, lda and pda were isolated. This was confirmed with IR and  $^1\text{H}$  NMR spectra.

The possibility of the substitution reactions with different ligands in solution at these pH values were eliminated by the study of the reactions between  $[\text{Co}(\text{lda})(\text{H}_2\text{O})_2]$  and strong acids with coordinating and non-coordinating anions. Similar reactions were followed between  $[\text{Co}(\text{pda})(\text{H}_2\text{O})_2]$  and these acids, see **Table 4.1**.

**Table 4.1:** Observed rate constants for the reaction between  $[\text{Co}(\text{L})(\text{H}_2\text{O})_2]$  ( $1 \times 10^{-2}$  M) (L = lda, pda) and different acids and anions, 25.0 °C,  $\mu = 1.0$  M ( $\text{NaClO}_4$ ).

	<b>lda</b>	<b>pda</b>
<b>Reactant</b>	<b><math>(10^3)k_{\text{obs}}</math> (<math>\text{s}^{-1}</math>)</b>	<b><math>(10^3)k_{\text{obs}}</math> (<math>\text{s}^{-1}</math>)</b>
0.2 M HCl	9.84(5)	9.58(6)
0.2 M HCl + 0.4 M NaCl	9.86(3)	9.64(5)
0.2 M $\text{HClO}_4$	9.88(4)	9.69(4)
0.4 M HCl	18.9(6)	18.9(6)

It can be seen from the results in **Table 4.1** that the observed rate constants remain the same within the experimental error upon addition of different acids (HCl and  $\text{HClO}_4$ ) to these solutions and that the rate remains the same even upon addition of an excessive amount of  $\text{Cl}^-$ . Furthermore, the increase in  $k_{\text{obs}}$  with increase in  $[\text{H}^+]$  clearly indicate that the observed reaction is in fact between  $[\text{Co}(\text{L})(\text{H}_2\text{O})_2]$  (L = lda, pda) and  $\text{H}^+$  ions.

A study of the reactions between  $[\text{Co}(\text{lda})(\text{H}_2\text{O})_2]$  and  $[\text{Co}(\text{pda})(\text{H}_2\text{O})_2]$  with  $\text{H}^+$  ions at different temperatures showed non-linear kinetics, see **Figures 4.3** and **4.4**. Keeping this in mind, as well as the fact that both lda and pda dissociates from the metal in acid solution, **Scheme 4.4** ( $L = \text{lda}, \text{pda}$ ) is proposed for describing the observed kinetics.

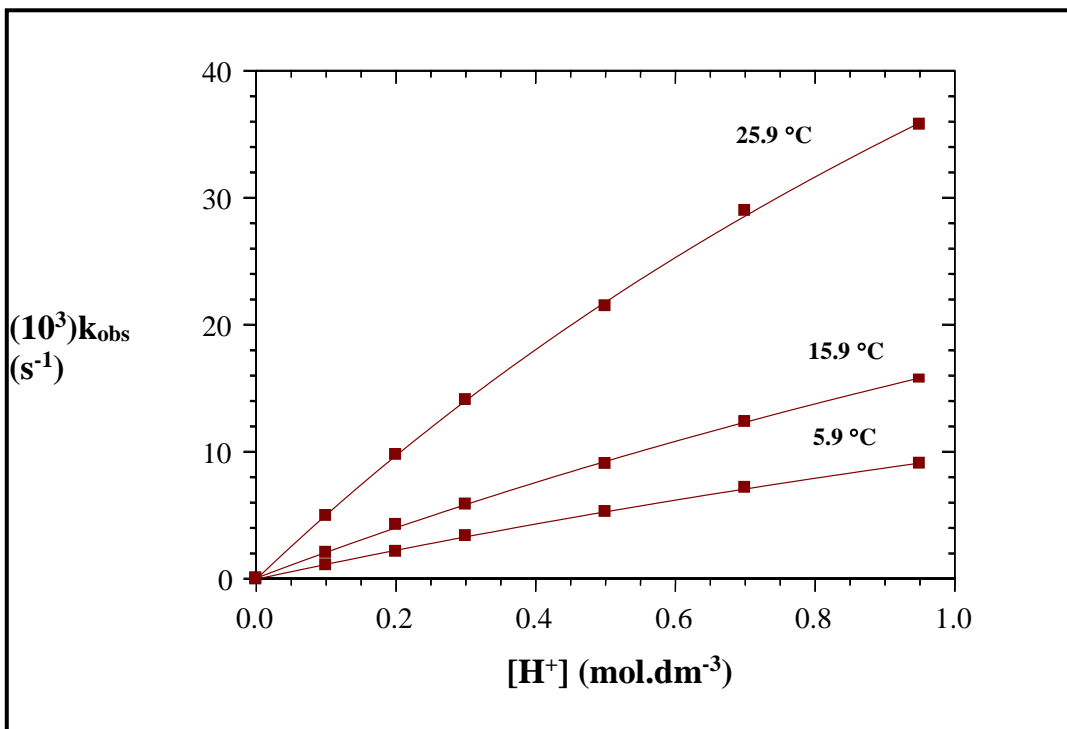


**Figure 4.3:** Plot of  $k_{\text{obs}}$  vs.  $[\text{H}^+]$  at different temperatures,  $\mu = 1.0 \text{ M}$  ( $\text{NaClO}_4$ ),  $\lambda = 355 \text{ nm}$ ,  $[\text{Co}(\text{lda})(\text{H}_2\text{O})_2] = 1 \times 10^{-2} \text{ M}$ .

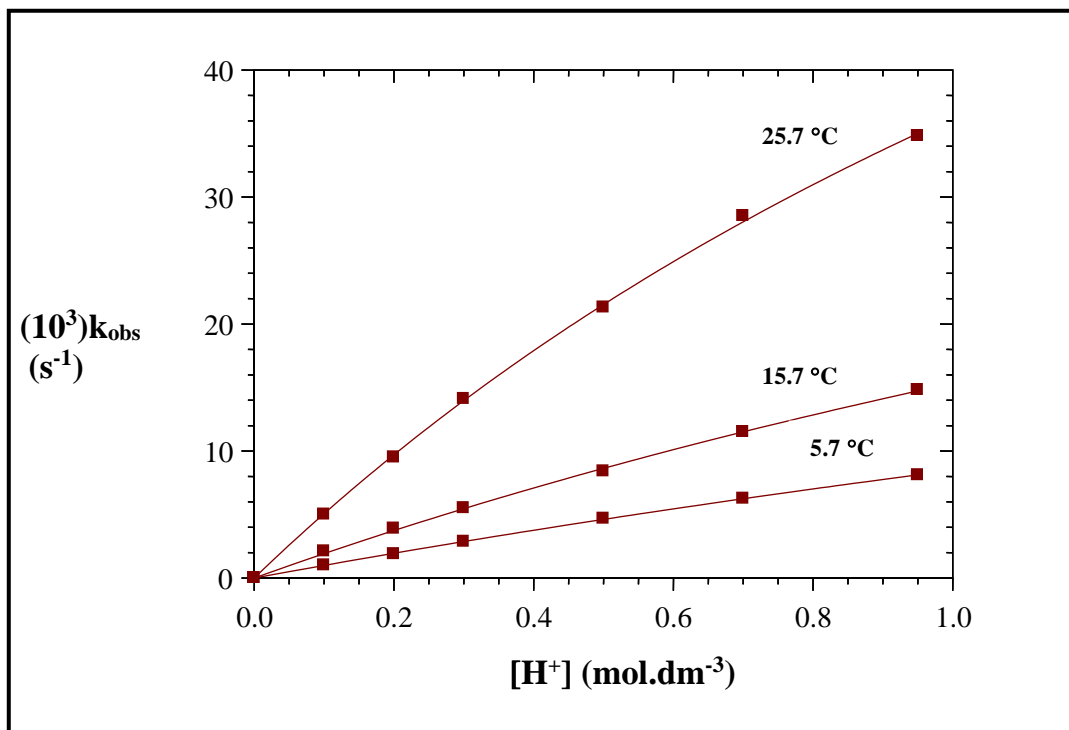
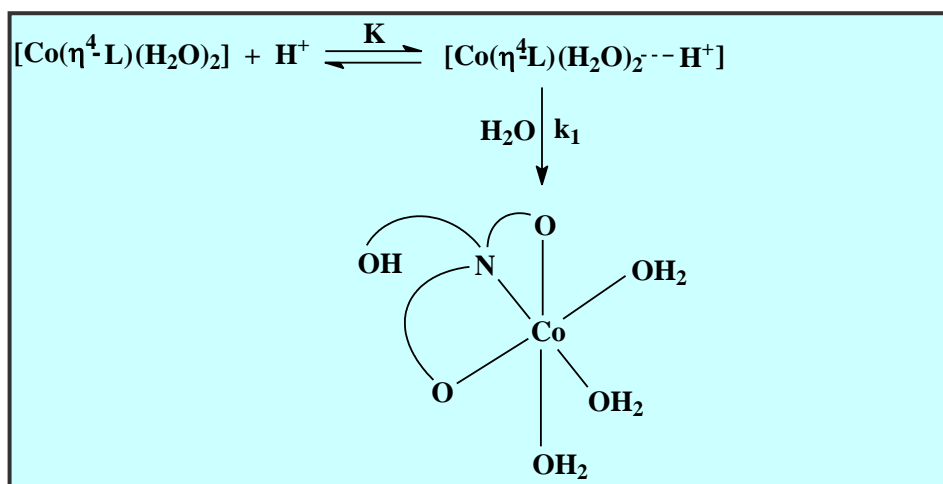


**Figure 4.4:** Plot of  $k_{\text{obs}}$  vs.  $[\text{H}^+]$  at different temperatures,  $\mu = 1.0 \text{ M}$  ( $\text{NaClO}_4$ ),  $\lambda = 355 \text{ nm}$ ,  $[\text{Co}(\text{pda})(\text{H}_2\text{O})_2] = 1 \times 10^{-2} \text{ M}$ .

The formation of an ion associated species between  $[\text{Co}(\text{L})(\text{H}_2\text{O})_2]$  ( $\text{L} = \text{lda}, \text{pda}$ ) and  $\text{H}^+$  ions upon addition of acid is postulated. This species dissociates in the rate determining step and is aquated to form the tridentate L complex ion,  $[\text{Co}(\eta^3\text{-L})(\text{H}_2\text{O})_3]^+$ .



**Scheme 4.4:** Proposed mechanism for the reaction of  $[\text{Co}(\text{L})(\text{H}_2\text{O})_2]$  ( $\text{L} = \text{lda}, \text{pda}$ ) with  $\text{H}^+$  ions.

The rate law for the first reaction according to **Scheme 4.4** is given by **Eq. 4.3**.

$$R = k_1[\text{Co}(\eta^4\text{-lda})(\text{H}_2\text{O})_2 \cdots \text{H}^+] \quad (4.3)$$

The total Co(III) concentration,  $[\text{Co}]_{\text{tot}}$  is indicated by **Eq. 4.4**.

$$[\text{Co}]_{\text{tot}} = [\text{Co}(\eta^3\text{-L})(\text{H}_2\text{O})_3]^+ + [\text{Co}(\eta^4\text{-L})(\text{H}_2\text{O})_2] \quad (4.4)$$

The acid dissociation constant,  $K_{\text{a1}}$  is given in **Eq. 4.5**

$$K_{\text{a1}} = \frac{[\text{Co}(\eta^4\text{-L})(\text{H}_2\text{O})_2][\text{H}^+]}{[\text{Co}(\eta^4\text{-L})(\text{H}_2\text{O})_2 \cdots \text{H}^+]} \quad (4.5)$$

Under pseudo first-order conditions with  $[\text{Co}]_{\text{tot}} \ll [\text{H}^+]$  the observed rate,  $k_{\text{obs}}$ , can be derived from **Eq. 4.3–4.5** (Appendix A, Section II).

$$k_{\text{obs}} = \frac{k_1 K [\text{H}^+]}{1 + K [\text{H}^+]} \quad (4.6)$$

The results in **Figures 4.3** and **4.4** were fitted to **Eq. 4.6**, respectively. The calculated  $k_1$  and  $K$  values, as well as the activation parameters (using the Eyring-Polanyi equation) are reported in **Table 4.2** for the reactions of  $[\text{Co}(\text{L})(\text{H}_2\text{O})_2]$  ( $\text{L} = \text{lda}, \text{pda}$ ) with  $\text{H}^+$  ions.

**Table 4.2:** Rate constants and activation parameters for the reaction between [Co(L)(H<sub>2</sub>O)<sub>2</sub>] (L = lda, pda) and H<sup>+</sup> ions.

Constants	lda	pda
<b>25 °C</b>		
k <sub>1</sub> (M <sup>-1</sup> s <sup>-1</sup> )	0.128(8)	0.115(7)
K (M <sup>-1</sup> )	0.41(1)	0.46(4)
ΔH <sup>#</sup> (k <sub>1</sub> ) (kJ mol <sup>-1</sup> )	33(2)	26(2)
ΔS <sup>#</sup> (k <sub>1</sub> ) (J mol <sup>-1</sup> K <sup>-1</sup> )	-153(6)	-177(8)
pK <sub>a1</sub> (25.0 °C) (spectrophotometrically determined)	6.11(2)	6.74(1)
<b>15 °C</b>		
k <sub>1</sub> (M <sup>-1</sup> s <sup>-1</sup> )	0.076(9)	0.068(8)
K (M <sup>-1</sup> )	0.27(4)	2.9(4)
<b>5 °C</b>		
k <sub>1</sub> (M <sup>-1</sup> s <sup>-1</sup> )	0.049(6)	0.052(4)
K (M <sup>-1</sup> )	0.24(4)	0.20(2)

#### 4.3.2 Substitution reactions of [Co(lda)(H<sub>2</sub>O)<sub>2</sub>] and [Co(pda)(H<sub>2</sub>O)<sub>2</sub>] with NCS<sup>-</sup> ions

The UV/VIS spectrum revealed two distinguishable substitution reactions of [Co(lda)(H<sub>2</sub>O)<sub>2</sub>] and [Co(pda)(H<sub>2</sub>O)<sub>2</sub>], respectively with NCS<sup>-</sup> at low pH. At higher pH (6–7) we only observed one reaction. Typical spectral changes for the reactions at low pH are shown in **Figures 4.5** and **4.6**. The addition of NaSCN to the solution containing [Co(L)(H<sub>2</sub>O)<sub>2</sub>] (pH = 2.00) resulted in an increase of spectrum in the 400 nm range (L = lda, pda).

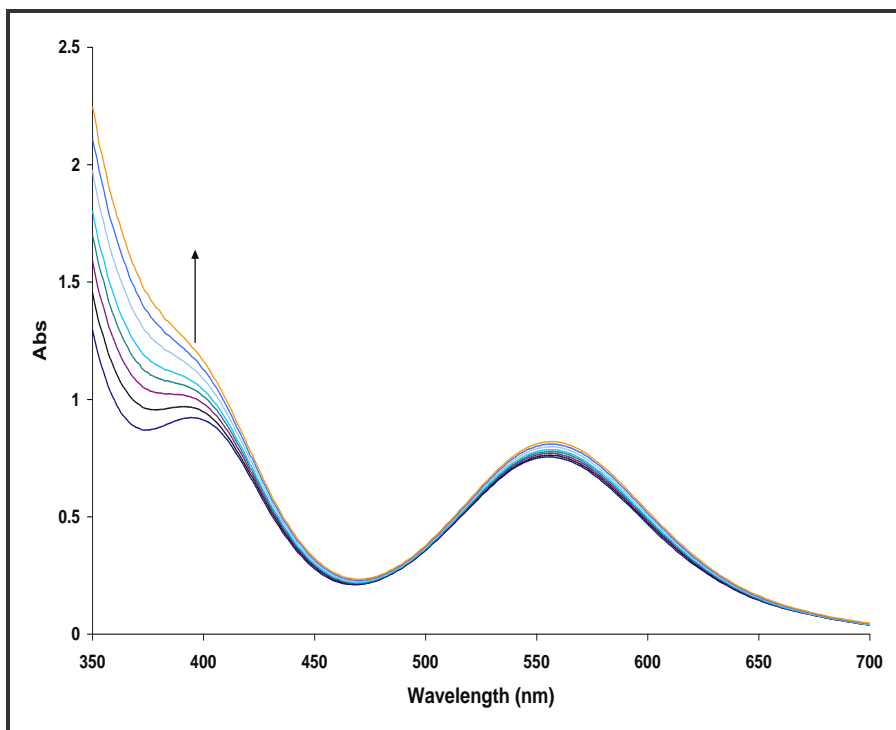


**Figure 4.5:** UV/VIS spectral changes for the reaction between  $[\text{Co}(\text{lda})(\text{H}_2\text{O})_2]$  ( $7.9 \times 10^{-3}$  M) with  $\text{NCS}^-$  ions.  $T = 25.3$  °C,  $[\text{NCS}^-] = 1.7 \times 10^{-2}$  M.

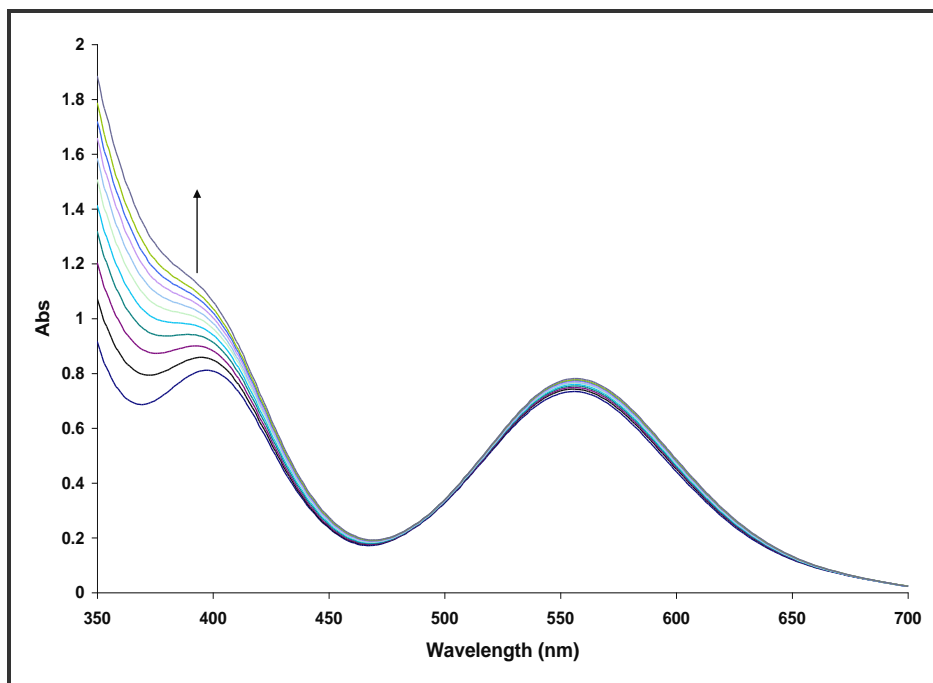
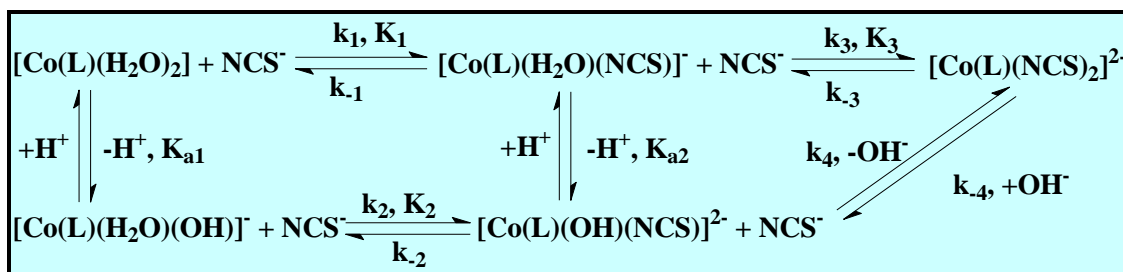


**Figure 4.6:** UV/VIS spectral changes for the reaction between  $[\text{Co}(\text{pda})(\text{H}_2\text{O})_2]$  ( $7.2 \times 10^{-3}$  M) with  $\text{NCS}^-$  ions.  $T = 25.3$  °C,  $[\text{NCS}^-] = 1.5 \times 10^{-2}$  M.

At these pH values (pH = 2–7), where both the Co(III)-L (L = lda, pda) species (see also Chapter 3) can react with NCS<sup>-</sup>, the following reaction scheme is proposed:



**Scheme 4.5:** Reactions of [Co(L)(H<sub>2</sub>O)<sub>2</sub>]/[Co(L)(H<sub>2</sub>O)(OH)]<sup>-</sup> (L = lda, pda) with NCS<sup>-</sup> ions.

The equilibrium constant for the reaction of [Co(L)(H<sub>2</sub>O)<sub>2</sub>] (L = lda, pda) with NCS<sup>-</sup> ions (as defined by **Eq. 4.7**) were determined spectrophotometrically at a pH of *ca.* 2 using **Eq. 4.8** (Appendix A, Section II).



$$A = \frac{A_r + A_p K_1 [\text{NCS}^-]}{1 + K_1 [\text{NCS}^-]} \quad (4.8)$$

This may be derived from the definition of  $K_1$ , see **Scheme 4.5**, mass balance and Beer's law.  $A$  is the absorbance at a given [NCS<sup>-</sup>] and  $A_r$  and  $A_p$  are the absorbance of [Co(L)(H<sub>2</sub>O)<sub>2</sub>] and [Co(L)(H<sub>2</sub>O)(NCS)]<sup>-</sup> (L = lda, pda), respectively. **Figures 4.7** and **4.8** are respective illustrations of the data used for the determination of  $K_1$  for the reaction with NCS<sup>-</sup> ions. The absorbances *vs.* [NCS<sup>-</sup>] data for the entering ligand were fitted to **Eq. 4.8** using a least-squares program to determine the  $K_1$  values. These results are in good agreement with that obtained kinetically as indicated in **Table 4.3**.

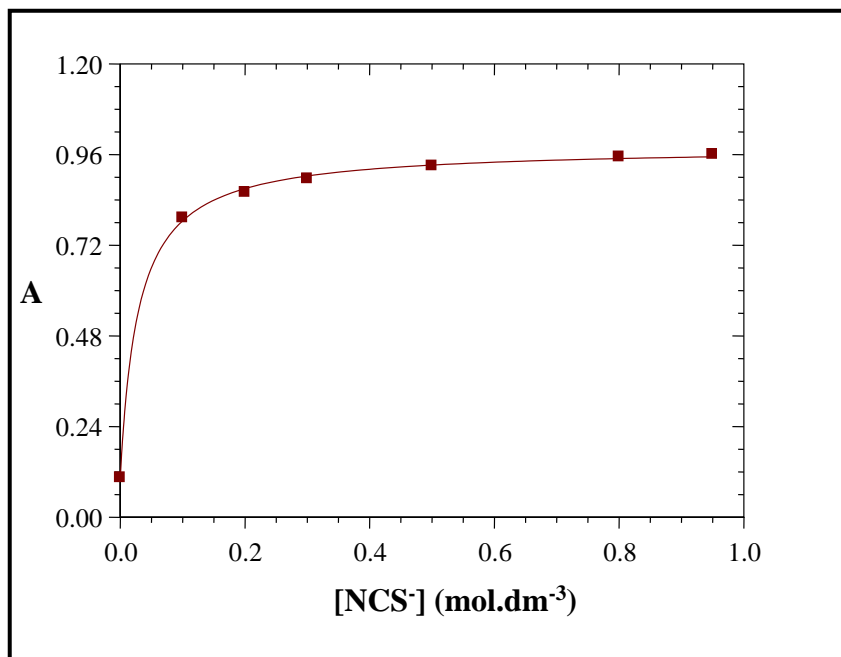


**Figure 4.7:** Plot of Abs ( $\lambda = 400$  nm) vs.  $[\text{NCS}^-]$  for  $[\text{Co}(\text{lda})(\text{H}_2\text{O})_2]$  ( $1 \times 10^{-3}$  M),  $25.1$  °C, pH = 2.0 and  $\mu = 1.0$  M ( $\text{NaClO}_4$ ).

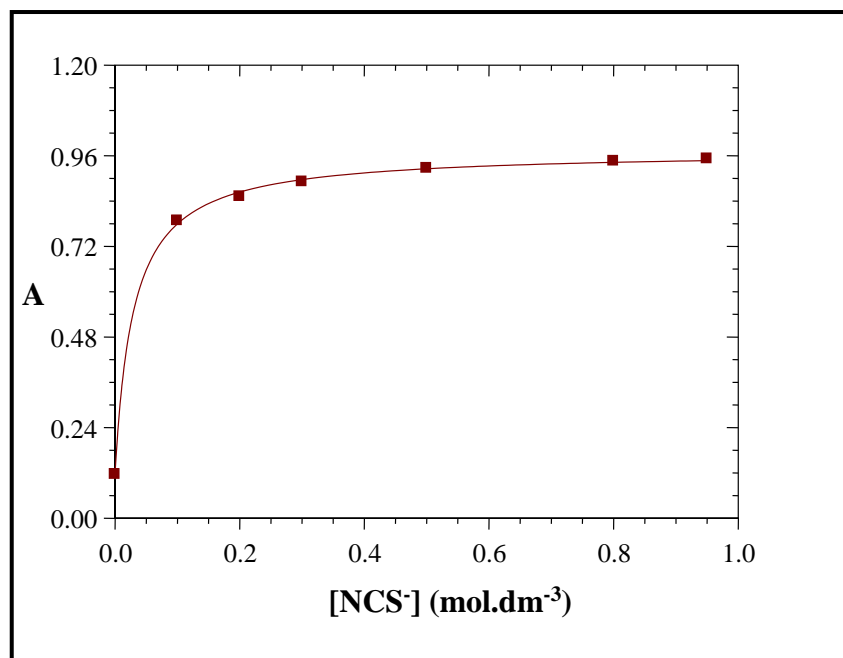


**Figure 4.8:** Plot of Abs ( $\lambda = 400$  nm) vs.  $[\text{NCS}^-]$  for  $[\text{Co}(\text{pda})(\text{H}_2\text{O})_2]$  ( $1 \times 10^{-3}$  M),  $25.3$  °C, pH = 2.0 and  $\mu = 1.0$  M ( $\text{NaClO}_4$ ).

The total rate law, according to general **Scheme 4.5**, is given by **Eq. 4.9**.

$$\begin{aligned}
 R = & k_1[\text{Co(L)(H}_2\text{O)}_2][\text{NCS}^-] + k_2[\text{Co(L)(H}_2\text{O)(OH)}^-][\text{NCS}^-] + \\
 & k_3[\text{Co(L)(H}_2\text{O)(NCS)}^-][\text{NCS}^-] + k_4[\text{Co(L)(NCS)(OH)}^{2-}][\text{NCS}^-] - \\
 & k_{-1}[\text{Co(L)(H}_2\text{O)(NCS)}^-] - k_{-2}[\text{Co(L)(NCS)(OH)}^{2-}] - k_{-3}[\text{Co(L)(NCS)}_2^{2-}] \\
 & - k_{-4}[\text{Co(L)(NCS)}_2^{2-}]
 \end{aligned} \tag{4.9}$$

The total concentration of the Co(III)-aqua complex,  $[\text{Co-H}_2\text{O}]_{\text{tot}}$ , is indicated by Eq. 4.10.

$$[\text{Co-H}_2\text{O}]_{\text{tot}} = [\text{Co(L)(H}_2\text{O)}_2] + [\text{Co(L)(H}_2\text{O)(OH)}^-] \tag{4.10}$$

The total concentration of the Co(III)-monothiocyanide complex,  $[\text{Co-NCS}]_{\text{tot}}$ , is illustrated by Eq. 4.11.

$$[\text{Co-NCS}]_{\text{tot}} = [\text{Co(L)(H}_2\text{O)(NCS)}^-] + [\text{Co(L)(NCS)(OH)}^{2-}] \tag{4.11}$$

The acid dissociation constants,  $K_{a1}$  and  $K_{a2}$ , are given in Eq. 4.12 and 4.13 respectively.

$$K_{a1} = \frac{[\text{Co(L)(H}_2\text{O)(OH)}^-][\text{H}^+]}{[\text{Co(L)(H}_2\text{O)}_2]} \tag{4.12}$$

$$K_{a2} = \frac{[\text{Co(L)(OH)(NCS)}_2^{2-}][\text{H}^+]}{[\text{Co(L)(H}_2\text{O)(NCS)}^-]} \tag{4.13}$$

Under pseudo first-order conditions with  $[\text{Co}]_{\text{tot}} \ll [\text{NCS}^-]$  and  $[\text{Co-NCS}]_{\text{tot}} \ll [\text{NCS}^-]$ , the observed rate,  $k_{\text{obs}}$ , can be derived from Eq. 4.9–4.13 (Appendix A, Section II).

$$k_{\text{obs}} = \frac{k_1[\text{H}^+] + k_2K_{a1}}{(K_{a1} + [\text{H}^+])}[\text{NCS}^-] + \frac{k_3[\text{H}^+] + k_4K_{a2}}{(K_{a2} + [\text{H}^+])}[\text{NCS}^-] + \frac{k_{-1}[\text{H}^+] + k_{-2}K_{a2}}{(K_{a2} + [\text{H}^+])} + k_{-3} + k_{-4}[\text{OH}^-]$$

(4.14)

In the pH range of 2–7.5 in which these substitution reactions were studied the  $[\text{OH}^-]$  is very small, resulting in the contribution of the  $k_4[\text{OH}^-]$  term in **Eq. 4.14** to become negligibly small. A provisional fit of the experimental data to **Eq. 4.14** (excluding the  $k_4[\text{OH}^-]$  factor) also gave a value for  $k_4$  approaching zero.

In order to verify the last assumption, the first reaction between  $[\text{Co}(\text{L})(\text{H}_2\text{O})_2]$  ( $\text{L} = \text{lda}, \text{pda}$ ) and  $\text{NCS}^-$  ions were allowed to go to completion at low pH after which the pH of the reaction solution was increased to  $\sim 6.5$ . The spectroscopic results did not indicate that hydroxide ions are substituted ( $k_4$  pathway). Taking the above into consideration **Eq. 4.14** can be simplified to **Eq. 4.15**.

$$k_{\text{obs}} = \frac{k_1[\text{H}^+] + k_2K_{a1}}{(K_{a1} + [\text{H}^+])}[\text{NCS}^-] + \frac{k_3[\text{H}^+]}{(K_{a2} + [\text{H}^+])}[\text{NCS}^-] + \frac{k_{-1}[\text{H}^+] + k_{-2}K_{a2}}{(K_{a2} + [\text{H}^+])} + k_{-3} \quad (4.15)$$

Initial calculations showed that  $K_{a2} \approx 7$ . This means the values for  $K_{a1}$  and  $K_{a2}$  becomes negligible at pH 2.00 so that **Eq. 4.15** can be simplified to **Eq. 4.16**.

$$k_{\text{obs}} = k_1[\text{NCS}^-] + k_{-1} + k_3[\text{NCS}^-] + k_{-3} \quad (4.16)$$

The substitution of the second aqua ligand from the coordination sphere ( $k_3$  in **Scheme 4.5**) is slower than the first aqua substitution step ( $k_1$  step) so that the rate equation for the formation of  $[\text{Co}(\text{L})(\text{H}_2\text{O})(\text{NCS})]^-$  and  $[\text{Co}(\text{L})(\text{NCS})]^{2-}$  in consecutive substitution steps, but different time scales, can be described by **Eq. 4.17** and **4.18**, respectively.

$$k_{\text{obs}} = k_1[\text{NCS}^-] + k_{-1} \quad (4.17)$$

$$k_{\text{obs}} = k_3[\text{NCS}^-] + k_{-3} \quad (4.18)$$

Plots of  $k_{\text{obs}}$  vs.  $[\text{NCS}^-]$  for the first reaction between  $[\text{Co(L)}(\text{H}_2\text{O})_2]$  and  $\text{NCS}^-$  ions at  $\text{pH} = 2.00$  and three different temperatures are shown in **Figure 4.9** and **4.10**. Due to the fact that the second reaction is very slow at  $15.0\text{ }^\circ\text{C}$ , plots of  $k_{\text{obs}}$  vs.  $[\text{NCS}^-]$  for the second substitution reaction between  $[\text{Co(L)}(\text{H}_2\text{O})_2]$  and  $\text{NCS}^-$  ions at  $\text{pH} 2.00$  were obtained between  $25.0\text{ }^\circ\text{C}$  and  $48.0\text{ }^\circ\text{C}$  as shown in **Figures 4.11** and **4.12**. The plots for both the first and second reactions were linear (refer to **Figures 4.9** and **4.10** as well as **4.11** and **4.12**) and the  $k_1$ ,  $k_{-1}$ ,  $k_3$  and  $k_{-3}$  values were calculated from **Eq. 4.17** and **4.18** and are reported in **Table 4.3**.

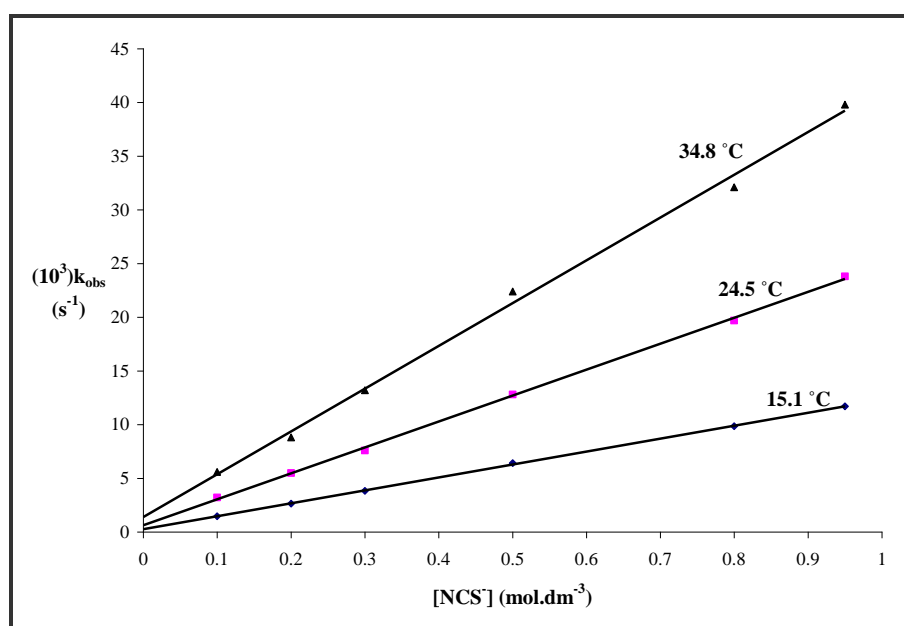


**Figure 4.9:** Plot of  $k_{\text{obs}}$  vs.  $[\text{NCS}^-]$  for the first reaction ( $k_1$  step, **Scheme 4.5**) at different temperatures,  $\mu = 1.0\text{ M}$  ( $\text{NaClO}_4$ ),  $\lambda = 400\text{ nm}$ ,  $[\text{Co}(\text{lda})(\text{H}_2\text{O})_2] = 1 \times 10^{-3}\text{ M}$ .

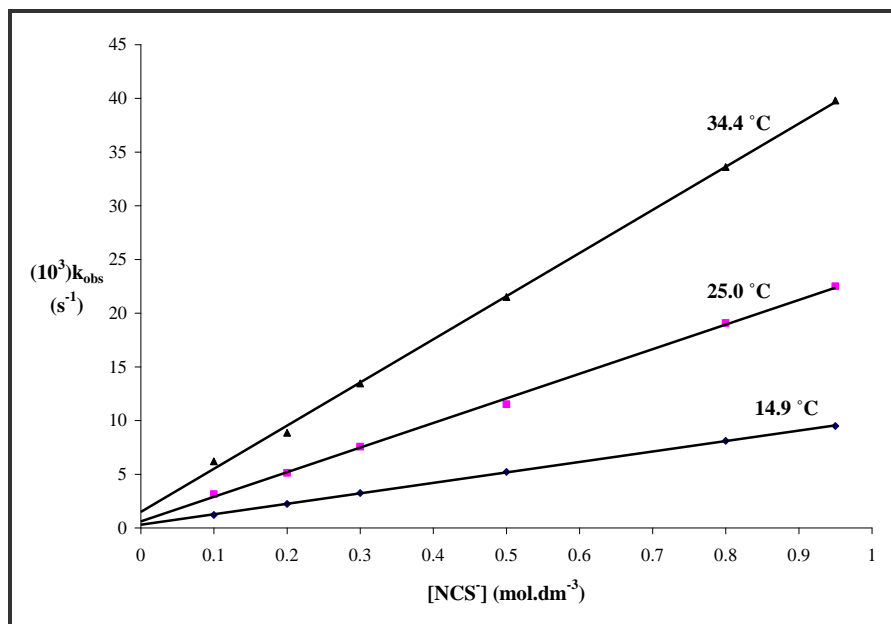


**Figure 4.10:** Plot of  $k_{\text{obs}}$  vs.  $[\text{NCS}^-]$  for the first reaction ( $k_1$  step, **Scheme 4.5**) at different temperatures,  $\mu = 1.0 \text{ M}$  ( $\text{NaClO}_4$ ),  $\lambda = 400 \text{ nm}$ ,  $[\text{Co}(\text{pda})(\text{H}_2\text{O}_2)] = 1 \times 10^{-3} \text{ M}$ .

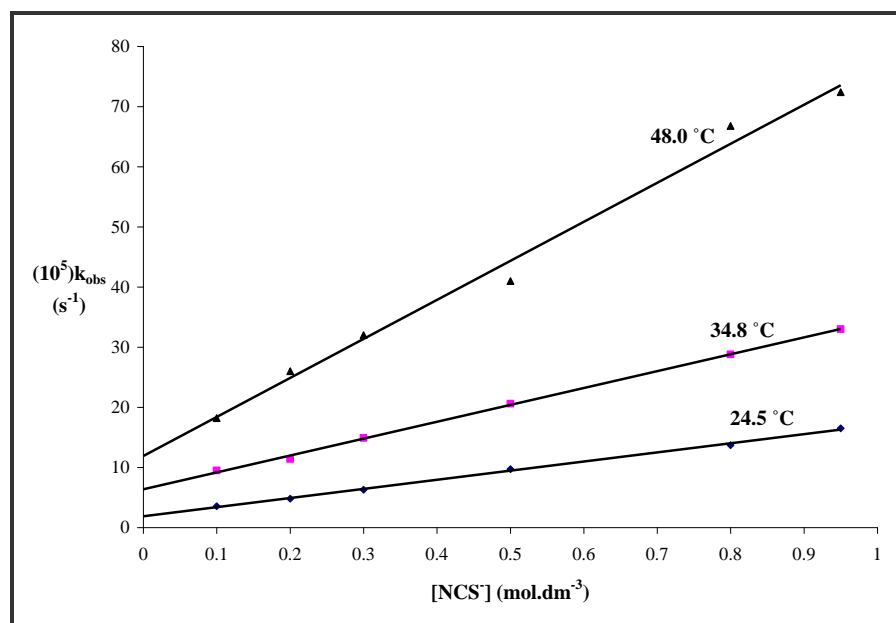


**Figure 4.11:** Plot of  $k_{\text{obs}}$  vs.  $[\text{NCS}^-]$  for the second reaction ( $k_3$  step, **Scheme 4.5**) at different temperatures,  $\mu = 1.0 \text{ M}$  ( $\text{NaClO}_4$ ),  $\lambda = 400 \text{ nm}$ ,  $[\text{Co}(\text{lda})(\text{H}_2\text{O}_2)] = 1 \times 10^{-3} \text{ M}$ .

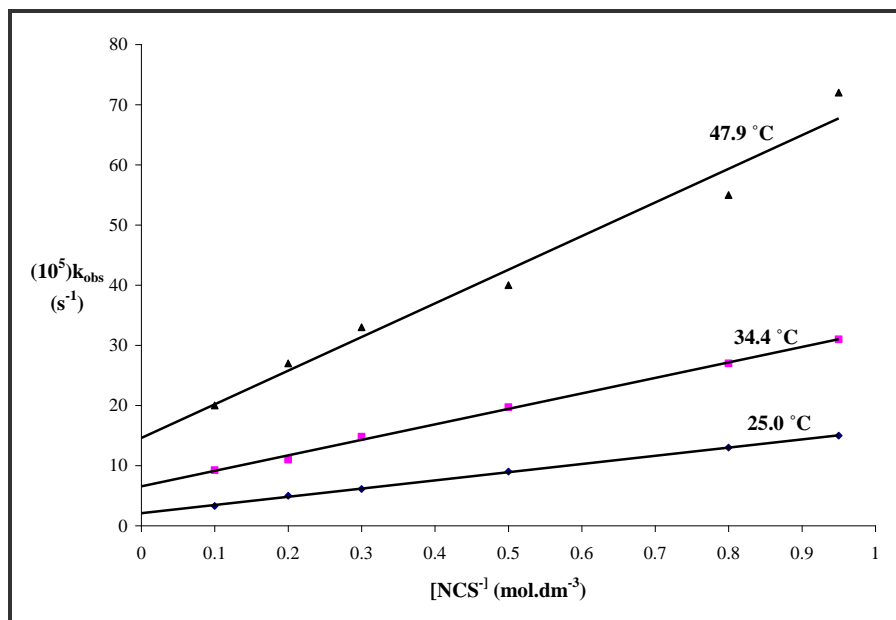


**Figure 4.12:** Plot of  $k_{\text{obs}}$  vs.  $[\text{NCS}^-]$  for the second reaction ( $k_3$  step, **Scheme 4.5**) at different temperatures,  $\mu = 1.0 \text{ M}$  ( $\text{NaClO}_4$ ),  $\lambda = 400 \text{ nm}$ ,  $[\text{Co}(\text{pda})(\text{H}_2\text{O}_2)] = 1 \times 10^{-3} \text{ M}$ .

According to **Scheme 4.5** the concentration of  $[\text{Co}(\text{L})(\text{H}_2\text{O})(\text{OH})]^-$  ( $\text{L} = \text{lda}, \text{pda}$ ) will increase with an increase in pH. The results in **Figure 4.13** and **4.14** clearly indicate an increase in substitution rate with an increase in pH. As mentioned earlier, the UV/VIS spectrum of  $[\text{Co}(\text{lda})(\text{H}_2\text{O})(\text{OH})]^-$  and  $[\text{Co}(\text{pda})(\text{H}_2\text{O})(\text{OH})]^-$  at  $\text{pH} > 7$  indicated competing reactions, possibly due to dimer formation. In order to prevent further complication of the reaction scheme it was decided to investigate the reaction between  $\text{Co}(\text{III})\text{-L}$  ( $\text{L} = \text{lda}, \text{pda}$ ) and  $\text{NCS}^-$  ions between  $\text{pH} 2\text{--}7$ . This meant that the values of  $k_2$ ,  $k_{-2}$  and  $\text{pK}_{\text{a}2}$  could only be determined from **Eq. 4.15** and the influence of the  $k_1$  and  $k_3$  pathways as well as the dissociation constants  $\text{K}_{\text{a}1}$  and  $\text{K}_{\text{a}2}$  could not be ignored under these conditions.

The values for  $k_2$ ,  $k_{-2}$  and  $\text{pK}_{\text{a}2}$  were calculated by fitting the data in **Figures 4.14** and **4.15** at  $\text{pH} 7$  simultaneously with the data in **Figures 4.12** and **4.13** into **Eq. 4.15**. This was achieved by keeping the values of  $k_1$ ,  $k_{-1}$ ,  $k_3$ ,  $k_{-3}$  and  $\text{pK}_{\text{a}1}$ , that was already

determined in the previous paragraphs, constant. These results are also reported in **Table 4.3**.

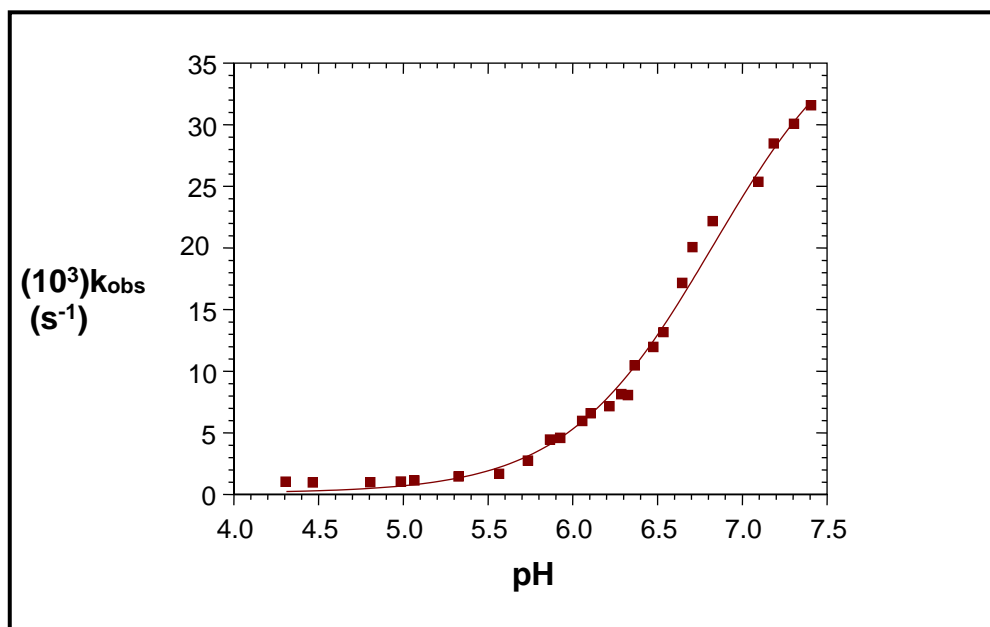


**Figure 4.13:** Plot of  $k_{\text{obs}}$  vs. pH at  $25.0^\circ\text{C}$  for the first reaction between  $[\text{Co}(\text{lda})(\text{H}_2\text{O}_2)]$  and  $\text{NCS}^-$  ions.  $\mu = 1.0 \text{ M}$  ( $\text{NaClO}_4$ ),  $\lambda = 400 \text{ nm}$ ,  $[\text{NCS}^-] = 1.25 \times 10^{-2} \text{ M}$ .

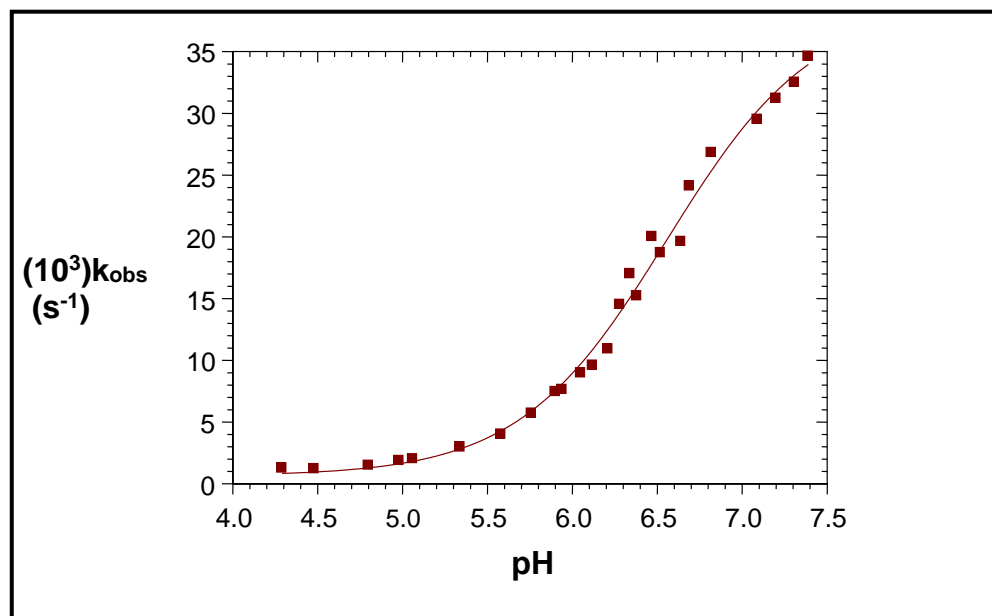


**Figure 4.14:** Plot of  $k_{\text{obs}}$  vs. pH at  $25.0^\circ\text{C}$  for the first reaction between  $[\text{Co}(\text{pda})(\text{H}_2\text{O}_2)]$  and  $\text{NCS}^-$  ions.  $\mu = 1.0 \text{ M}$  ( $\text{NaClO}_4$ ),  $\lambda = 400 \text{ nm}$ ,  $[\text{NCS}^-] = 1.25 \times 10^{-2} \text{ M}$ .

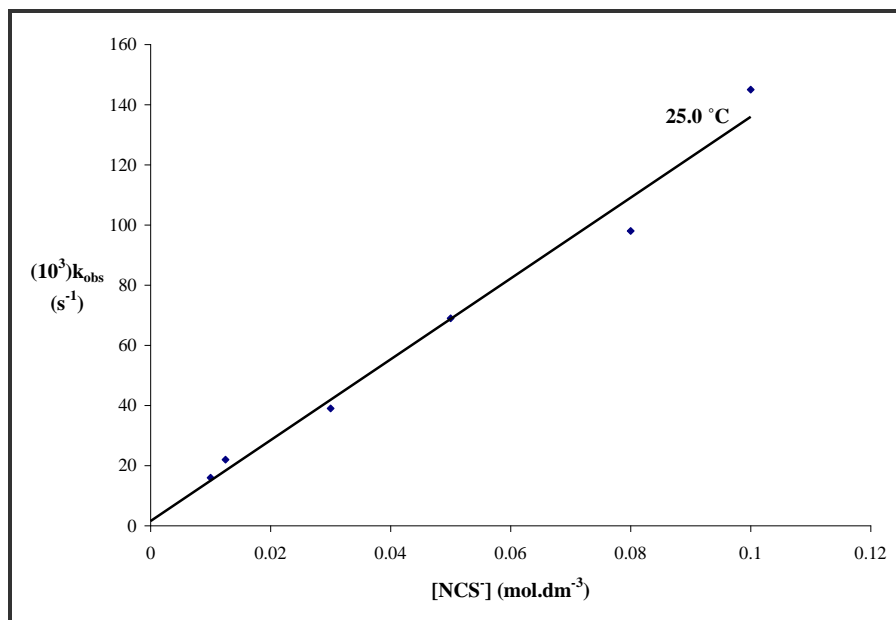


**Figure 4.15:** Plot of  $k_{\text{obs}}$  vs.  $[\text{NCS}^-]$  for the first reaction at  $\text{pH} = 7.00$ ,  $25.0\text{ }^\circ\text{C}$ ,  $\mu = 1.0\text{ M}$  ( $\text{NaClO}_4$ ),  $\lambda = 400\text{ nm}$ ,  $[\text{Co}(\text{lda})(\text{H}_2\text{O}_2)] = 2 \times 10^{-4}\text{ M}$ .

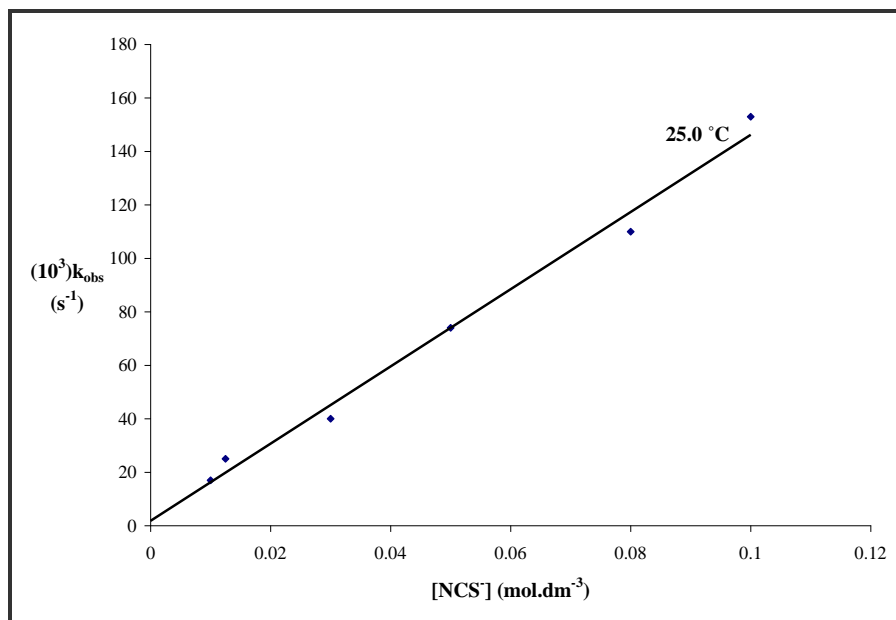


**Figure 4.16:** Plot of  $k_{\text{obs}}$  vs.  $[\text{NCS}^-]$  for the first reaction at  $\text{pH} = 7.00$ ,  $25.0\text{ }^\circ\text{C}$ ,  $\mu = 1.0\text{ M}$  ( $\text{NaClO}_4$ ),  $\lambda = 400\text{ nm}$ ,  $[\text{Co}(\text{pda})(\text{H}_2\text{O}_2)] = 2 \times 10^{-4}\text{ M}$ .

The calculation of activation parameters from kinetic data supplies information regarding the reaction mechanism. The Eyring Equation (refer to Chapter 2) that is used to calculate the activation parameters,  $\Delta H^\ddagger$  and  $\Delta S^\ddagger$ , is shown in **Eq. 4.19**.

$$\ln\left(\frac{k}{T}\right) = \ln\left(\frac{k_b}{h}\right) + \frac{\Delta S^\ddagger}{R} - \frac{\Delta H^\ddagger}{RT} \quad (4.19)$$

In **Eq. 4.19**, T = Temperature in Kelvin,  $k_b$  = Boltzman's constant, h = Planck's constant and R = universal gas constant. The activation parameters  $\Delta H^\ddagger$  and  $\Delta S^\ddagger$  can be obtained experimentally from a plot of  $\ln(k/T)$  vs.  $(1/T)$ . The activation enthalpy,  $\Delta H^\ddagger$ , is calculated from the slope  $\{-\Delta H^\ddagger/R\}$  of the graph while the activation entropy,  $\Delta S^\ddagger$ , is calculated from the section  $\{\ln(k_b/h) + (\Delta S^\ddagger/R)\}$  of the graph.

From **Table 4.3** below as well as the preceding figures it is clear that the experimental data fits well with the rate law (**Eq. 4.9**) and we conclude that **Scheme 4.5** is a fair representation of the mechanism of the substitution reactions between  $[\text{Co}(\text{L})(\text{H}_2\text{O})_2]$  and  $\text{NCS}^-$  ions (L= lda, pda).

**Table 4.3:** Rate constants and activation parameters for the reaction between [Co(L)(H<sub>2</sub>O)<sub>2</sub>] (L= lda, pda) and NCS<sup>-</sup> ions.

Constants	lda	pda
<b>48 °C</b>		
(10 <sup>4</sup> )k <sub>3</sub> (M <sup>-1</sup> s <sup>-1</sup> )	6.3(4)	5.6(5)
(10 <sup>5</sup> )k <sub>-3</sub> (s <sup>-1</sup> )	13(2)	14(3)
K <sub>3</sub> (M <sup>-1</sup> ) <sup>a</sup>	5(7)	4(7)
<b>35 °C</b>		
(10 <sup>2</sup> )k <sub>1</sub> (M <sup>-1</sup> s <sup>-1</sup> )	4.0(1)	4.01(6)
(10 <sup>4</sup> )k <sub>-1</sub> (s <sup>-1</sup> )	14(7)	15(4)
K <sub>1</sub> (M <sup>-1</sup> ) <sup>a</sup> (kinetically determined)	29(8)	27(2)
(10 <sup>4</sup> )k <sub>3</sub> (M <sup>-1</sup> s <sup>-1</sup> )	2.8(5)	2.8(5)
(10 <sup>5</sup> )k <sub>-3</sub> (s <sup>-1</sup> )	6.4(3)	6.4(3)
K <sub>3</sub> (M <sup>-1</sup> ) <sup>a</sup>	4(6)	4(6)
<b>25 °C</b>		
(10 <sup>2</sup> )k <sub>1</sub> (M <sup>-1</sup> s <sup>-1</sup> )	2.43(3)	2.3(4)
(10 <sup>4</sup> )k <sub>-1</sub> (s <sup>-1</sup> )	6(2)	6(2)
K <sub>1</sub> (M <sup>-1</sup> ) <sup>a</sup> (kinetically determined)	41(6)	38(7)
K <sub>1</sub> <sup>#</sup> (M <sup>-1</sup> ) (spectrophotometrically determined)	35(3)	34(2)
(10 <sup>4</sup> )k <sub>3</sub> (M <sup>-1</sup> s <sup>-1</sup> )	1.52(6)	1.36(2)
(10 <sup>5</sup> )k <sub>-3</sub> (s <sup>-1</sup> )	1.9(2)	2.07(9)
K <sub>3</sub> (M <sup>-1</sup> ) <sup>a</sup>	8(5)	7(8)
k <sub>2</sub> (M <sup>-1</sup> s <sup>-1</sup> )	1.34(9)	1.44(8)
(10 <sup>2</sup> ) k <sub>-2</sub> (s <sup>-1</sup> )	1.55(5)	1.84(4)
K <sub>2</sub> (M <sup>-1</sup> ) <sup>a</sup>	86(4)	78(7)
pK <sub>a2</sub> (kinetically determined)	6.82(4)	6.6(3)
ΔH <sup>#</sup> (k <sub>1</sub> ) (kJ mol <sup>-1</sup> )	42(6)	51(4)
ΔS <sup>#</sup> (k <sub>1</sub> ) (J mol <sup>-1</sup> K <sup>-1</sup> )	-133(9)	-107(6)
<b>15 °C</b>		
(10 <sup>2</sup> )k <sub>1</sub> (M <sup>-1</sup> s <sup>-1</sup> )	1.20(9)	0.974(7)
(10 <sup>4</sup> )k <sub>-1</sub> (s <sup>-1</sup> )	2.7(6)	2.9(4)
K <sub>1</sub> (M <sup>-1</sup> ) <sup>a</sup> (kinetically determined)	44(5)	34(8)

<sup>a</sup>determined as k<sub>n</sub>/k<sub>-n</sub>

#### 4.4 Discussion of kinetics results

The values for  $pK_{a1}$  that were reported in **Table 4.2** for  $[\text{Co}(\text{lda})(\text{H}_2\text{O})_2]$  and  $[\text{Co}(\text{pda})(\text{H}_2\text{O})_2]$  are similar to the value of 6.52(2) determined by Visser and co-workers (2002:461) for  $[\text{Co}(\text{nta})(\text{H}_2\text{O})_2]$ . These  $pK_{a1}$  values are also higher than the value of 5.43 found for the similar acid dissociation equilibrium involving  $[\text{Cr}(\text{nta})(\text{H}_2\text{O})_2]$  complex (Hualin & Xu, 1990:137).

The mechanism that was proposed in **Scheme 4.4** is similar to that was found for the reaction between  $[\text{Cr}(\eta^3\text{-nta})(\text{H}_2\text{O})_3]^+$  and  $\text{H}^+$  ions (Visser *et al.*, 1994:1051) and involves the formation of an ion pair. Protonation of one of the carboxylate groups of the lda and pda ligands then occurs, which result in the dissociation of these bonds to give the tridentate lda and pda complexes,  $[\text{Co}(\eta^3\text{-lda})(\text{H}_2\text{O})_3]^+$  and  $[\text{Co}(\eta^3\text{-pda})(\text{H}_2\text{O})_3]^+$ , respectively.

As in the case of  $[\text{Co}(\text{nta})(\text{H}_2\text{O})_2]$  (Visser *et al.*, 2002:461), the UV/VIS studies of both  $[\text{Co}(\text{lda})(\text{H}_2\text{O})_2]$  and  $[\text{Co}(\text{pda})(\text{H}_2\text{O})_2]$  complexes (refer to Chapter 3) indicate competitive reactions at pH values  $> 7$ , possibly due to dimer formation. In order to avoid complications by these reactions, the substitution reactions of  $[\text{Co}(\text{L})(\text{H}_2\text{O})_2]/[\text{Co}(\text{L})(\text{H}_2\text{O})(\text{OH})]^-$  (L = lda, pda) with  $\text{NCS}^-$  ions were studied in the pH range between 2 and 7. The ligand substitution of  $[\text{Co}(\text{L})(\text{H}_2\text{O})_2]/[\text{Co}(\text{L})(\text{H}_2\text{O})(\text{OH})]^-$  with various ligands ( $\text{NCS}^-$ ,  $\text{N}_3^-$  *etc.*) were studied. In the pH 2-7 range, only ligand substitution of  $[\text{Co}(\text{L})(\text{H}_2\text{O})_2]/[\text{Co}(\text{L})(\text{H}_2\text{O})(\text{OH})]^-$  with  $\text{NCS}^-$  ions provided satisfactory results.

Thacker and Higginson (1975:704) also investigated the substitution reactions between  $[\text{Co}(\text{nta})(\text{H}_2\text{O})_2]$  and different incoming ligands ( $\text{NCS}^-$ ,  $\text{HCN}$ ,  $\text{N}_3^-/\text{thiourea}$ ). Unfortunately, none of these ligands provided satisfactory results.  $\text{HCN}$  did not react with  $[\text{Co}(\text{nta})(\text{H}_2\text{O})_2]$  in the pH range 2-7, while the reactions between  $[\text{Co}(\text{nta})(\text{H}_2\text{O})_2]$  and  $\text{N}_3^-/\text{thiourea}$  were complicated by the reduction of the metal centre in each case.

They concluded that only  $\text{NCS}^-$  ions did not reduce the metal centre in the pH range studied.

The rate of substitution of the first aqua ligand of  $[\text{Co}(\text{lda})(\text{H}_2\text{O})_2]$  and  $[\text{Co}(\text{pda})(\text{H}_2\text{O})_2]$  ( $k_1 = 2.43(3) \times 10^{-3} \text{ M}^{-1} \text{ s}^{-1}$  at  $24.5 \text{ }^\circ\text{C}$ ) and ( $k_1 = 2.3(4) \times 10^{-2} \text{ M}^{-1} \text{ s}^{-1}$  at  $25.0 \text{ }^\circ\text{C}$ ), respectively, at low pH is about 125 times faster than the rate of substitution of the second aqua ligand, respectively ( $k_3 = 1.52(6) \times 10^{-4} \text{ M}^{-1} \text{ s}^{-1}$  at  $25.0 \text{ }^\circ\text{C}$ ) and ( $k_3 = 1.36(2) \times 10^{-4} \text{ M}^{-1} \text{ s}^{-1}$  at  $25.0 \text{ }^\circ\text{C}$ ). Similar results was observed by Visser *et al.* (2002:461) for the reaction of  $[\text{Co}(\text{nta})(\text{H}_2\text{O})_2]$  with  $\text{NCS}^-$  ions. They observed that the rate of substitution of the first aqua ligand at low pH was about 120 times faster than the rate of substitution of the second aqua ligand. The reason for this is not well understood, but one would not expect the  $\text{NCS}^-$  ligand to have a high *cis*-labilising effect on the remaining aqua ligand. It is possible that additional  $d \rightarrow \pi^*$  backbonding for strengthening the Co-NCS bond will enhance the  $\sigma$ -donation of  $\text{H}_2\text{O}$  to Co and thus strengthen this Co- $\text{H}_2\text{O}$  bond in the ground state. More information, e.g. crystallographic data, is required in order to explain this decrease in rate successfully.

The  $[\text{Co}(\text{lda})(\text{H}_2\text{O})(\text{OH})]^-$  and  $[\text{Co}(\text{pda})(\text{H}_2\text{O})(\text{OH})]^-$  complexes reacts about 70 times faster at  $25.0 \text{ }^\circ\text{C}$  respectively with  $\text{NCS}^-$  than  $[\text{Co}(\text{lda})(\text{H}_2\text{O})_2]$  and  $[\text{Co}(\text{pda})(\text{H}_2\text{O})_2]$  complexes respectively with  $\text{NCS}^-$  ( $k_2 = 1.34(9) \text{ M}^{-1} \text{ s}^{-1}$  vs.  $2.43(3) \times 10^{-2} \text{ M}^{-1} \text{ s}^{-1}$  for  $k_1$  at  $24.5 \text{ }^\circ\text{C}$ ) and ( $k_2 = 1.44(8) \text{ M}^{-1} \text{ s}^{-1}$  vs.  $2.3(4) \times 10^{-2} \text{ M}^{-1} \text{ s}^{-1}$  for  $k_1$  at  $25.0 \text{ }^\circ\text{C}$ ). A corresponding increase was observed in the similar reaction of  $[\text{Co}(\text{nta})(\text{H}_2\text{O})(\text{OH})]^-$  /  $[\text{Co}(\text{nta})(\text{H}_2\text{O})_2]$  with  $\text{NCS}^-$  ions (Visser *et al.*, 2002:461). This clearly indicates that the hydroxo ligand labilises the *cis*-aqua bond so that an increase in rate is observed. This *cis*-labilising effect of the hydroxo ligand was also observed in the reaction of  $[\text{Cr}(\text{nta})(\text{H}_2\text{O})(\text{OH})]^-$  /  $[\text{Cr}(\text{nta})(\text{H}_2\text{O})_2]$  with  $\text{NCS}^-$  ions where an increase of 8 times was observed (Visser *et al.*, 1994:1051). The same increase was also observed in the formation of  $[\text{Co}(\text{TPPS})(\text{H}_2\text{O})(\text{NCS}^-)]^{4-}$  and  $[\text{Co}(\text{TMpyP})(\text{H}_2\text{O})(\text{NCS}^-)]^{4+}$  (Ashley & Leipoldt, 1981:2326).

The values of  $k_1$  at 25.0 °C is in the same order of magnitude as the value calculated for the reaction of  $[\text{Co}(\text{nta})(\text{H}_2\text{O})_2]$  with  $\text{NCS}^-$  ions ( $k_1 = 2.4(1) \times 10^{-2} \text{ M}^{-1} \text{ s}^{-1}$  at 24.7 °C, Visser *et al.*, 2002:461) as well as the value calculated for the reaction of  $[\text{Co}(\text{TPPS})(\text{H}_2\text{O})_2]^{3-}$  with  $\text{NCS}^-$  ions ( $k_1 = 3.24(2) \times 10^{-2} \text{ M}^{-1} \text{ s}^{-1}$ , Ashley & Leipoldt, 1981:2326) and about 105 times faster than the reaction of  $[\text{Co}(\text{NH}_3)_5(\text{H}_2\text{O})]^{3+}$  with  $\text{NCS}^-$  ions (Van Eldik *et al.*, 1979:1520). This indicates that ligands such as lda, pda and nta exert a very high labilising effect on cobalt(III) complexes. This labilisation can be contributed to the fact that lda and pda donates electron density to the central metal ion which in turn weakens the metal-aqua bond. This also indicates that the electron donating ability of the lda and pda ligands is in the same order of magnitude as that of the porphine ligand. This trend was also observed for the similar Cr(III)-nta complexes (Visser *et al.*, 1994:1051).

The stability constants,  $K_1$ , of  $[\text{Co}(\text{lda})(\text{H}_2\text{O})(\text{OH})]^-$  and  $[\text{Co}(\text{pda})(\text{H}_2\text{O})(\text{OH})]^-$  at 25.0 °C were calculated as 41(6)  $\text{M}^{-1}$  and 38(7)  $\text{M}^{-1}$ , respectively. These values correlate very well with the value of 40(7) obtained by Visser *et al.* (2002:461) for  $[\text{Co}(\text{nta})(\text{H}_2\text{O})(\text{OH})]^-$  at 24.7 °C. The values obtained is almost 70 times smaller than the similar value obtained for  $[\text{Co}(\text{TPPS})(\text{H}_2\text{O})(\text{NCS}^-)]^{4-}$  and 160 times smaller than the value obtained for the formation of  $[\text{Co}(\text{TMpyP})(\text{H}_2\text{O})(\text{NCS}^-)]^{4+}$  (2.6(4)  $\times 10^3 \text{ M}^{-1}$  and 6.4(2)  $\times 10^3 \text{ M}^{-1}$ , respectively, Ashley & Leipoldt, 1981:2326) (TPPS and TMpyP are both N donor ligands). The increase in stability for the porphyrine complexes is probably due to the fact that the formal charge on these complexes is spread over a very large planar surface area, which does not exist for the lda, pda or nta complexes. The mode of bonding of the thiocyanide ion is unknown, but one would anticipate that the ligand is nitrogen bonded because of the apparent hard acid character of cobalt(III) (Huheey *et al.*, 2<sup>nd</sup> Edition, p. 278).

The  $k_1$  values for  $[\text{Co}(\text{lda})(\text{H}_2\text{O})_2]$  and  $[\text{Co}(\text{pda})(\text{H}_2\text{O})_2]$  are factor of 4 times faster than the  $k_1$  value obtained for the reaction of  $[\text{Cr}(\text{nta})(\text{H}_2\text{O})_2]$  with  $\text{NCS}^-$  ions ( $k_1$  was determined as  $5.8 \times 10^{-3} \text{ M}^{-1} \text{ s}^{-1}$  for the chromium complex, Visser *et al.*, 1994:1051). The value of  $k_2$  at 24.7 °C (1.68(5)  $\text{M}^{-1} \text{ s}^{-1}$ ) was approximately 70 times faster than the

value obtained for the similar reaction of  $[\text{Cr}(\text{nta})(\text{H}_2\text{O})(\text{OH})]/[\text{Cr}(\text{nta})(\text{H}_2\text{O})_2]$  with  $\text{NCS}^-$  ions at 35.0 °C. This indicated that Co(III) complexes are more labile than Cr(III) complexes. This was also observed for several M(III)-porphyrin (M = Co/Cr) complexes (Ashley *et al.*, 1980:1608).

The values of  $\Delta H^\ddagger$  for the substitution of the first aqua ligand ( $k_1$ ) in the reaction of  $[\text{Co}(\text{L})(\text{H}_2\text{O})_2]$  (L = lda, pda), respectively with  $\text{NCS}^-$  ions are 42(2) and 51(4)  $\text{kJ mol}^{-1}$  and  $\Delta S^\ddagger$  values are -133(9) and -107(6)  $\text{J mol}^{-1} \text{K}^{-1}$ , respectively. These high negative values for  $\Delta S^\ddagger$  would suggest an associative mechanism, in total contrast to normal substitution reactions of Co(III) complexes (Van Eldik, 1986:115 and Wilkins, 1991:199) where  $I_d$  mechanisms are usually observed. Hung and Busch (1977:4977) observed similar tendencies for the aquation of a range of dichlorotetraamine complexes of Co(III). It was postulated that these aquation reactions are still dissociatively activated, but that the tetragonal pyramidal intermediate states are more polar so that one could expect a larger degree of solvation in which case  $\Delta S^\ddagger$  would become more negative. Until more data are acquired, additional discussion is inappropriate at this time.

# 5

## Critical evaluation

---

*In this chapter the relevance and successes regarding the initial aims of this study are discussed as well as some future research possibilities related to cobalt(III)-lda and-pda complexes.*

---

All the initial aims of this study have to a large extent successfully been met. The synthesis and characterisation of  $[\text{Co}(\text{lda})(\mu\text{-OH})_2]^{2-}$  and  $[\text{Co}(\text{pda})(\mu\text{-OH})_2]^{2-}$  by way of  $^1\text{H}$  NMR and IR together with the UV/VIS spectral study have removed a lot of doubt regarding the structures of the cobalt(III)-lda and-pda complexes first prepared by Uehara *et al.* (1971:1552). The Co(III)-lda and-pda complexes that were isolated and characterised (Chapter 3) can successfully be used as biological model complexes in future studies. These complexes could for example be used to simulate the bonding of metal ion to functional groups of wool fibre or might have uses as models in pharmacology.

The available  $^1\text{H}$  NMR and IR spectra of cobalt(III)-lda and-pda complexes have also been increased substantially and should be of assistance in future studies.

The study of the pH dependence of  $[\text{Co}(\text{lda})(\text{H}_2\text{O})_2]$  and  $[\text{Co}(\text{pda})(\text{H}_2\text{O})_2]$  was successful and the  $\text{pK}_a$  values for the acid dissociation reactions of these complexes were determined. The formation of  $[\text{Co}(\text{lda})(\text{H}_2\text{O})_2]$  and  $[\text{Co}(\text{pda})(\text{H}_2\text{O})_2]$  by acidifying  $[\text{Co}(\text{lda})(\mu\text{-OH})_2]^{2-}$  and  $[\text{Co}(\text{pda})(\mu\text{-OH})_2]^{2-}$  respectively, could be investigated in more detail in the future, especially if multi-probe stopped-flow spectrophotometers can be applied.

The study of the substitution reactions of  $[\text{Co}(\text{lda})(\text{H}_2\text{O})_2]$  and  $[\text{Co}(\text{pda})(\text{H}_2\text{O})_2]$  with thiocyanide, respectively, at different pH values in order to determine the mechanism was successfully undertaken and the values of  $\text{pK}_{a2}$  (**Scheme 4.5**) was determined successfully.

## Chapter 5

High pressure kinetic studies will provide more information on the intimate reaction mechanism for the acid cleavage and substitution reactions in future studies.

## References

---

- ALMAZAN, F., GARCIA-ESPANA, E., MOLLAR, M., LLORET, F., JULVE, M., FAUS, J., SOLANS, X. and ALINS, N., 1990. *J. Chem. Soc. Dalton Trans.*, p. 2565.
- ASHELY, K.R. & LEIPOLDT, J.G., 1981. *Inorg. Chem.*, 20:2326.
- ASHELY, K.R., LEIPOLDT, J.G. and JOSHI, V.K., 1980. *Inorg. Chem.*, 19:1608.
- BARROW, G.M., 1973. *Physical Chemistry* (3<sup>rd</sup> ed.). Tokyo: McGraw-Hill Kogakusha Ltd. p. 190.
- BASOLO, F. and PEARSON, R.G., 1967. *Mechanisms of Inorganic Reactions* (4<sup>th</sup> ed.). New York: John Wiley & Sons. p. 124-164.
- BOCARSLY, J.R., CHIANG, M.Y., BRYANT, L. and BARTON, J.K., 1990. *Inorg. Chem.*, 29: 4898.
- CANDLIN, J.P., TAYLOR, K.A. and THOMPSON, D.T., 1968. *Reactions of Transition-Metal Complexes*. London: Elsevier Publishing Company. p. 12.
- CAPELLOS, C. and BIELSKI, H.J., 1972. *Mathematical Description of Chemical Kinetics in Solutions*. New York: John Wiley & Sons Inc. p. 1.
- COTTON, F.A. and WILKINSON, G., 1988. *Advanced Inorganic Chemistry* (5<sup>th</sup> ed.). New York: John Wiley & Sons. p. 1283-1296.
- DASGUPTA, T.P. & HARRIS, G.M., 1974. *Inorg. Chem.*, 13:1275.
- DASSARMA, S. & DASSARMA, B., 1979. *Inorg. Chem.*, 18:3618.
- DOUGLAS, B.E., McDANIEL, D.H. and ALEXANDER, J.J., 1983. *Concepts and Models of Inorganic Chemistry*. New York: John Wiley & Sons Inc. p. 341.
- ESPESON, J.H., 1995. *Chemical Kinetics and Reaction Mechanisms* (2<sup>nd</sup> ed.). McGraw-Hill Inc. p. 1-15.
- FROST, A.A. and PEARSON, R.G., 1953. *Kinetics and Mechanism*. New York: John Wiley & Sons. p. 74.
- GARLATTI, R.D., TAUZHER, G. and COSTA, G., 1986. *Inorg. Chim. Acta.*, 121:27.
- GLADKIKH, O.P., POZNYAK, A.L., POLYNOVA, T.N. and PORAI-KOSHITS, M.A., 1992. *Koord. Khim.*, 18:908.

## References

- GLADKIKH, O.P., POZNYAK, A.L., POLYNOVA, T.N. and PORAI-KOSHITS, M.A.**, 1992. *Koord. Khim.*, 18:1231.
- GLADKIKH, O.P., POZNYAK, A.L., POLYNOVA, T.N. and PORAI-KOSHITS, M.A.**, 1997. *Russian J. Inorg. Chem.*, 42:1346.
- HALPERN, J., PALMER, R.A. and BLAKELY, L.M.**, 1966. *J. Am. Chem. Soc.*, 88: 2877.
- HAULIN, Z. & XU, Z.**, 1990. *Polyhedron.*, 9:137.
- HAY, R.W.**, 1984. *Coord. Chem. Rev.*, 57:1.
- HOUSE, D.A., BROWNING, J., ZIPPER, L. and MARTY, W.**, 1999. *Inorg. Chim. Acta.*, 288:181.
- HUHEEY, J.E., KEITER, E.A., and KEITER, R.L.**, *Inorganic Chemistry: Principles, Structure and Reactivity* (2<sup>nd</sup> ed.), p. 278.
- HUNG, Y. and BUSCH, D.H.**, 1977. *J. Am. Chem. Soc.*, 99:4977.
- JITSUKAWA ,K., MORIOKA, T., MASUDA, H., OGOSHI, H. and EINAGA, H.**, 1994. *Inorg. Chim. Acta*, 216:249.
- JORDAN, R.B.**, 1991. *Reaction Mechanisms of Inorganic and Organometallic Systems*. New York: Oxford University Press. p. 1-57.
- KUMITA, H., JITSUKAWA, K., and EINAGA, H.**, 1998. *Inorg. Chim. Acta*, 283:160.
- LANGFORD, C.H. and GRAY, H.B.**, 1966. *Ligand Substitution Processes*. New York: W.A. Benjamin Inc. p. 55.
- LLEWELLYN, D.R., O'CONNOR, C.J. and ODEB, A.A.**, 1964. *J. Chem. Soc.* p. 196.
- LUČKA, A. & HOLEČEK, J.**, 2003. *Dyes and Pigments.*, 57:115.
- MELOON, D.R. & HARRIS, G.M.**, 1977. *Inorg. Chem.*, 16:434.
- MORI, M., SHIBATA, M., KYUNO, E. and OKUBO, Y.**, 1958. *Studies on the Synthesis of Metal Complexes*, 31:940.
- MORRAL, F.R.**, 1967. *Adv. Chem. Ser.* 62:70.
- MORRAL, F.R.**, 1979. Cobalt compounds. (In GRAYSON, M., ed. *Kirk-Othmer Encyclopedia of Chemical Technology*. New York: John Wiley & Sons. p. 495–510).

## References

- NAKAMOTO, K.**, 1963. *Infrared Spectra of Inorganic and Coordination Compounds*. New York: John Wiley & Sons. p. 206.
- PLANISEK, F & NEWKIRK, J.B.**, 1979. Cobalt and cobalt alloys. (In **GRAYSON, M.**, ed. *Kirk-Othmer Encyclopedia of Chemical Technology*. New York: John Wiley & Sons. p. 481-494).
- PLUMB, W. and HARRIS, G.M.**, 1964. *Inorg. Chem.*, 3:542.
- PORTERFIELD, W.W.**, 1993. *Inorganic Chemistry* (2<sup>nd</sup> ed.). Academic Press Inc. p. 703.
- POTGIETER, H., PURCELL, W., VISSER, H.G. and NICLÓS-GUTIÉRREZ, J.**, 2005. *Polyhedron.*, 24:1968.
- PURCELL, K.F. & KOTZ, J.C.**, 1980. *An Introduction to Inorganic Chemistry*. Philadelphia: Saunders College Publishing. p. 412.
- SCIENTIST FOR WINDOWS**, 1990. Least Square Parameter Estimation, Version 4.00, Micromath.
- SKRZYPCZAK-JANKUN, E., and SMITH, D.A.**, 1994. *Acta Cryst.*, Section C:1097
- SMITH, A., ALAM, J., ESCRIBA, P.V. and MORGAN, W.T.**, 1993. *J. Biol. Chem.*, 268:7365.
- SWADDLE, T.W. and GUASTALLA, G.**, 1969. *Inorg.Chem.*, 8:1604.
- SWAMINATHAN, K., SINHA, U.C., CHATTERJEE, C., PHULAMBRIKAR, A., PADMANABHAN, V.M. and BOHRA, R.**, 1989. *Acta Cryst.*, 45:566.
- SYKES, A.G.**, 1966. *Kinetics of Inorganic Reactions*. Pergamon Press Ltd. p. 43.
- TANNENBAUM, R. & BOR, G.**, 2004. *Journal of Molecular Catalysis A: Chemical.*, 215:33.
- THACKER, M.A. & HIGGINSON, W.C.E.**, 1975. *J. Chem. Soc. Dalton Trans.*, p. 704.
- TSUCHIYA, R., UEHARA, A. and KYUNO, E.**, 1969. *Bull. Chem. Soc. Jpn.*, 42:1886.
- UEHARA, A., KYUNO, E. and TSUCHIYA, R.**, 1971. *Bull. Chem. Soc. Jpn.*, 44:1548.
- UEHARA, A., KYUNO, E. and TSUCHIYA, R.**, 1971. *Bull. Chem. Soc. Jpn.*, 44:1552.
- VAN ELDIK, R., PALMER, D.A. and KELM, H.**, 1979. *Inorg. Chem.*, 18:1520.
- VAN ELDIK, R.**, 1986. *Kinetics and Mechanisms*. New York: Elsevier Science Publishing Company Inc. p. 115.

## References

- VISSER, H.G., LEIPOLDT, J.G., PURCELL, W. and MOSTERT, D.,** 1994. *Polyhedron.*, 13:1051.
- VISSER, H.G., PURCELL, W., BASSON, S.S. and CLAASEN, Q.,** 1997. *Polyhedron*, 16:2851.
- VISSER, H.G., PURCELL, W. and BASSON, S.S.,** 2001. *Polyhedron*, 20:185.
- VISSER, H.G., PURCELL, W. and BASSON, S.S.,** 2001. *Trans. Metal Chem.*, 26:175.
- VISSER, H.G., PURCELL, W. and BASSON, S.S.,** 2002. *Trans. Metal Chem.*, 27:461.
- VISSER, H.G., PURCELL, W. and BASSON, S.S.,** 2003. *Trans. Metal Chem.*, 28:235.
- WILKINS, R.G.,** 1974. *The Study of Kinetics and Mechanism of Reactions of the Transitional Metal Complexes.* Allyn and Bacon Inc. p. 181.
- WILKINS, R.G.,** 1991. *Kinetics and Mechanism of Reactions of the Transitional Metal Complexes.* New York: VCH Publishers Inc. p. 199.
- WITHLOW, S.H.,** 1972. *Acta Cryst.*, B28:1914.

## Appendix A: Supplementary data

---

### Section I Kinetic data

The tables in this section give the observed first-order rate constant for the reactions described in Chapter 4. Where applicable, the figure number representing a specific data set is included in brackets after the Table number.

**Table A.1 (Figure 4.1)** Plot of Abs ( $\lambda = 400$  nm) vs. pH for [Co(lda)(H<sub>2</sub>O)<sub>2</sub>] ( $2 \times 10^{-3}$  M), 25.1 °C,  $\mu = 1.0$  M (NaClO<sub>4</sub>).

pH	A	pH	A
3.55	0.4841	6.10	0.4258
3.82	0.4832	6.14	0.4253
3.98	0.4854	6.19	0.4273
4.28	0.4800	6.24	0.4199
4.82	0.4851	6.29	0.4134
4.89	0.4817	6.35	0.4110
5.01	0.4767	6.40	0.4052
5.21	0.4763	6.46	0.4025
5.31	0.4723	6.50	0.4023
5.38	0.4702	6.56	0.3992
5.46	0.4639	6.62	0.3933
5.51	0.4663	6.71	0.3939
5.56	0.4614	6.76	0.3936
5.75	0.4588	6.90	0.3959
5.80	0.4503	7.03	0.3860
5.86	0.4460	7.07	0.3807
5.91	0.4409	7.18	0.3812
5.96	0.4410	7.26	0.3803
5.99	0.4464	7.48	0.3805
6.05	0.4373	7.57	0.3789

## Appendix A

**Table A.2 (Figure 4.2)** Plot of Abs ( $\lambda = 400$  nm) vs. pH for [Co(pda)(H<sub>2</sub>O)<sub>2</sub>] ( $2 \times 10^{-3}$  M), 25.2 °C,  $\mu = 1.0$  M (NaClO<sub>4</sub>).

pH	A	pH	A
3.56	0.4097	6.11	0.3729
3.64	0.4091	6.17	0.3695
3.74	0.4100	6.25	0.3624
3.88	0.4097	6.31	0.3574
4.00	0.4066	6.38	0.3522
4.18	0.4061	6.45	0.3483
4.34	0.4047	6.52	0.3446
4.56	0.4048	6.57	0.3360
4.75	0.4037	6.62	0.3352
4.94	0.4027	6.67	0.3265
5.02	0.4012	6.73	0.3237
5.12	0.3997	6.77	0.3183
5.19	0.3989	6.85	0.3102
5.24	0.3970	6.89	0.3086
5.32	0.3960	6.96	0.3007
5.37	0.3948	7.03	0.2941
5.42	0.3932	7.13	0.2857
5.49	0.3921	7.25	0.2766
5.53	0.3915	7.33	0.2710
5.59	0.3907	7.43	0.2650
5.67	0.3887	7.52	0.2620
5.75	0.3861	7.63	0.2539
5.81	0.3852	7.72	0.2531
5.88	0.3834	7.84	0.2515
5.92	0.3810	7.94	0.2462
5.97	0.3759	8.02	0.2418
6.03	0.3740	8.17	0.2410

## Appendix A

**Table A.3 (Figure 4.3)** Plot of  $k_{\text{obs}}$  vs.  $[\text{H}^+]$  at different temperatures,  $\mu = 1.0 \text{ M}$  ( $\text{NaClO}_4$ ),  $\lambda = 355 \text{ nm}$ ,  $[\text{Co}(\text{l}da)(\text{H}_2\text{O})_2] = 1 \times 10^{-2} \text{ M}$ .

$[\text{H}^+]$ ( $\text{mol} \cdot \text{dm}^{-3}$ )	$(10^3)k_{\text{obs}}$ ( $\text{s}^{-1}$ )		
	5.9 °C	15.9 °C	25.9 °C
0.1	1.10(2)	2.0(2)	4.98(3)
0.2	2.16(1)	4.2(2)	9.79(2)
0.3	3.40(2)	5.8(3)	14.1(3)
0.5	5.30(3)	9.0(1)	21.5(1)
0.7	7.20(4)	12.3(3)	29.0(2)
0.95	9.10(3)	15.8(4)	35.8(5)

**Table A.4 (Figure 4.4)** Plot of  $k_{\text{obs}}$  vs.  $[\text{H}^+]$  at different temperatures,  $\mu = 1.0 \text{ M}$  ( $\text{NaClO}_4$ ),  $\lambda = 355 \text{ nm}$ ,  $[\text{Co}(\text{p}da)(\text{H}_2\text{O})_2] = 1 \times 10^{-2} \text{ M}$ .

$[\text{H}^+]$ ( $\text{mol} \cdot \text{dm}^{-3}$ )	$(10^3)k_{\text{obs}}$ ( $\text{s}^{-1}$ )		
	5.7 °C	15.7 °C	25.7 °C
0.1	1.10(2)	2.1(3)	5.0(2)
0.2	1.88(1)	3.9(2)	9.5(1)
0.3	2.86(3)	5.5(4)	14.1(3)
0.5	4.67(4)	8.4(3)	21.3(3)
0.7	6.25(2)	11.5(3)	28.5(2)
0.95	8.1(5)	14.8(4)	34.8(2)

**Table A.5 (Figure 4.7)** Plot of Abs ( $\lambda = 400 \text{ nm}$ ) vs.  $[\text{NCS}^-]$  for  $[\text{Co}(\text{l}da)(\text{H}_2\text{O})_2]$  ( $1 \times 10^{-3} \text{ M}$ ),  $25.1 \text{ °C}$ ,  $\text{pH} = 2.0$  and  $\mu = 1.0 \text{ M}$  ( $\text{NaClO}_4$ ).

$[\text{NCS}^-]$ ( $\text{mol} \cdot \text{dm}^{-3}$ )	<b>A</b>
0.0	0.105
0.1	0.793
0.2	0.860
0.3	0.896
0.5	0.930
0.8	0.954
0.95	0.961

## Appendix A

**Table A.6 (Figure 4.8)** Plot of Abs ( $\lambda = 400$  nm) vs.  $[\text{NCS}^-]$  for  $[\text{Co}(\text{pda})(\text{H}_2\text{O})_2]$  ( $1 \times 10^{-3}$  M),  $25.3$  °C,  $\text{pH} = 2.0$  and  $\mu = 1.0$  M ( $\text{NaClO}_4$ ).

$[\text{NCS}^-]$ ( $\text{mol.dm}^{-3}$ )	<b>A</b>
0.0	0.116
0.1	0.788
0.2	0.852
0.3	0.891
0.5	0.927
0.8	0.946
0.95	0.952

**Table A.7 (Figure 4.9)** Plot of  $k_{\text{obs}}$  vs.  $[\text{NCS}^-]$  for first reaction ( $k_1$  step, **Scheme 4.5**) at different temperatures,  $\mu = 1.0$  M ( $\text{NaClO}_4$ ),  $\lambda = 400$  nm,  $[\text{Co}(\text{lda})(\text{H}_2\text{O})_2] = 1 \times 10^{-3}$  M.

$[\text{NCS}^-]$ ( $\text{mol.dm}^{-3}$ )	$(10^3)k_{\text{obs}}$ ( $\text{s}^{-1}$ )		
	15.1 °C	24.5 °C	34.8 °C
0.1	1.47(3)	3.21(4)	5.6(2)
0.2	2.65(4)	5.50(1)	8.81(2)
0.3	3.83(2)	7.60(3)	13.2(4)
0.5	6.42(1)	12.8(4)	22.4(3)
0.7	9.86(4)	19.7(3)	32.1(5)
0.95	11.7(3)	23.8(4)	39.8(1)

## Appendix A

**Table A.8 (Figure 4.10)** Plot of  $k_{\text{obs}}$  vs.  $[\text{NCS}^-]$  for first reaction ( $k_1$  step, **Scheme 4.5**) at different temperatures,  $\mu = 1.0 \text{ M}$  ( $\text{NaClO}_4$ ),  $\lambda = 400 \text{ nm}$ ,  $[\text{Co}(\text{pda})(\text{H}_2\text{O})_2] = 1 \times 10^{-3} \text{ M}$ .

$[\text{NCS}^-]$ ( $\text{mol.dm}^{-3}$ )	$(10^3)k_{\text{obs}}$ ( $\text{s}^{-1}$ )		
	14.9 °C	25.0 °C	34.4 °C
0.1	1.2(1)	3.15(4)	6.2(2)
0.2	2.239(2)	5.122(4)	8.85(3)
0.3	3.249(3)	7.566(4)	13.45(3)
0.5	5.207(4)	11.51(2)	21.5(4)
0.7	8.114(2)	19.08(3)	33.6(8)
0.95	9.484(3)	22.51(1)	39.8(6)

**Table A.9 (Figure 4.11)** Plot of  $k_{\text{obs}}$  vs.  $[\text{NCS}^-]$  for second reaction ( $k_3$  step, **Scheme 4.5**) at different temperatures,  $\mu = 1.0 \text{ M}$  ( $\text{NaClO}_4$ ),  $\lambda = 400 \text{ nm}$ ,  $[\text{Co}(\text{lada})(\text{H}_2\text{O})_2] = 1 \times 10^{-3} \text{ M}$ .

$[\text{NCS}^-]$ ( $\text{mol.dm}^{-3}$ )	$(10^5)k_{\text{obs}}$ ( $\text{s}^{-1}$ )		
	24.5 °C	34.8 °C	48.0 °C
0.1	3.55(2)	9.5(2)	18.2(5)
0.2	4.8(1)	11.4(1)	26(1)
0.3	6.3(3)	14.9(3)	32(2)
0.5	9.7(3)	20.6(2)	41(2)
0.7	13.7(5)	28.8(3)	66.8(4)
0.95	16.5(5)	33.0(4)	72.4(4)

## Appendix A

**Table A.10 (Figure 4.12)** Plot of  $k_{\text{obs}}$  vs.  $[\text{NCS}^-]$  for second reaction ( $k_3$  step, **Scheme 4.5**) at different temperatures,  $\mu = 1.0 \text{ M}$  ( $\text{NaClO}_4$ ),  $\lambda = 400 \text{ nm}$ ,  $[\text{Co}(\text{pda})(\text{H}_2\text{O})_2] = 1 \times 10^{-3} \text{ M}$ .

$[\text{NCS}^-]$ ( $\text{mol.dm}^{-3}$ )	$(10^4)k_{\text{obs}}$ ( $\text{s}^{-1}$ )		
	25.0 °C	34.4 °C	47.9 °C
0.1	3.3(2)	9.25(3)	20(7)
0.2	5(1)	11(2)	27(9)
0.3	6.1(4)	14.8(3)	33(6)
0.5	9(5)	19.7(3)	40(5)
0.7	13(6)	27(4)	55(4)
0.95	15(4)	31(5)	72(4)

**Table A.11 (Figure 4.13)** Plot of  $k_{\text{obs}}$  vs. pH at 25.0 °C for the first reaction between  $[\text{Co}(\text{lda})(\text{H}_2\text{O})_2]$  and  $\text{NCS}^-$  ions.  $\mu = 1.0 \text{ M}$  ( $\text{NaClO}_4$ ),  $\lambda = 400 \text{ nm}$ ,  $[\text{NCS}^-] = 1.25 \times 10^{-2} \text{ M}$ .

pH	$(10^3)k_{\text{obs}}$ ( $\text{s}^{-1}$ )	pH	$(10^3)k_{\text{obs}}$ ( $\text{s}^{-1}$ )
4.31	0.95(4)	6.29	8.07(5)
4.47	0.91(4)	6.33	8.00(6)
4.81	0.93(4)	6.37	10.4(4)
4.99	0.97(3)	6.48	11.9(5)
5.07	1.07(4)	6.54	13.1(5)
5.33	1.39(7)	6.65	17.7(5)
5.57	1.61(7)	6.71	20.0(6)
5.74	2.69(8)	6.83	22.1(4)
5.87	4.39(6)	7.1	25.3(5)
5.93	4.53(6)	7.19	28.4(4)
6.06	5.89(6)	7.31	30.0(4)
6.11	6.51(5)	7.41	31.5(4)
6.22	7.10(4)		

## Appendix A

**Table A.12 (Figure 4.14)** Plot of  $k_{\text{obs}}$  vs. pH at 25.0 °C for the first reaction between  $[\text{Co}(\text{pda})(\text{H}_2\text{O})_2]$  and  $\text{NCS}^-$  ions.  $\mu = 1.0 \text{ M}$  ( $\text{NaClO}_4$ ),  $\lambda = 400 \text{ nm}$ ,  $[\text{NCS}^-] = 1.25 \times 10^{-2} \text{ M}$ .

pH	$(10^3)k_{\text{obs}}$ ( $\text{s}^{-1}$ )	pH	$(10^3)k_{\text{obs}}$ ( $\text{s}^{-1}$ )
4.29	1.255(4)	6.28	14.5(5)
4.48	1.195(5)	6.34	17.0(6)
4.80	1.482(3)	6.38	15.2(6)
4.98	1.863(3)	6.47	20.0(4)
5.06	2.000(6)	6.52	18.7(3)
5.34	2.961(6)	6.64	19.6(3)
5.58	4.001(5)	6.69	24.1(2)
5.76	5.686(5)	6.82	26.8(4)
5.90	7.448(5)	7.09	29.5(4)
5.94	7.62(3)	7.20	31.2(3)
6.05	8.95(3)	7.31	32.5(2)
6.12	9.57(4)	7.39	34.6(3)
6.21	10.9(2)		

**Table A.13 (Figure 4.15)** Plot of  $k_{\text{obs}}$  vs.  $[\text{NCS}^-]$  for first reaction at pH = 7.00, 25.0 °C,  $\mu = 1.0 \text{ M}$  ( $\text{NaClO}_4$ ),  $\lambda = 400 \text{ nm}$ ,  $[\text{Co}(\text{lida})(\text{H}_2\text{O})_2] = 2 \times 10^{-4} \text{ M}$ .

$[\text{NCS}^-]$ ( $\text{mol}\cdot\text{dm}^{-3}$ )	$(10^2)k_{\text{obs}}$ ( $\text{s}^{-1}$ )
0.0100	1.6(4)
0.0125	2.22(4)
0.0300	3.9(3)
0.0500	6.9(2)
0.0800	9.8(2)
0.1000	14.5(1)

## Appendix A

**Table A.14 (Figure 4.16)** Plot of  $k_{\text{obs}}$  vs.  $[\text{NCS}^-]$  for first reaction at pH = 7.00, 25.0 °C,  $\mu = 1.0 \text{ M}$  ( $\text{NaClO}_4$ ),  $\lambda = 400 \text{ nm}$ ,  $[\text{Co}(\text{pda})(\text{H}_2\text{O})_2] = 2 \times 10^{-4} \text{ M}$ .

$[\text{NCS}^-]$ ( $\text{mol.dm}^{-3}$ )	$(10^2)k_{\text{obs}}$ ( $\text{s}^{-1}$ )
0.0100	1.7(4)
0.0125	2.5(3)
0.0300	4.0(3)
0.0500	7.4(2)
0.0800	11.0(1)
0.1000	15.3(2)

## Section II Theoretical aspects of kinetics

### Spectrophotometric determination of ionization constants:

For diprotic species:



The observed absorption coefficient,  $\epsilon$  at the analytical wavelength for a given pH value, when all these species are present, is

$$\epsilon = \epsilon_{\text{A}^{2-}} F_{\text{A}^{2-}} + \epsilon_{\text{HA}^-} F_{\text{HA}^-} + \epsilon_{\text{H}_2\text{A}} F_{\text{H}_2\text{A}} \quad (\text{A.2})$$

where  $\epsilon_{\text{A}^{2-}}$ ,  $\epsilon_{\text{HA}^-}$  and  $\epsilon_{\text{H}_2\text{A}}$  are the molar absorption coefficients for the *diprotonated*, *monoprotonated* and *nonprotonated* species, respectively. The fractions of these species present is given by

$$F_{\text{H}_2\text{A}} = [\text{H}^+]^2 / G \quad (\text{A.3})$$

$$F_{\text{HA}^-} = K_{a1}' [\text{H}^+] / G \quad (\text{A.4})$$

$$F_{\text{A}^{2-}} = K_{a1}' K_{a2}' / G \quad (\text{A.5})$$

Where G, the denominator, is  $[\text{H}^+]^2 + K_{a1}' [\text{H}^+] + K_{a1}' K_{a2}'$ . Substituting these relevant factors into the total molar absorption coefficient equation, multiplying with the denominator and rearranging, yields

$$[\text{H}^+]^2 (\epsilon - \epsilon_{\text{H}_2\text{A}}) + K_{a1}' [\text{H}^+] (\epsilon - \epsilon_{\text{HA}^-}) + K_{a1}' K_{a2}' (\epsilon - \epsilon_{\text{A}^{2-}}) = 0 \quad (\text{A.6})$$

## Appendix A

Provided that the same total concentration is used for all the measurements, the expression may be written with the appropriate absorbance ( $A$ ) replacing the molar absorption ( $\epsilon$ ).

The equation can be then arranged to:

$$[\text{H}^+]^2(A_{\text{tot}} - A_{\text{H}_2\text{A}}) + K_{\text{a}1}[\text{H}^+](A_{\text{tot}} - A_{\text{HA}^-}) + K_{\text{a}1}K_{\text{a}2}(A_{\text{tot}} - A_{\text{A}^{2-}}) = 0 \quad (\text{A.7})$$

Rearrangement of this expression after dividing this equation by  $[\text{H}^+]^2$  throughout gives:

$$A_{\text{tot}} = \frac{A_{\text{H}_2\text{A}} + A_{\text{HA}^-}(K_{\text{a}1}/[\text{H}^+]) + A_{\text{A}^{2-}}(K_{\text{a}1}K_{\text{a}2}/[\text{H}^+]^2)}{1 + (K_{\text{a}1}/[\text{H}^+]) + K_{\text{a}1}K_{\text{a}2}/[\text{H}^+]^2} \quad (\text{A.8})$$

For monoprotic species:



The total absorbance  $A_{\text{tot}}$  is the sum of the ionised species,  $A_{\text{B}^-}$ , and the molecular species,  $A_{\text{HB}}$ .

$$A_{\text{tot}} = A_{\text{HB}} + A_{\text{B}^-} \quad (\text{A.10})$$

The absorbance of either component is related to its molar concentration ( $c$ ) by a general expression ( $A = \epsilon lc$ ), where  $\epsilon$  is the molar absorption coefficient of the particular species and  $l$  is the optical length of the cell. The concentration of the ionized species in the mixture is  $F_{\text{B}^-}c$ , where  $F_{\text{B}^-}$  is the fraction ionised. **Eq. A.11** gives the fraction ionised for acids.

$$F_{\text{B}^-} = [\text{B}^-]/([\text{B}^-] + [\text{HB}]) \quad (\text{A.11})$$

## Appendix A

Hence the contribution of  $F_{B^-}$  to the observed absorbance of the mixture is  $\varepsilon_{B^-}F_{B^-}lc$ . Similarly the contribution of the molecular species to the observed absorbance of the mixture is  $\varepsilon_{HB}F_{HB}lc$ , where  $F_{HB}$  is the fraction present in the molecular form. The terms  $\varepsilon_{HB}$  and  $\varepsilon_{B^-}$  are the molar absorption coefficients of the molecular and ionised species, respectively, which are related directly to the absorbance. The ionisation constant is defined by the expression:

$$K_{a1} = \frac{[H^+][B^-]}{[HB]} \quad (\text{A.12})$$

The fractions of ionized and molecular species are then given by expression obtained by replacing  $[HB]$  with  $[H^+][B^-]/K_{a1}$ :

$$F_{B^-} = K_{a1}/([H^+] + K_{a1}) \quad (\text{A.13})$$

$$F_{HB} = [H^+]/([H^+] + K_{a1}) \quad (\text{A.14})$$

If the same cell optical length is used throughout then

$$A = (\varepsilon_{B^-}F_{B^-} + \varepsilon_{HB}F_{HB}) \quad (\text{A.15})$$

and therefore, because  $\varepsilon = A/c$ , and  $F_{B^-}$  and  $F_{HB}$  are defined above,

$$\varepsilon = ((\varepsilon_{B^-}K_{a1}/([H^+] + K_{a1}) + (\varepsilon_{HB}[H^+]/([H^+] + K_{a1}))) \quad (\text{A.16})$$

Provided that the same total concentration is used for all the measurements, the expression may be written with the appropriate absorbance ( $A$ ) replacing the molar absorption ( $\varepsilon$ ). The equation can be then be arranged to:

$$A_{\text{tot}} = \frac{A_{HB} + A_{B^-}(K_{a1}/[H^+])}{1 + (K_{a1}/[H^+])} \quad (\text{A.17})$$

**Spectrophotometric determination of the equilibrium constant of the reaction:**

Consider the following equilibrium reaction between a complex (M) and a ligand (L):



The equilibrium constant for the above-mentioned reaction is given by the following **Eq. A.19**.

$$K = \frac{[ML]}{[M][L]} \quad (\text{A.19})$$

**Eq. A.20** can be applied for the observed absorbance ( $A_{\text{obs}}$ ) according to Beer-Lambert law.

$$A_{\text{obs}} = \varepsilon_M [M] + \varepsilon_{ML} [ML] \quad (\text{A.20})$$

where  $A_{\text{obs}}$  = observed absorbance,  $\varepsilon_M$  = molar extinction coefficient of M and  $\varepsilon_{ML}$  = molar extinction coefficient of ML.

**Eq. A.21** can be applied for the total metal concentration according to the law of Gulberg and Waage (the law of conservation of mass).

$$[M]_t = [M] + [ML] \quad (\text{A.21})$$

where  $[M]_t$  = total concentration of the absorbed M,  $[M]$  = concentration of the metal complex and  $[ML]$  = concentration of the ML-complex.

$[M]$  and  $[ML]$  can be defined respectively, as in **Eq. A.22** and **A. 23** by using **Eq. A.19**.

## Appendix A

$$[M] = \frac{[ML]}{K[L]} \quad (\text{A.22})$$

$$[ML] = K[M][L] \quad (\text{A.23})$$

Separate substitution of **Eq. A.22** and **A.23** in **Eq. A.21** gives **Eq. A.24** and **A.25**, respectively.

$$\begin{aligned} [M]_t &= \frac{[ML]}{K[L]} + [ML] \\ &= [ML] \left( 1 + \frac{1}{K[L]} \right) \\ \therefore [ML] &= \frac{[M]_t}{1 + \frac{1}{K[L]}} \end{aligned} \quad (\text{A.24})$$

$$\begin{aligned} [M]_t &= [M] + K[M][L] \\ &= [M](1 + K[L]) \\ \therefore [M] &= \frac{[M]_t}{1 + K[L]} \end{aligned} \quad (\text{A.25})$$

In **Eq. A.24** and **A.25**,  $[M]$  and  $[ML]$  are express in terms of experimental determined values. Similar substitution of the above-mentioned equations in **Eq. A.20** will give the result in **Eq. A.26**.

## Appendix A

$$A_{\text{obs}} = \frac{\varepsilon_M [M]_t}{1 + K[L]} + \frac{\varepsilon_{ML} [M]}{1 + \frac{1}{K[L]}} \quad (\text{A.26})$$

For **Eq. A.26** the following apply: if  $[L] = 0$ , then  $[ML] = 0$  so that  $A_{\text{obs}} = A_M = \varepsilon_M [M]_t$ . If  $[L] \gg [M]_t$  then  $[M] = 0$  and  $A_M = \varepsilon_{ML} [ML]_t$ . Through substitution of the last mentioned absorbance in **Eq. A.26** and further manipulation gives the results as in **Eq. A.27**.

$$A_{\text{obs}} = \frac{A_M}{1 + K[L]} + \frac{A_{ML} K[L]}{1 + K[L]}$$

$$A_{\text{obs}} = \frac{A_M + A_{ML} K[L]}{1 + K[L]} \quad (\text{A.27})$$

where  $A_M$  = absorbance at the beginning of the reaction and  $A_{ML}$  = absorbance when the reaction is finished.

### Pseudo-first-order reactions (mono-variation)

The rate of a reaction is defined by the change in concentration of any of the reacting species per time unit. For the reaction



the rate can be expressed in terms of the disappearance of A or B or in terms of the formation of C, as shown in **Eq. A.29**.

$$\text{Rate} = \frac{-d[A]}{dt} = \frac{-d[B]}{dt} = \frac{d[C]}{dt} \quad (\text{A.29})$$

## Appendix A

**Eq. A.30** is representative of a typical rate law for Reaction **A.28**, if the rate of the reaction is only dependent on the concentrations of A and B.

$$\text{Rate} = k[\text{A}]^a[\text{B}]^b \quad (\text{A.30})$$

In **Eq. A.30**,  $k$  represents the rate constant whilst  $a$  and  $b$  represent the order of the reaction with respect to the concentrations of A and B. The total order of the reaction is given by the sum of  $a$  and  $b$ . If the reaction proceeds by more than one step, the order of the reaction is determined by the reactions that precede the rate-determining step.

It is often impossible to determine the order of the reaction with respect to the different reactants in one kinetic experiment. The problem can be solved to a large extent by the mono-variation (isolation). This type of experiment is conducted where  $[\text{B}] \gg [\text{A}]$ , which cause  $[\text{B}]$  to be constant during the whole reaction. The rate of this reaction is presented in **Eq. A.31**.

$$\text{Rate} = k_{\text{obs}}[\text{A}]^a \quad (\text{A.31})$$

In **Eq. A.31**,  $k_{\text{obs}}$  is the observed rate constant with

$$k_{\text{obs}} = k[\text{B}]^b \quad (\text{A.32})$$

It often happens that  $a = 1$ , which means that the kinetics of Reaction **A.28** simplifies to that of a first order reaction where  $k_{\text{obs}}$  is the pseudo-first-order rate constant.

In practice  $k_{\text{obs}}$  is determined at different concentrations of  $[\text{B}]$ . If the reaction were first-order with respect to  $[\text{B}]$ , a plot of  $k_{\text{obs}}$  vs.  $[\text{B}]$  would, according to **Eq. A.32**, produce a straight line through the origin. The slope of the graph then give the second-order rate constant.

## Appendix A

If the straight does not pass through the origin of the graph it indicates that there is a second reaction independent of [B]. The rate of the reaction is then given by the **Eq. A.33**.

$$\text{Rate} = k_1[\text{A}][\text{B}] + k_2[\text{A}] \quad (\text{A.33})$$

From **Eq. A.32** and the above discussion, the pseudo-first-order reaction constant is given by **Eq. A.34**.

$$k_{\text{obs}} = k_1[\text{B}] + k_2 \quad (\text{A.34})$$

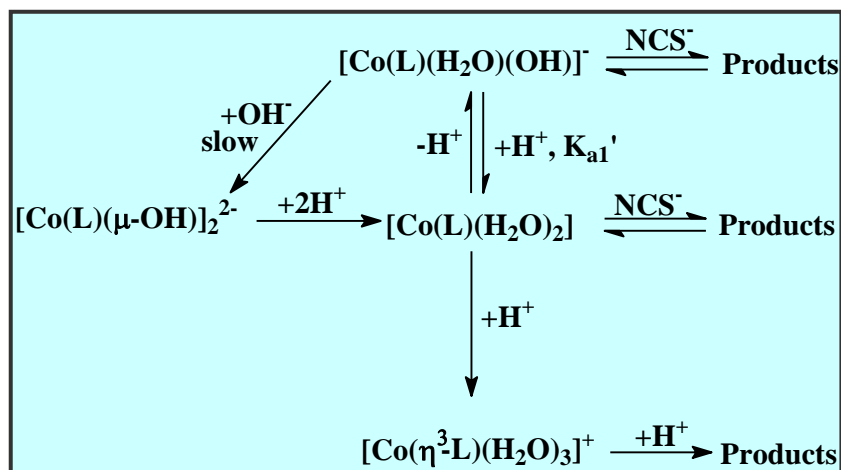
A plot of  $k_{\text{obs}}$  vs. [B] would produce a straight line with slope  $k_1$  and a section of  $k_2$ .

## Abstract

---

The synthesis and reactions of Co(III) complexes with tripod-type ligands such as *l*-leucine-*N,N*-diacetic acid (lda) and *l*-phenylalanine-*N,N*-diacetic acid (pda) have a widespread interest, mainly because of the fact that these complexes can be used as biological model complexes and because lda as well as pda labilises usually inert metal centres. Uehara and co-workers (1971:1552) were the first to prepare Co(III)-lda and-pda complexes. Unfortunately metal complexes of cobalt(III) containing lda and pda as possible multidentate or tripod ligand are rarely mentioned in the literature and little information on their structure and chemistry is available. No kinetic studies on cobalt(III)-lda and-pda complexes have been published.

The question regarding the identity of the different Co(III)-L (L = lda, pda) species in solution at different pH levels has been accounted for in this study (see **Scheme 1**).



**Scheme 1:** Complexes and reactions of cobalt(III)-L (L = lda, pda)

*l*-Leucine-*N,N*-diacetic acid (lda) and *l*-phenylalanine-*N,N*-diacetic acid (pda) were synthesised according to the procedure developed by Bocarsly *et al.* (1990:4898). The synthesis of lda and pda were confirmed by means of IR and <sup>1</sup>H NMR spectrometry.

## Abstract

Both  $[\text{Co}(\text{lda})(\mu\text{-OH})]_2^{2-}$  and  $[\text{Co}(\text{pda})(\mu\text{-OH})]_2^{2-}$  were prepared similar to the method described by Uehara and co-workers (1971:1552). The synthesis of  $[\text{Co}(\text{lda})(\mu\text{-OH})]_2^{2-}$  and  $[\text{Co}(\text{pda})(\mu\text{-OH})]_2^{2-}$  were confirmed by means of IR, UV/VIS and  $^1\text{H}$  NMR spectrometry. The IR stretching frequencies obtained for above-mentioned complexes are indicative of  $\text{COO}^-$  groups coordinated to a metal centre such as Co(III). The  $^1\text{H}$  NMR spectra for both  $[\text{Co}(\text{lda})(\mu\text{-OH})]_2^{2-}$  and  $[\text{Co}(\text{pda})(\mu\text{-OH})]_2^{2-}$  also indicated that all the protons of lda and pda are non-equivalent.

$[\text{Co}(\text{lda})(\mu\text{-OH})]_2^{2-}$  and  $[\text{Co}(\text{pda})(\mu\text{-OH})]_2^{2-}$  undergo bridge-cleavage upon acidification with  $\text{H}^+$  ions to form  $[\text{Co}(\text{lda})(\text{H}_2\text{O})_2]$  and  $[\text{Co}(\text{pda})(\text{H}_2\text{O})_2]$ , respectively. Further acidification of  $[\text{Co}(\text{lda})(\text{H}_2\text{O})_2]$  and  $[\text{Co}(\text{pda})(\text{H}_2\text{O})_2]$  leads to the stepwise dissociation of lda and pda, respectively. The formation of an ion association species between  $[\text{Co}(\text{L})(\text{H}_2\text{O})_2]$  (L = lda, pda) and  $\text{H}^+$  ions upon addition of acid is postulated. This ion associated species dissociates in the rate determining step to form the tridentate L (L = lda, pda) complex,  $[\text{Co}(\eta^3\text{-L})(\text{H}_2\text{O})_3]^+$ . The values of  $k_1$  were determined as  $0.128(8) \text{ s}^{-1}$  at  $25.9 \text{ }^\circ\text{C}$  for lda complex and as  $0.115(7) \text{ s}^{-1}$  at  $25.7 \text{ }^\circ\text{C}$  for pda complex.

Another acid-base equilibrium is observed when the pH of both  $[\text{Co}(\text{lda})(\text{H}_2\text{O})_2]$  and  $[\text{Co}(\text{pda})(\text{H}_2\text{O})_2]$  solutions are increased. It was concluded that the newly formed species are not the dimer, but rather  $[\text{Co}(\text{lda})(\text{H}_2\text{O})(\text{OH})]^-$  and  $[\text{Co}(\text{pda})(\text{H}_2\text{O})(\text{OH})]^-$  which reverts back to the dimer at pH 6 - 7 after several days. The acid dissociation constants of  $[\text{Co}(\text{lda})(\text{H}_2\text{O})_2]$  and  $[\text{Co}(\text{pda})(\text{H}_2\text{O})_2]$  were spectrophotometrically determined as 6.11(2) and 6.74(1), respectively.

The substitution reactions between  $[\text{Co}(\text{L})(\text{H}_2\text{O})_2]/[\text{Co}(\text{L})(\text{H}_2\text{O})(\text{OH})]^-$  (L = lda, pda) and  $\text{NCS}^-$  ions have been investigated. At pH = 2.00  $\text{NCS}^-$  ions substitute the aqua ligands in a stepwise fashion. The substitution of the first aqua ligand of  $[\text{Co}(\text{lda})(\text{H}_2\text{O})_2]$  and  $[\text{Co}(\text{pda})(\text{H}_2\text{O})_2]$  ( $k_1 = 2.43(3) \times 10^{-3} \text{ M}^{-1} \text{ s}^{-1}$  at  $24.5 \text{ }^\circ\text{C}$ ) and ( $k_1 = 2.3(4) \times 10^{-2} \text{ M}^{-1} \text{ s}^{-1}$  at  $25.0 \text{ }^\circ\text{C}$ ), respectively, at low pH is about 125 times faster than the rate of substitution of the second aqua ligand ( $k_3 = 1.52(6) \times 10^{-4} \text{ M}^{-1} \text{ s}^{-1}$  at  $25.0 \text{ }^\circ\text{C}$ ) and ( $k_3 = 1.36(2) \times 10^{-4} \text{ M}^{-1} \text{ s}^{-1}$  at  $25.0 \text{ }^\circ\text{C}$ ), respectively. The  $[\text{Co}(\text{lda})(\text{H}_2\text{O})(\text{OH})]^-$  and  $[\text{Co}(\text{pda})(\text{H}_2\text{O})(\text{OH})]^-$

## Abstract

complexes reacts about 70 times faster at 25.0 °C with  $\text{NCS}^-$ , respectively, than the  $[\text{Co}(\text{lda})(\text{H}_2\text{O})_2]$  and  $[\text{Co}(\text{pda})(\text{H}_2\text{O})_2]$  complexes with  $\text{NCS}^-$  ( $k_2 = 1.34(9) \text{ M}^{-1} \text{ s}^{-1}$  vs.  $2.43(3) \times 10^{-2} \text{ M}^{-1} \text{ s}^{-1}$  for  $k_1$  at 24.5 °C) and ( $k_2 = 1.44(8) \text{ M}^{-1} \text{ s}^{-1}$  vs.  $2.3(4) \times 10^{-2} \text{ M}^{-1} \text{ s}^{-1}$  for  $k_1$  at 25.0 °C), respectively. This clearly indicates that the hydroxo ligand labilises the *cis*-aqua bond so that an increase in rate is observed. Hydroxide is not substituted by  $\text{NCS}^-$  ions at higher pH so that only one reaction is observed spectrophotometrically.

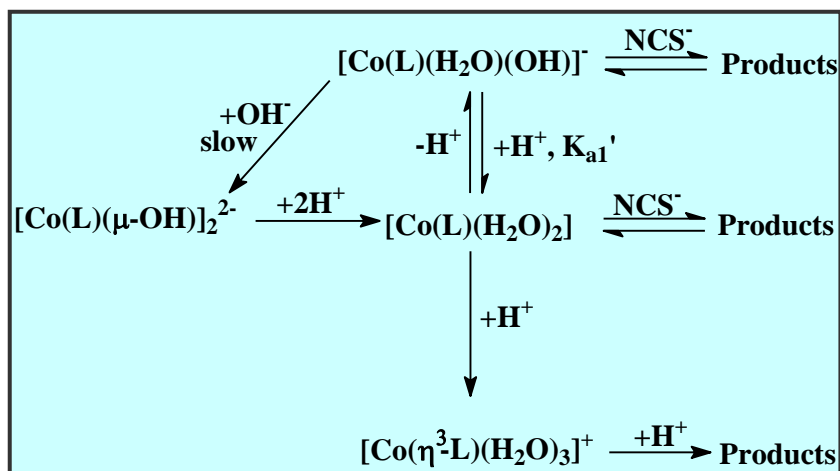
The Co(III)-lda and-pda complexes that were isolated and characterised can successfully be used as biological model complexes in future studies. These complexes could for example be used to simulate the bonding of metal ion to functional groups of wool fibre or might have uses as models in pharmacology.

**Keywords:** cobalt(III), *l*-leucine-*N,N*-diacetic acid (lda) and *l*-phenylalanine-*N,N*-diacetic acid (pda), ionisation constants, substitution reactions.

# Opsomming

Die sintese en reaksies van Co(III) komplekse met driepoot-tipe ligande soos *l*-leusien-*N,N*-diasynsuur (lda) en *l*-fenielalanien-*N,N*-diasynsuur (pda) lok wye belangstelling omdat hierdie komplekse as biologiese modelkomplekse gebruik kan word en omdat die lda en pda ligande metaalsentra wat gewoonlik inert is, labiliseer. Die eerste bereiding van Co(III)-lda en-pda komplekse is gedoen deur Uehara en medewerkers (1971:1552). Ongelukkig word metaalkomplekse van cobalt(III) wat lda en pda as moonklike multidentate of driepootligand bevat, selde in die literatuur vermeld. Daar is dus min beskikbare inligting oor die struktuur en chemie van hierdie komplekse. Daar is nog geen kinetiese studie van cobalt(III)-lda en-pda komplekse gepubliseer nie.

Die vraag rondom die indentiteit van die verskillende Co(III)-L (L = lda, pda) spesies in oplossing (sien **Skema 1**) by verskillende pH's is grootliks in hierdie studie beantwoord.



**Skema 1:** Komplekse en reaksies van cobalt(III)-L (L = lda, pda).

*l*-Leusien-*N,N*-diasynsuur (lda) en *l*-fenielalanien-*N,N*-diasynsuur (pda) was gesintetiseer volgens die prosedure van Bocarsly *et al.* (1990:4898). Die sintese van lda en pda was bevestig met behulp van IR en  $^1\text{H}$  KMR spektrometrie.

## Opsomming

Beide  $[\text{Co}(\text{lda})(\mu\text{-OH})]_2^{2-}$  en  $[\text{Co}(\text{pda})(\mu\text{-OH})]_2^{2-}$  was gesintetiseer volgens die metode wat beskryf is deur Uehara and medewerkers (1971:1552). Die sintese van  $[\text{Co}(\text{lda})(\mu\text{-OH})]_2^{2-}$  en  $[\text{Co}(\text{pda})(\mu\text{-OH})]_2^{2-}$  was bevestig met behulp van IR, UV/VIS en  $^1\text{H}$  KMR spektrometrie. Die IR strekkingsfrekwensies van die bogenoemde komplekse dui op  $\text{COO}^-$  groepe wat gekoördineer is aan metale soos  $\text{Co}(\text{III})$ . Die  $^1\text{H}$  KMR spektrum van beide  $[\text{Co}(\text{lda})(\mu\text{-OH})]_2^{2-}$  en  $[\text{Co}(\text{pda})(\mu\text{-OH})]_2^{2-}$  het ook bewys dat al die protone van lda en pda nie-ekwivalent is.

Hierdie studie het bevind dat die hidrokso-brûe van  $[\text{Co}(\text{lda})(\mu\text{-OH})]_2^{2-}$  en  $[\text{Co}(\text{pda})(\mu\text{-OH})]_2^{2-}$  gesplyt word met byvoeging van  $\text{H}^+$  ione om  $[\text{Co}(\text{lda})(\text{H}_2\text{O})_2]$  en  $[\text{Co}(\text{pda})(\text{H}_2\text{O})_2]$ , respektiewelik te vorm. Verdere byvoeging van suur lei tot die stapsgewyse dissosiasie van die lda en pda ligande. Dit word gepostuleer dat 'n ioongeassosieerde spesie tydens die reaksie tussen  $[\text{Co}(\text{L})(\text{H}_2\text{O})_2]$  ( $\text{L} = \text{lda}, \text{pda}$ ) en  $\text{H}^+$  ione met byvoeging van suur vorm. Hierdie ioongeassosieerde spesie dissosieer in die tempobepalende stap om 'n tridentate  $\text{L}$  ( $\text{L} = \text{lda}, \text{pda}$ ) kompleks,  $[\text{Co}(\eta^3\text{-L})(\text{H}_2\text{O})_3]^+$ , te vorm. Die waarde van  $k_1$  by  $25.9^\circ\text{C}$  is as  $0.128(8) \text{ s}^{-1}$  van die lda kompleks en is as  $0.115(7) \text{ s}^{-1}$  by  $25.7^\circ\text{C}$  van die pda kompleks bepaal.

Nog 'n suur-basis ewewig is waargeneem toe die pH van beide  $[\text{Co}(\text{lda})(\text{H}_2\text{O})_2]$  en  $[\text{Co}(\text{pda})(\text{H}_2\text{O})_2]$  oplossing verhoog is. Die gevolgtrekking is dat die nuutgevormde spesies nie die dimeer is nie, maar eerder  $[\text{Co}(\text{lda})(\text{H}_2\text{O})(\text{OH})]^-$  en  $[\text{Co}(\text{pda})(\text{H}_2\text{O})(\text{OH})]^-$  wat terugkeer na die dimeer by pH 6 - 7 na verloop van 'n paar dae. Die  $\text{pK}_a$  van  $[\text{Co}(\text{lda})(\text{H}_2\text{O})_2]$  en  $[\text{Co}(\text{pda})(\text{H}_2\text{O})_2]$  was spektrofotometries as 6.11(2) en 6.74(1), respektiewelik bepaal.

Die substitusiereaksies tussen  $[\text{Co}(\text{L})(\text{H}_2\text{O})_2]/[\text{Co}(\text{L})(\text{H}_2\text{O})(\text{OH})]^-$  ( $\text{L} = \text{lda}, \text{pda}$ ) en  $\text{NCS}^-$  ione is ook ondersoek.  $\text{NCS}^-$  substitueer die akwaligande stapsgewys by pH = 2.00. Die substitusie van die eerste akwa ligand van  $[\text{Co}(\text{lda})(\text{H}_2\text{O})_2]$  en  $[\text{Co}(\text{pda})(\text{H}_2\text{O})_2]$  ( $k_1 = 2.43(3) \times 10^{-3} \text{ M}^{-1} \text{ s}^{-1}$  by  $24.5^\circ\text{C}$ ) en ( $k_1 = 2.3(4) \times 10^{-2} \text{ M}^{-1} \text{ s}^{-1}$  by  $25.0^\circ\text{C}$ ), respektiewelik by lae pH is ongeveer 125 keer vinniger as die tempo van die tweede akwa-substitusie ( $k_3 = 1.52(6) \times 10^{-4} \text{ M}^{-1} \text{ s}^{-1}$  by  $25.0^\circ\text{C}$ ) en ( $k_3 = 1.36(2) \times 10^{-4} \text{ M}^{-1} \text{ s}^{-1}$  by

## Opsomming

25.0 °C), respektiewelik. Die  $[\text{Co}(\text{lda})(\text{H}_2\text{O})(\text{OH})]^-$  en  $[\text{Co}(\text{pda})(\text{H}_2\text{O})(\text{OH})]^-$  komplekse reageer ongeveer 70 keer vinniger by 25.0 °C met  $\text{NCS}^-$ , respektiewelik as die  $[\text{Co}(\text{lda})(\text{H}_2\text{O})_2]$  en  $[\text{Co}(\text{pda})(\text{H}_2\text{O})_2]$  komplekse met  $\text{NCS}^-$  ( $k_2 = 1.34(9) \text{ M}^{-1} \text{ s}^{-1}$  vs.  $2.43(3) \times 10^{-2} \text{ M}^{-1} \text{ s}^{-1}$  vir  $k_1$  by 24.5 °C) en ( $k_2 = 1.44(8) \text{ M}^{-1} \text{ s}^{-1}$  vs.  $2.3(4) \times 10^{-2} \text{ M}^{-1} \text{ s}^{-1}$  vir  $k_1$  by 25.0 °C), respektiewelik. Hierdie resultate toon duidelik dat die hidroksoligand die cis-akwa binding sodanig labiliseer dat 'n toename in tempo waargeneem word. Verder toon dit aan dat die hidroksied ligande nie deur  $\text{NCS}^-$  ione by hoër pH gesubstitueer word nie, aangesien slegs een reaksie by hierdie pH waargeneem word.

Die Co(III)-lda en-pda komplekse wat geïsoleer en gekarakteriseer is in hierdie studie kan suksesvol as biologiese modelkomplekse gebruik word in toekomstige studies. Hierdie komplekse kan byvoorbeeld gebruik word om die binding van 'n metaal aan 'n funksionele groep van wol na te boots of kan gebruik word as modelkomplekse in farmakologie.

**Sleutelwoorde:** cobalt(III), *l*-leusien-*N,N*-diasynsuur (lda) en *l*-fenielalanien-*N,N*-diasynsuur (pda), ionisasie ewewig konstantes, substitusiereaksies.